PASSIVE NOSETIP TECHNOLOGY (PANT) PROGRAM. VOLUME XI. ANALYSIS AND REVIEW OF THE ABRES COMBUSTION TEST FACILITY FOR HIGH PRESSURE HYPERTHERMAL REENTRY NOSETIP SYSTEMS TESTS

R. E. Maurer, et al

Acurex Corporation

Prepared for:

Space and Missile Systems Organization

April 1974

SAMSO-TR-74-86
Volume XI

INTERIM REPORT
PASSIVE NOSETIP TECHNOLOGY
(PANT) PROGRAM

Volume XI. Analysis and Review of the ABRES Combustion Test Facility for High Pressure Hyperthermal Reentry Nosetip Systems Tests

R. E. Maurer
E. K. Chu

Aerotherm Division/Acurex Corporation

SAMSO-TR-74-86

April 1974

AEROTHERM REPORT 74-100

Air Force Space and Missile
Systems Organization
Los Angeles, California

Contract F04701-71-C-0027

SAMSO-TR-74-86
Volume XI

C/N 7045.394

INTERIM REPORT
PASSIVE NOSETIP TECHNOLOGY
(PANT) PROGRAM

Volume XI. Analysis and Review of the ABRES Combustion Test Facility for High Pressure Hyperthermal Reentry Nosetip Systems Tests

R. E. Maurer
E. K. Chu

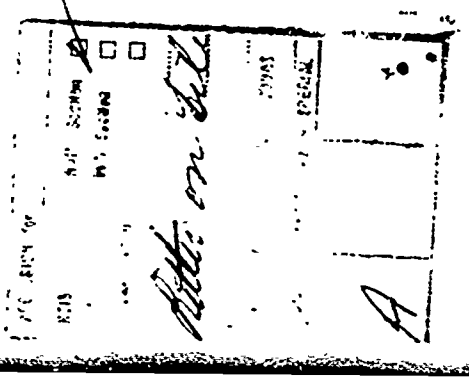

FOREWORD

This document is Volume XI of the Interim Report series for the Passive Nosetip Technology (PANT) program. A summary of the documents in this series prepared to date is as follows:

Volume I - Program Overview (U)

Volume II - Environment and Material Response Procedures for Nosetip Design (U)

Volume III - Surface Roughness Effects

- Part I - Experimental Data
- Part II - Roughness Augmented Heating Data Correlation and Analysis (U)
- Part III - Boundary Layer Transition Data Correlation and Analysis (U)

Volume IV - Heat Transfer and Pressure Distributions on Ablated Shapes

- Part I - Experimental Data
- Part II - Data Correlation

Volume V - Definition of Shape Change Phenomenology from Low Temperature Ablator Experiments

- Part I - Experimental Data, Series C (Preliminary Test Series)
- Part II - Experimental Data, Series D (Final Test Series)
- Part III - Shape Change Data Correlation and Analysis

Volume VI - Graphite Ablation Data Correlation and Analysis (U)

Volume VII - Computer User's Manual, Steady-State Analysis of Ablating Nosetips (SAANT) Program

Volume VIII - Computer User's Manual, Passive Graphite Ablating Nosetip (PAGAN) Program

Volume IX - Unsteady Flow on Ablated Nosetip Shapes - PANT Series G Test and Analysis Report

Volume X - Summary of Experimental and Analytical Results

Volume XI - Analysis and Review of the ABRES Combustion Test Facility for High Pressure Hyperthermal Reentry Nosetip Systems Tests

Volume XII - Nosetip Transition and Shape Change Tests in the AFFDL 50 MW RENT Arc - Data Report

Volume XIII - An Experimental Study to Evaluate Heat Transfer Rates to Scalloped Surfaces - Data Report

Volume XIV - An Experimental Study to Evaluate the Irregular Nosetip Shape Regime - Data Report

Volume XV - Roughness Induced Transition Experiments - Data Report

This report was prepared by Aerotherm Division/Acurex Corporation under Contract F04701-71-C-0027. Volumes I through IX covered PANT activities from April 1971 through April 1973. Volumes X through XV represent contract efforts from May 1973 to December 1974. Volume X summarizes the respective test programs and describes improvements in nosetip analysis capabilities. Volume XI presents an evaluation of the ABRES test facility in terms of performing thermostructural and reentry flight simulation testing. Volumes XII through XV are data reports which summarize the experiments performed for the purpose of defining the irregular flight regime. The analysis of these data are presented in Volume X.

This work was administered under the direction of the Space and Missile Systems Organization with Lieutenant A. T. Hopkins and Lieutenant E. G. Taylor as Project Officers with Mr. W. Portenier and Dr. R. L. Baker of the Aerospace Corporation serving as principal technical monitors. Mr. R. E. Maurer and Mr. E. K. Chu were the Aerotherm investigators on the ABRES facility review activity.

This technical report has been reviewed and is approved.

E G Taylor

E. G. Taylor, Lt., USAF
Project Officer
Aero and Materials Division
Directorate of Systems Engineering
Deputy for Reentry Systems

ABSTRACT

The ABRES Combustion Test Facility located at the Air Force Rocket Propulsion Laboratory (AFRPL) is a high pressure liquid rocket combustor which is used for high pressure hyperthermal ablation testing. The oxidizer and fuel (O/F) currently burned in this facility is nitrogen tetroxide and Aerozine-50 at a nominal O/F ratio of 2.1. Calorimeter and pressure calibration data from this facility are compared with predictions. The agreement between these data and predictions is good with the exception that measured stagnation point heat rates are about double predictions. Additional calibration measurements and analyses are recommended to resolve the stagnation point heating anomaly and other facility uncertainties.

The current ABRES facility is evaluated from the standpoint of thermostructural and reentry flight simulation and is compared with other current high pressure ablation test facilities. Results show that the level of thermostructural and reentry ablation flight simulation achieved in the ABRES facility is relatively low; although, full scale flight hardware can be tested in this facility (even at angle of attack) which is a relatively unique capability.

Alternate propellant combinations are evaluated from the standpoint of upgrading the severity of the ABRES facility hyperthermal test environment. The hydrocarbon/LOX propellant combinations are assessed to be the optimum propellants for upgrading the ABRES ablation test facility due to (1) the moderate increase in severity of the hyperthermal environment that they provide, (2) their low toxicity, and (3) their relatively low cost. The upgraded ABRES combustion test facility is compared with other advanced ablation test facilities and found to be quite competitive.

TABLE OF CONTENTS

LIST OF FIGURES

LIST OF FIGURES (Concluded)

LIST OF TABLES

SECTION 1

INTRODUCTION

The ABRES Combustion Test Facility located at the Air Force Rocket Propulsion Laboratory was developed by AFRPL personnel under sponsorship of the Space and Missiles Systems Organization, Advance Ballistic Reentry Systems Division (SAMSO/ABRES). This high pressure hyperthermal liquid rocket combustor was designed to provide a nosetip design test facility, capable of testing full scale flight hardware, even at angle-of-attack. The facilities nominal operating conditions are (1) a peak chamber pressure of 3000psi (2) two contoured supersonic nozzles which yield impact pressures of either 50 or 100 atmospheres at free-stream Mach numbers of 2.93 and 2.32 respectively (3) a nominal total run time of 15 seconds and (4) a propellant combination of N_2O_4/Aerozine-50 at an O/F mixture ratio in the range of 2.0 to 2.2. The facility became operational in the fall of 1972. Since that time several ablation test series and many calibration models have been exposed in the facilities hyperthermal test stream.

The intent of this study within the PANT program was to evaluate the ABRES Combustion Test Facility compared with typical flight environmental requirements and other existing and projected ablation test facilities. This study started with a complete and detailed review of all calorimeter and pressure measurements made to date in the ABRES facility. These data were reviewed in order to assess the status of the characterization of the high pressure hyperthermal environment, including the Mach 2.32 and 2.93 test rhombuses. Results of this study, including recommendations for additional calibration measurements are reviewed in Section 2.

Results of the ABRES facility application studies are presented in Section 3. This part of the study considered the current degree of simulation of flight environmental conditions achieved in the ABRES facility. Also included in this portion of the study was a comparison of the nosetip transition and ablation (shape change) response achieved in the ABRES facility compared with other operational hyperthermal ablation test facilities.

Section 4 summarizes the highlights of the ABRES facility propellant optimization study. This phase of the study considered optimization of the high pressure hyperthermal environmental test conditions from three different standpoints: (1) nosetip thermostructural tests (2) reentry ablation simulation tests and (3) transpiration systems testing. Results of these analyses were used to recommend optimum propellant combinations for each of the above ablation test requirements. In addition one propellant combination was recommended as optimum from the standpoint of overall facility test requirements and ease of operation.

Based on the upgraded environmental test conditions selected in Section 4, the "advanced" ABRES test facility is compared with other advanced or proposed hyperthermal ablation test facilities in Section 5. Results of the entire ABRES facility evaluation study are summarized in Section 6.

SECTION 2

ABRES FACILITY CALIBRATION DATA EVALUATION

Calibration measurements of the ABRES combustion facility test stream have been made since it became operational in the fall of 1972 and they include both static pressure and calorimeter measurements. The propellant combination burned in the ABRES facility during this time was N_2O_4/Aerozine-50 at a nominal oxidizer to fuel (O/F) ratio of 2.1.

Analyses of the pressure and calorimeter data from the ABRES combustion test facility are reviewed in Section 2.1. Results of the calibration data analyses are interpreted to predict the nominal heating distribution over a sphere-cone configuration (R_N = 1 inch, CHA = 7°) at both the 50 and 100 atmosphere impact pressure test conditions. These estimates are presented in Section 2.2. Based on the calibration data reviewed herein and observations regarding materials thermal response in this facility, additional calibration measurements are recommended. These recommendations are presented in Section 2.3.

2.1 ABRES FACILITY CALIBRATION DATA EVALUATION

The ABRES facility calibration data analyzed herein were derived from calibration model exposures during the time interval of October 1972 to June 1973. A total of nineteen calibration models were exposed in the ABRES test stream which included 14 calorimeter models and 5 pressure models. Calibration models are generally exposed to the hyperthermal test stream by sweeping the copper model onto the centerline position, holding it on the centerline for a short time (10-20 miliseconds) and retracting it from the test stream before the copper melts. Details regarding the operation of the model positioner sting system are discussed in Reference 1.

The calorimeter data are reviewed in Section 2.1.1. The pressure calibration data are analyzed in Section 2.1.2. Both the pressure and calorimeter data were interpreted to establish the boundaries and uniformity of the test rhombus of the underexpanded test stream. The test rhombus boundaries for both the Mach 2.32 and 2.93 nozzles derived from the pressure and calorimeter calibration data are discussed in Section 2.1.3.

2.1.1 Calorimeter Data Analyses

The fourteen calorimeter models exposed in the ABRES test stream were of three basic designs. All calorimeters were sphere/cone models with 7° cone half angles. The distinguishing feature of the three model geometries were the three different nose radii. The radius of the spherical tips on the calorimeter models were 0.5 inch, 0.75 inch, and 1.35 inches. All null point calorimeter models were fabricated by the Aerotherm Division of Acurex Corporation. The 0.5 and 0.75 inch radius models were purchased as calibration models by the AFRPL directly. The 1.35 inch radius models were tested by Lockheed Missiles and Space Company in support of the Navy Trident Program.

The 0.5 inch radius models had only one null point calorimeter at the stagnation point, but both the 0.75 and 1.35 inch radius models had multiple null point calorimeters. The 0.75 inch radius models had a total of 6 null point calorimeters distributed along their length. The 1.35 inch radius models had a total of 17 calorimeters distributed along their length. Table 1 lists the null point calorimeter locations for both the 0.75 and 1.35 inch radius calorimeter models.

As previously discussed, the calorimeter models were exposed to the ABRES test stream in a modified swept mode. The calorimeters were swept onto the test stream centerline, held on the centerline for a few milliseconds and removed prior to melting. During their exposure in the hyperthermal test stream, the response of the null point calorimeters can be equated to the thermal response of a semi-infinite slab (Reference 2). The temperature response of the null point thermocouples were reduced to a hot wall heat flux by AFRPL personnel through use of the Aerotherm developed PANDA computer program (Reference 3). The hot wall heat flux were reduced to cold wall values through use of the following correction factor, $\dot{q}_{CW} = \{(H_R - H_{CW})/(H_R - H_{HW})\}\dot{q}_{HW}$ The calorimeter data analyzed herein are all cold-wall values.

The fourteen calorimeter exposures in the ABRES combustion test facility analyzed herein are listed in Table 2. This list of calorimeter tests is sequential with respect to the date of their exposure. The half inch radius calorimeters were exposed a total of five times. This included three calibration tests at the low Mach number condition and two at the high Mach number test condition. Four of the calorimeter exposures used the nominal sweep/hold/sweep mode whereas the fifth model (Run 46.01) was positioned on the centerline with a protective teflon cap which ablated off after several milliseconds in the test stream. This technique of calorimeter model exposure provided high quality stagnation point heating data, although the technique is not consistent with the desire of multiple calorimeter model exposures. It would be difficult to expose calorimeter models in this manner without destroying them since the precise time of teflon cap removal can not be predicted within 10-20 milliseconds

TABLE 1

NULL POINT CALORIMETER LOCATIONS ON THE
0.75 AND 1.35 INCH RADIUS CALORIMETERS

R_N = 0.75 Inch				R_N = 1.35 Inch			
Null Point Calorimeter	Azimuth	Radial Dist. from Axis (In.)	Axial Dist. from Stag. Pt. (In.)	Null Point Calorimeter	Azimuth	Radial Dist. from Axis (In.)	Axial Dist. from Stag. Pt. (In.)
C-1	0°	0.	0.	C-1	0°	0.	0
C-2	0°	.48	.175	C-2	0°	.960	.400
C-3	0°	.76	.75	C-3	90°	.960	.400
C-4	0°	.85	1.5	C-4	0°	1.310	1.0
C-5	180°	.85	1.5	C-5	90°	1.310	1.0
C-6	0°	1.03	3.0	C-6	0°	1.35	1.5
				C-7	270°	1.35	1.5
				C-8	90°	1.395	1.6
				C-9	0°	1.43	2.0
				C-10	90°	1.43	2.0
				C-11	270°	1.43	2.0
				C-12	0°	1.495	2.25
				C-13	0°	1.56	2.75
				C-14	90°	1.68	3.75
				C-15	0°	1.80	4.75
				C-16	90°	1.92	5.75
				C-17	270°	1.92	5.75

TABLE 2

CALORIMETER TESTS IN THE ABRES TEST FACILITY

Run No.	R_N ~ in.	P_{t_2} ~ atm.	M_∞	Date	Comments
15.01	0.5	100.	2.32	6 Oct. '72	
19.01	0.5	100.	2.32	19 Oct. '72	
20.01	0.75	100.	2.32	20 Oct. '72	melting on nosetip
22.01	1.35	100.	2.32	30 Oct. '72	calorimeter positioned 0.7" off of stream ℄
23.01	1.35	50.	2.32	9 Nov. '72	
25.01	1.35	100.	2.32	27 Nov. '72	
29.01	0.75	50.	2.93	8 Jan. '73	δ_o = 0.25 inch stand-off from nozzle exit plane
30.01	0.75	50.	2.93	8 Jan. '73	δ_o = 5 inch stand-off from nozzle exit plane
32.01	0.75	25.	2.93	19 Jan. '73	δ_o = 0.25 inch stand-off from nozzle exit plane
41.01	0.5	100.	2.32	4 May '73	
43.01	0.75	25.	2.93	15 May '73	
45.01	0.5	50.	2.93	31 May '73	
46.01	0.5	50.	2.93	1 June '73	teflon covered model held on ℄ to destruction
49.01	1.35	100.	2.32	5 June '73	calorimeter position 1." off of stream ℄

which is about the time required to melt copper in the ABRES test stream. The 0.75 inch and 1.35 inch calorimeters were all exposed to the test stream in the nominal sweep/hold/sweep mode. Two of the 1.35 inch calorimeters missed the centerline by more than 0.5 inches. When this occurs the response of calorimeters located on the frustum of the model can be adversely affected since they may be erroneously positioned in the expansion region of the test stream. Anomalies of this nature are indicated in Table 2.

The cold wall heat rate data from the calorimeter models are compared to theoretical predictions in Figures 1 through 3. The heating distribution data derived from the 1.35 and 0.75 inch calorimeters are compared to theoretical predictions made with the ARGEIBL computer program (Reference 4) in Figures 1 and 2. The ARGEIBL computer code predicts the convective heating distribution over surfaces with prescribed velocity and pressure distributions by solving the boundary layer equations using an energy integral technique. The velocity and pressure distributions over these sphere cone models in the ABRES combustion test facility were calculated using the RAZZIB computer code (Reference 5) assuming $\gamma = 1.2$. The real gas transport properties of the exhaust gas products required as input into the ARGEIBL code were predicted with the ACE computer program (Reference 6). The gas composition in the test rhombus for the above ACE solutions was assumed to be in chemical equilibrium.

Figure 1 compares the cold-wall heat flux data from the 1.35 inch radius calorimeters at both the 100 and 50 atmosphere impact pressure test conditions. Observations regarding the comparison of the ARGEIBL heating distribution predictions with the cold wall heating data from these large models are summarized below.

1. The measured stagnation point cold wall heat flux is consistently above the laminar stagnation point prediction by about a factor of of two.

2. The trend in the data from Run 22.01 follows the expected behavior since the model was positioned 0.7 inches off the nozzle centerline. The calorimeters located along the 270° ray at both the 1.5 and 2.0 inch stations were within the expansion region of the test stream, thus the measured heat rates along this ray are extremely low. The 90° ray calorimeter was within the test cone to an axial station of 4 inches.

3. The data scatter from Run 49.01 is large. Film records of this test show that the calibration model missed the centerline position by about 1 inch. The generally higher heat flux measurements along the 90° ray result from the fact that this ray is completely immersed in the test stream. The high heat flux measurement at the 2 inch station (0° ray) appears anomalous when compared with the other data at this calorimeter station.

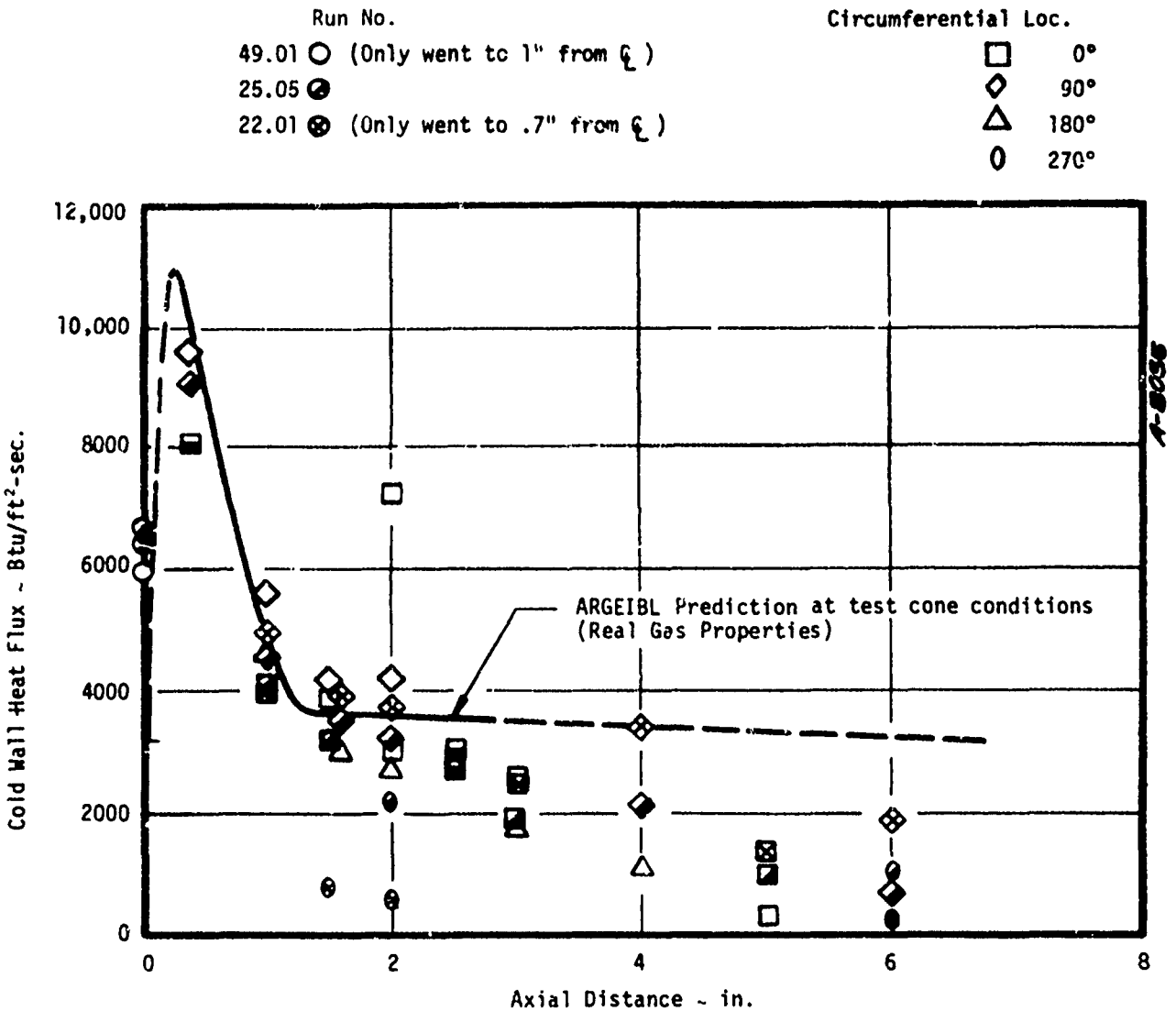

Figure 1. Heating Bistribution Data from the 1.35 inch Radius Calorimeter Models Compared with Predictions

a) ABRES Test Condition - P_{t_2} = 100 atm, M_∞ = 2.32

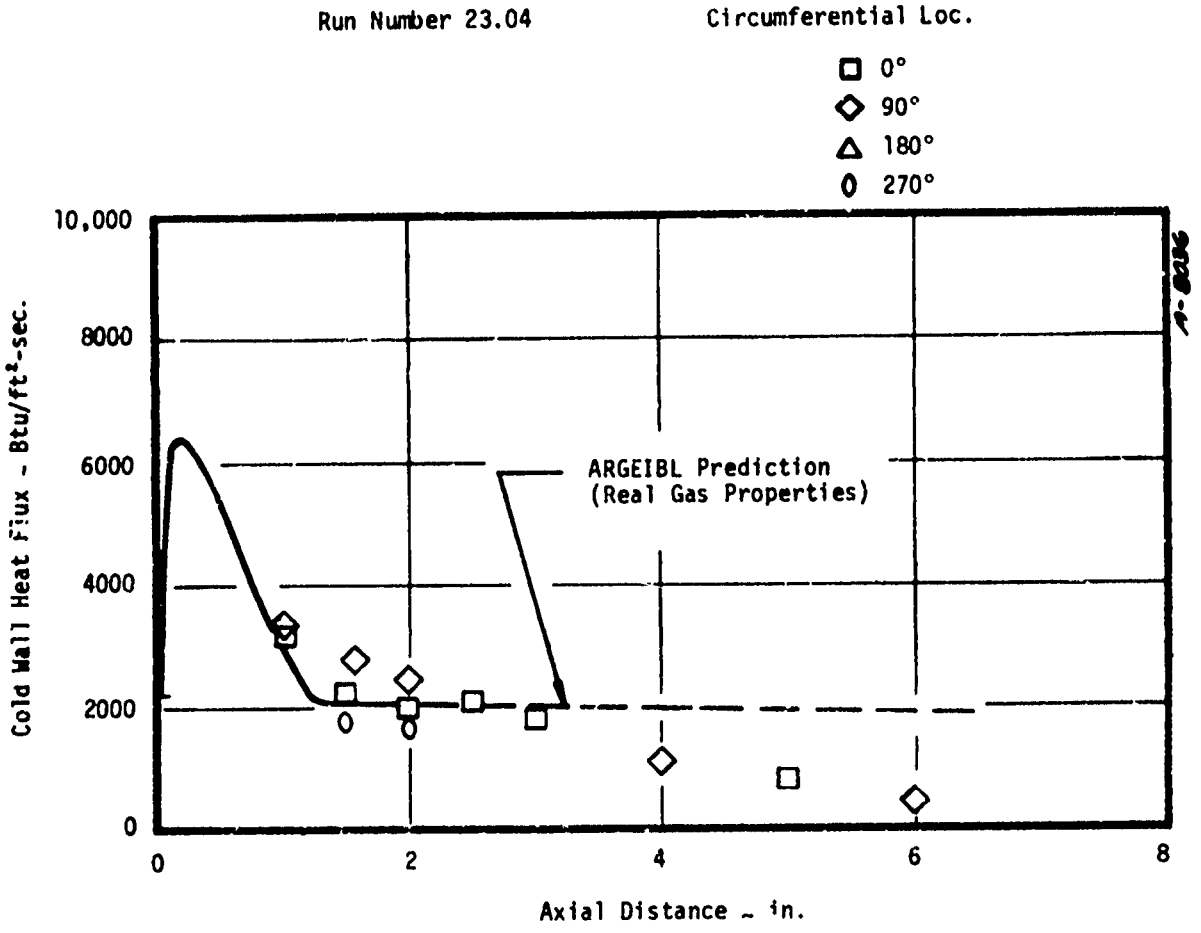

Figure 1. Concluded

b) ABRES Test Condition - P_{t_2} = 50 atm, M_∞ = 2.93

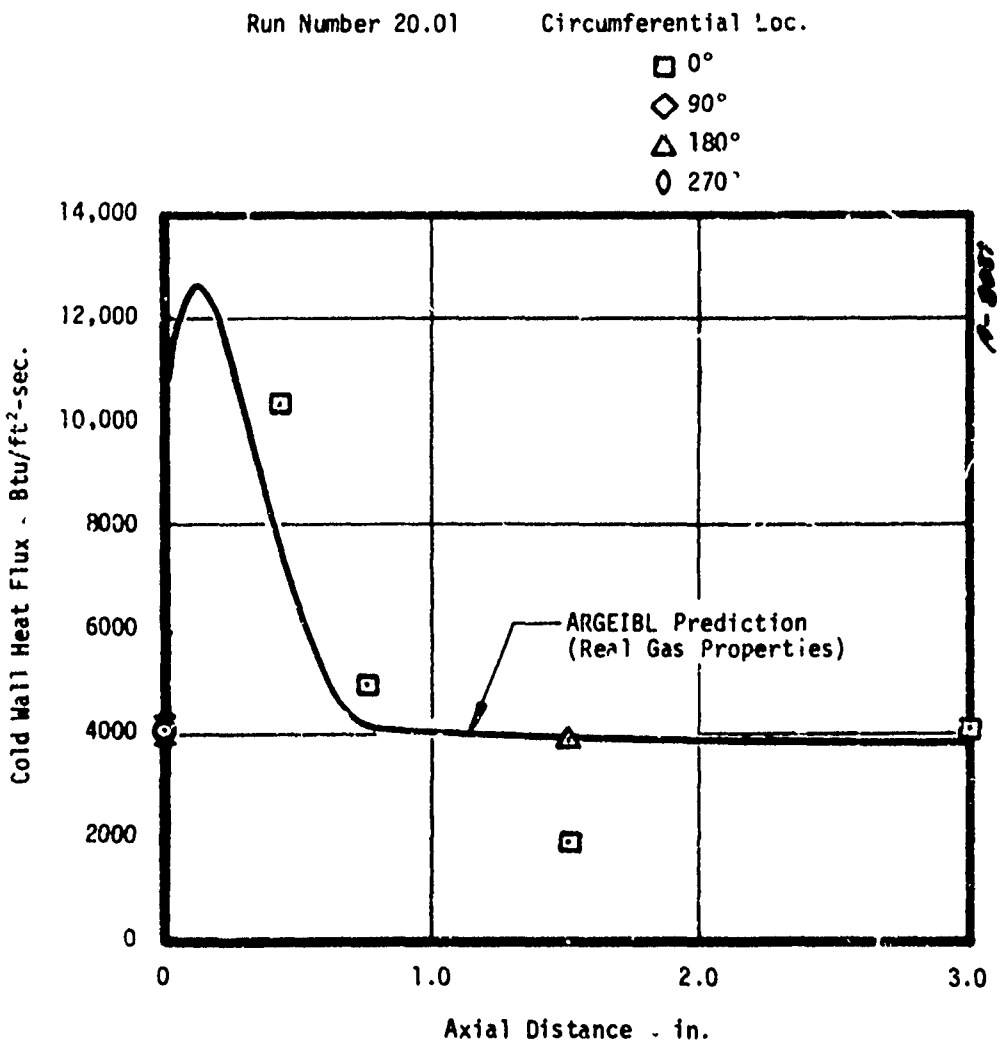

Figure 2. Heating Distribution Data from the 0.75 inch Radius Calorimeter Models Compared with Predictions

a) ABRES Test Condition - P_{t_2} = 100 atm, M_∞ = 2.32

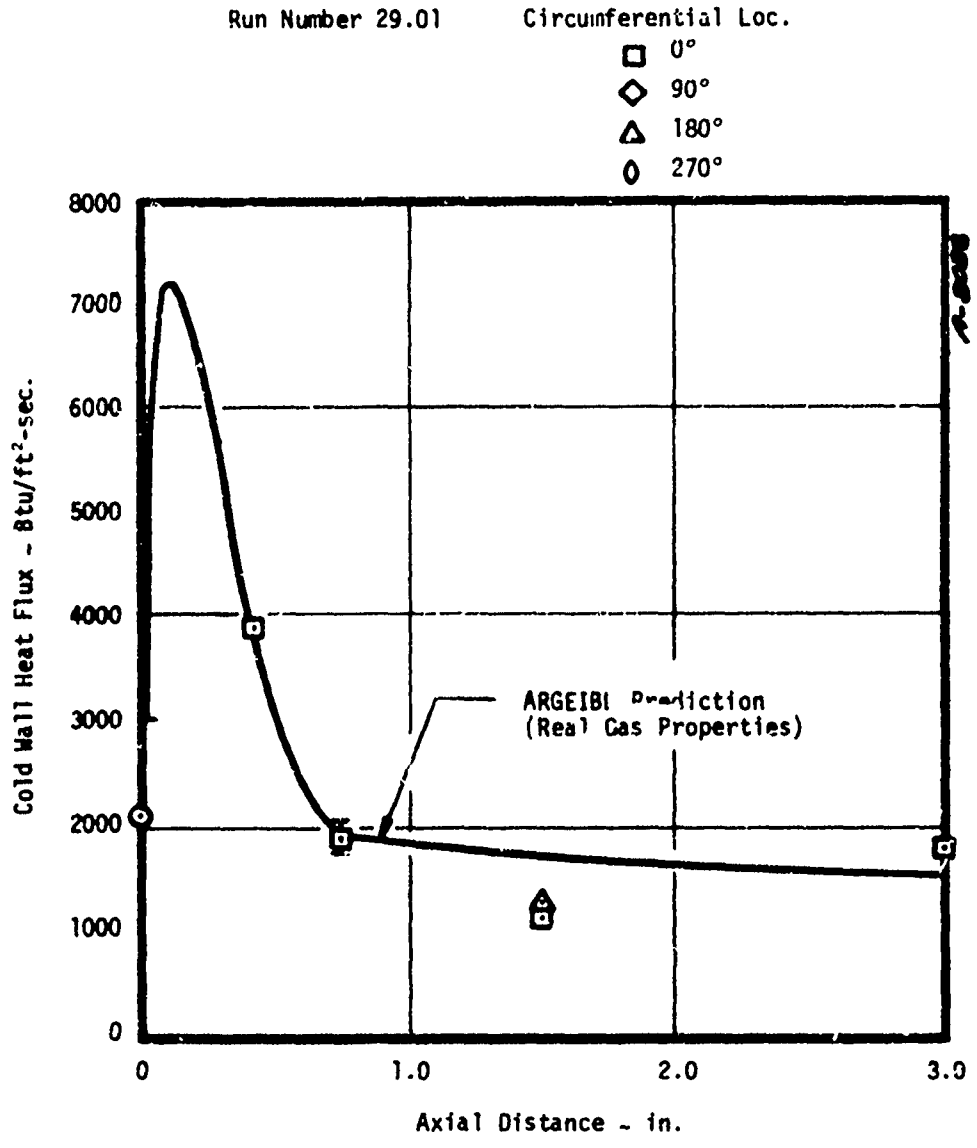

Figure 2. Continued

b) ABRES Test Condition - P_{t_2} = 50 atm, M_∞ = 2.93

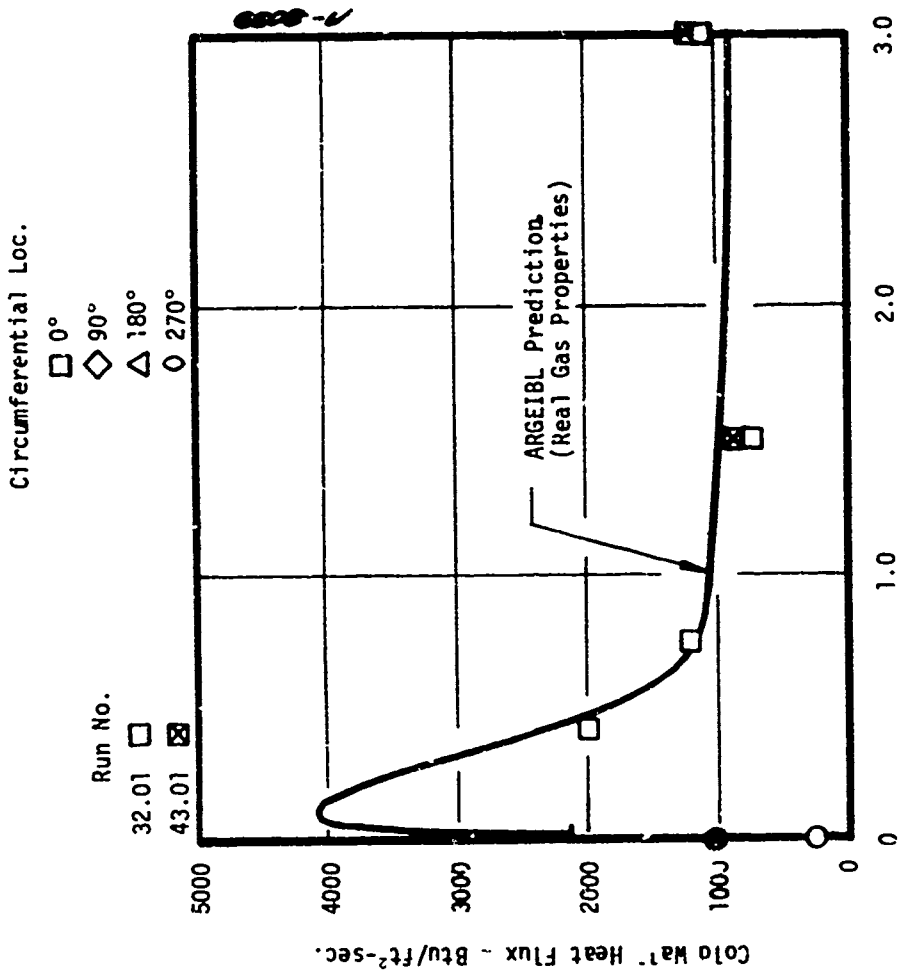

Figure 2. Concluded

c) ABRES Test Condition - P_{t_2} = 25 atm, M_∞ = 2.93

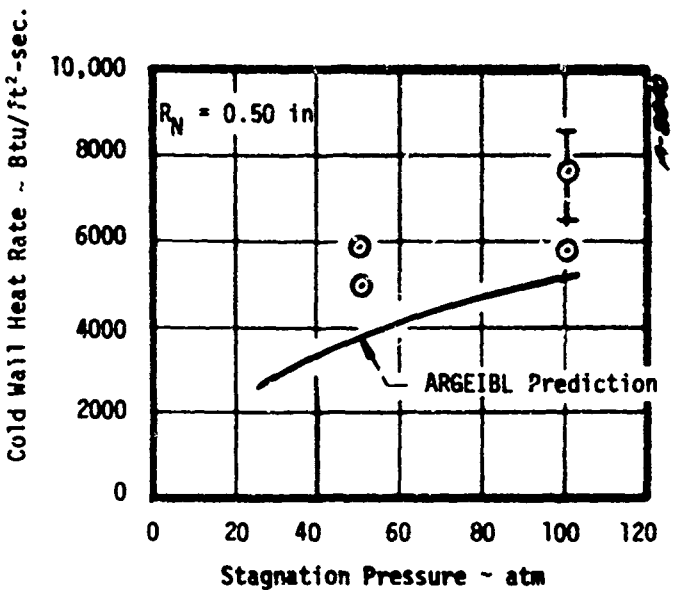

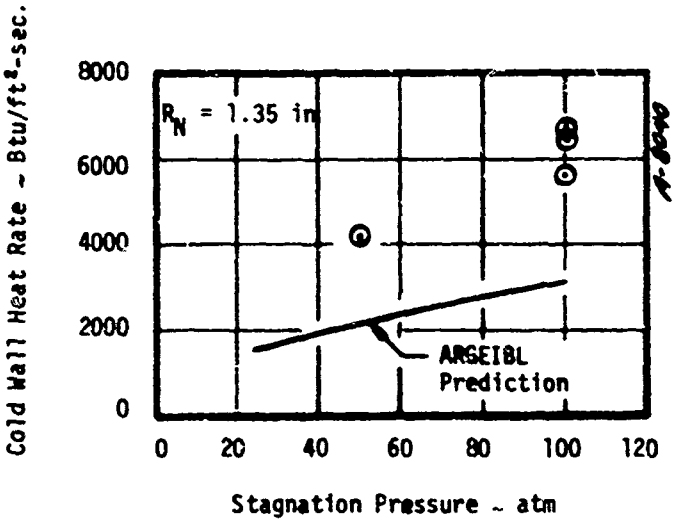

Figure 3. Comparison of Stagnation Point Calorimeter Data with ARGEIBL Predictions (Real Gas Properties)

4. Calorimeter data beyond the 3 inch axial station exhibit a substantial amount of scatter (caused in part by the misalignment of models and variability in the expansion region flow field).

5. The general agreement between the heat flux distribution data at the high pressure test condition and ARGEIBL predictions is good with the above mentioned exceptions.

6. Data consistency and agreement between the data and the ARGEIBL prediction at the 50 atmosphere impact pressure test condition (Run 23.04) is excellent.

7. A definite drop in the measured heat rates occurs beyond the 2 inch axial station. This location on the calorimeter model corresponds to the approximate location of frustum intersection with the test stream expansion fan.

In general the agreement between the 1.35 inch radius calorimeter data and the ARGEIBL real gas heating distribution predictions is good. The lack of agreement between the stagnation point heat flux measurements and laminar stagnation point predictions will be discussed subsequently.

Figure 2 compares the cold-wall heat flux data from the 0.75 inch radius calorimeters at the 100, 50, and 25 atmosphere impact pressure test conditions. Observations regarding the comparison of the ARGEIBL heating distribution predictions with the data for the intermediate sized models are summarized below.

1. The stagnation point calorimeter data are consistently below the laminar predictions. This behavior is felt to be a result of unknowingly damaged calorimeter sheaths which were used in these models. The sheaths were subsequently found to be degraded by water absorption. Heating data from these calorimeters are disregarded for this reason.

2. The general agreement between measured and predicted heat rates for Run 20.0 (P_{t_2} = 100 atm) is good with the following exceptions: (1) the measured heat flux at the 40° location on the spherical tip is above the ARGEIBL prediction (2) the measured heat rate at the 1.5 inch station is below the ARGEIBL prediction.

3. At the 50 atmosphere impact pressure test condition (Run 29.01) the agreement between the measured heat rates and predictions is good with the exception that the measured rates are slightly below the predictions at the 1.5 inch station.

4. At the 25 atmosphere impact pressure test condition (Runs 32.01 and 45.01) the agreement between the measured and predicted heating rates is good with the exception that the heat flux measurements at the 1.5 inch station are slightly below the turbulent predictions.

5. The consistency with which the calorimeter measurements at the 1.5 inch station are below the turbulent predictions suggests that relaminarization may be occuring in this region on the 0.75 inch models.

The general agreement between the ARGEIBL turbulent heating distribution predictions and the measured heat rates for the 0.75 inch models is good with the above noted exceptions. There are no anomalies between the measured cold-wall heat rates and predictions which suggests that the ABRES test stream environment is in generally good agreement with theory. The consistent lack of agreement between the stagnation point heat rate measurements and predictions is discussed subsequently when the data from the small nose radii calorimeters are reviewed.

Figure 3 compares the four stagnation point heat flux measurements from the small nose radii calorimeter models with ARGEIBL predictions. The predicted and observed variation of stagnation point cold wall heat flux with impact pressure exhibit good agreement in Figure 3 despite the fact that the measured heat rates are about double the predicted rates. This result is consistent with the level of agreement between the measured and predicted stagnation point heat rates for the large radius calorimeter models. The cause of this discrepancy between measured and predicted stagnation point heat rates can only be speculated at this time. It is apparent from the measured heating distributions on the 0.75 and 1.35 inch calorimeter models that transition occurs very near the stagnation point. A sharp rise in the heat flux distribution near the stagnation point provides the mechanism for strong two dimensional conduction effects which would effect the response of the stagnation line null point calorimeter. Reduction of the null point calorimeter data to heat flux data by the PANDA computer code does not account for lateral conduction effects. To resolve this question, detailed two-dimensional conduction analyses of the null point calorimeter response with a sharply increasing convective heating distribution in the lateral direction from the stagnation point must be made. More will be said regarding proposed anlayses to assess this apparent anomaly in the measured stagnation point heat rates in Section 2.3. The variation of the stagnation point heat flux measurements with pressure for the 1.35 inch radius calorimeters also exhibit good agreement with predictions as shown in Figure 3. Both sets of stagnation point heat flux measurements are about 1.5 to 2. times the laminar ARGEIBL predictions.

In summary, the calorimeter data from the ABRES combustion test facility show the following:

1. Transition on a relatively cold copper calorimeter model occurs within 40° of the stagnation point.
2. Peak turbulent cold wall heat rates measured on 1.35 and 0.75 inch radius spherically tipped calorimeters are about 9000-9500 Btu/ft^{2}sec and over 10,000 Btu/ft^{2}sec respectively at the high impact pressure test condition (e.g., P_{t_2} = 100 atm).
3. Measured cold wall convective heating distributions on a 7° conic frustum agree well with turbulent flow convective heating predictions made with the ARGEIBL computer code.
4. The exhaust products of the N_2O_4/Aerozine-50 propellant are assessed to be in equilibrium since all of the heat transfer predictions were all based on equilibrium gas properties.

2.1.2 Pressure Calibration Data Analyses

The pressure calibration data were derived from sphere cone models of the following geometry.

(1) R_N = 0.5" , CHA = 7°

(2) R_N = 0.75", CHA = 7°

(3) R_N = 1.35", CHA = 7°

The half inch radius model had only one pressure port at the stagnation point. The two larger nose radii geometries had multiple pressure ports along the length of the model. The locations of the pressure ports on these models are listed in Table 3.

The pressure calibration models were generally swept completely across the test stream to evaluate the uniformity and symmetry of the test rhombus. The 1.35 inch nose radius models were not swept, but rather held on the centerline for several milliseconds, since both null point calorimeters and pressure transducers were contained in these models. The results of nine pressure calibration tests are reviewed herein. These calibration tests are listed in Table 4 in the sequence in which they were exposed.

These data are presented in Figures 4 and 5. Figure 4 compares the pressure distribution data from the 1.35 inch radius models with predicted distributions at both the 100 and 50 atmosphere impact pressure test conditions.

TABLE 3

PRESSURE PORT LOCATIONS ON THE 0.75 AND
1.35 INCH RADIUS CALIBRATION MODELS

R_N = 0.75 Inch				R_N = 1.35 Inch			
Pressure Port	Azimuth	Radial Distance (in)	Axial Distance (in)	Pressure Port	Azimuth	Radial Distance (in)	Axial Distance (in)
P-1	0°	0	0	P-1	180°	1.31	1.
P-2	0°	.48	.175	P-2	180°	1.38	1.5
P-3	0°	.76	.750	P-3	180°	1.43	2.0
P-4	0°	.85	1.50	P-4	180°	1.56	3.0
P-5	180°	.85	1.50	P-5	180°	1.68	4.0
P-6	0°	1.03	3.00	P-6	180°	1.80	5.0

TABLE 4

PRESSURE CALIBRATION TESTS IN THE ABRES TEST FACILITY

Run No.	R_N ~ in.	P_{t_2} ~ atm.	M_∞	Date	Comments
18.01	0.5	100	2.32	18 Oct. '72	
21.01	0.75	100	2.32	26 Oct. '72	
22.01	1.35	100	2.32	30 Oct. '72	Calibration model positioned 0.7" off of stream $\mathbb{Q}$
23.04	1.35	50	2.32	9 Nov. '72	
25.05	0.75	100	2.32	27 Nov. '72	
28.01	0.75	50	2.93	8 Jan. '73	δ_o = 0.25" stand-off
31.02	0.75	50	2.93	17 Jan. '73	δ_o = 5" stand-off
42.01	0.75	25	2.93	15 May '73	no good data
49.01	1.35	100	2.32	5 June '73	Calibration model positioned 1.0" off of stream $\mathbb{Q}$

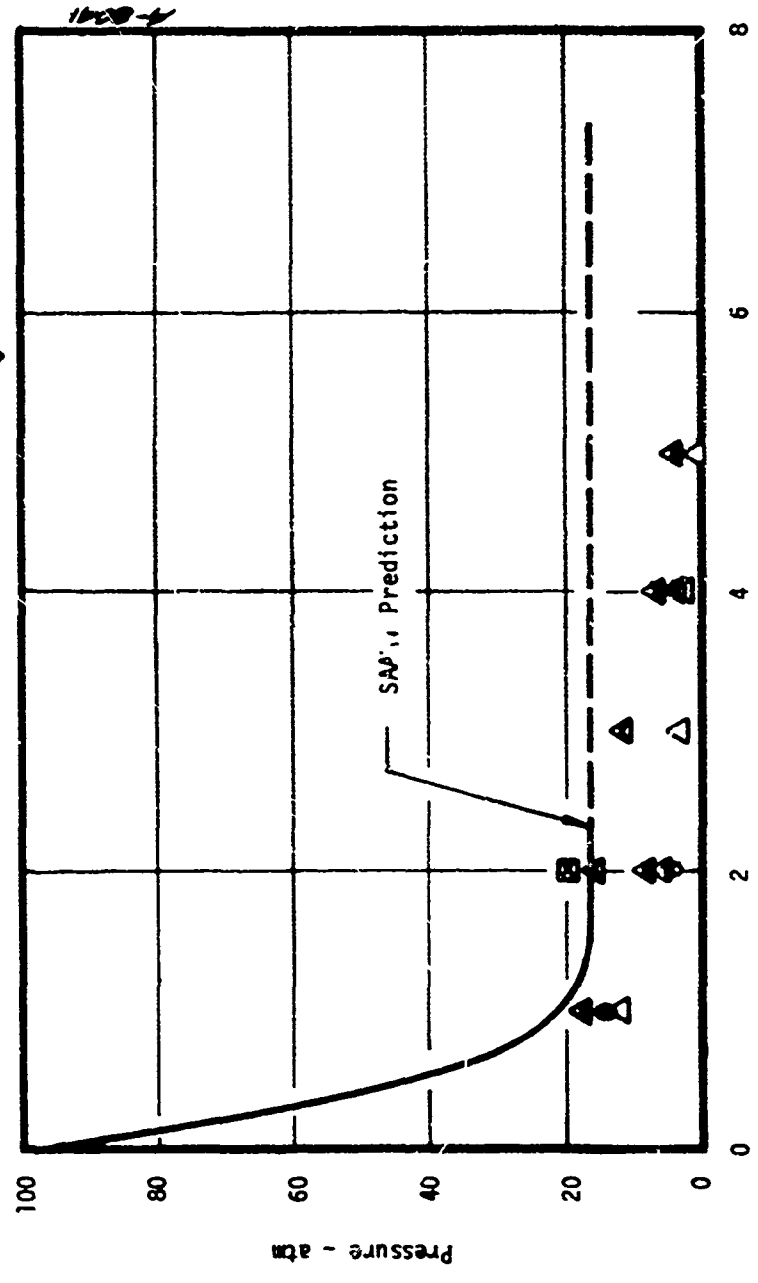

Figure 4. Pressure Distribution Data from the 1 35 inch Radius Models Compared with Predictions

a) ABRES Test Condition - P_{t_2} = 100 atm, M_∞ = 2.32

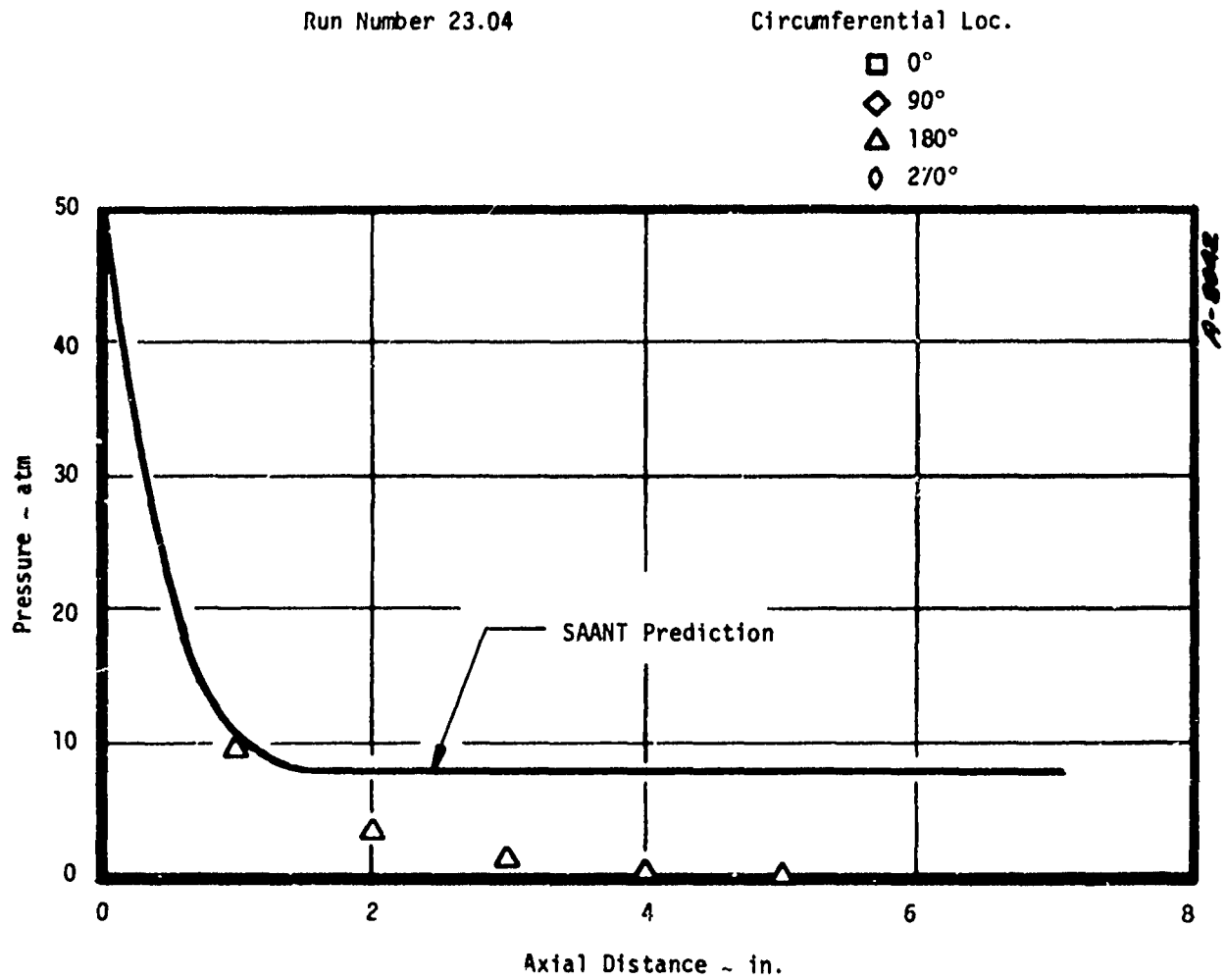

Figure 4. Concluded

b) ABRES Test Condition - P_{t_2} = 50 atm, M_∞ = 2.93

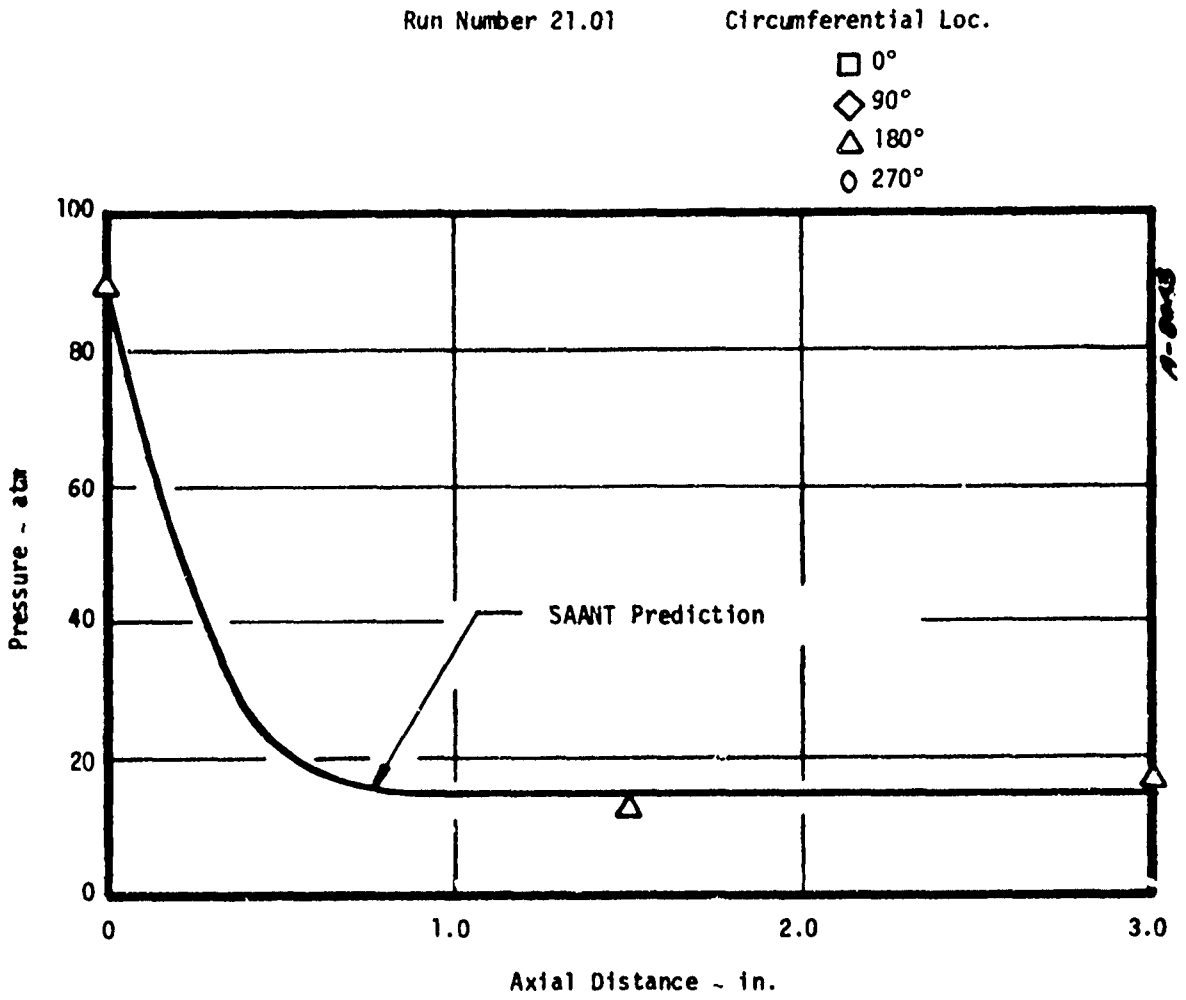

Figure 5. Pressure Distribution Data from the 0.75 inch Radius Models Compared with Predictions

a) ABRES Test Condition - P_{t_2} = 100 atm, M_∞ = 2.32

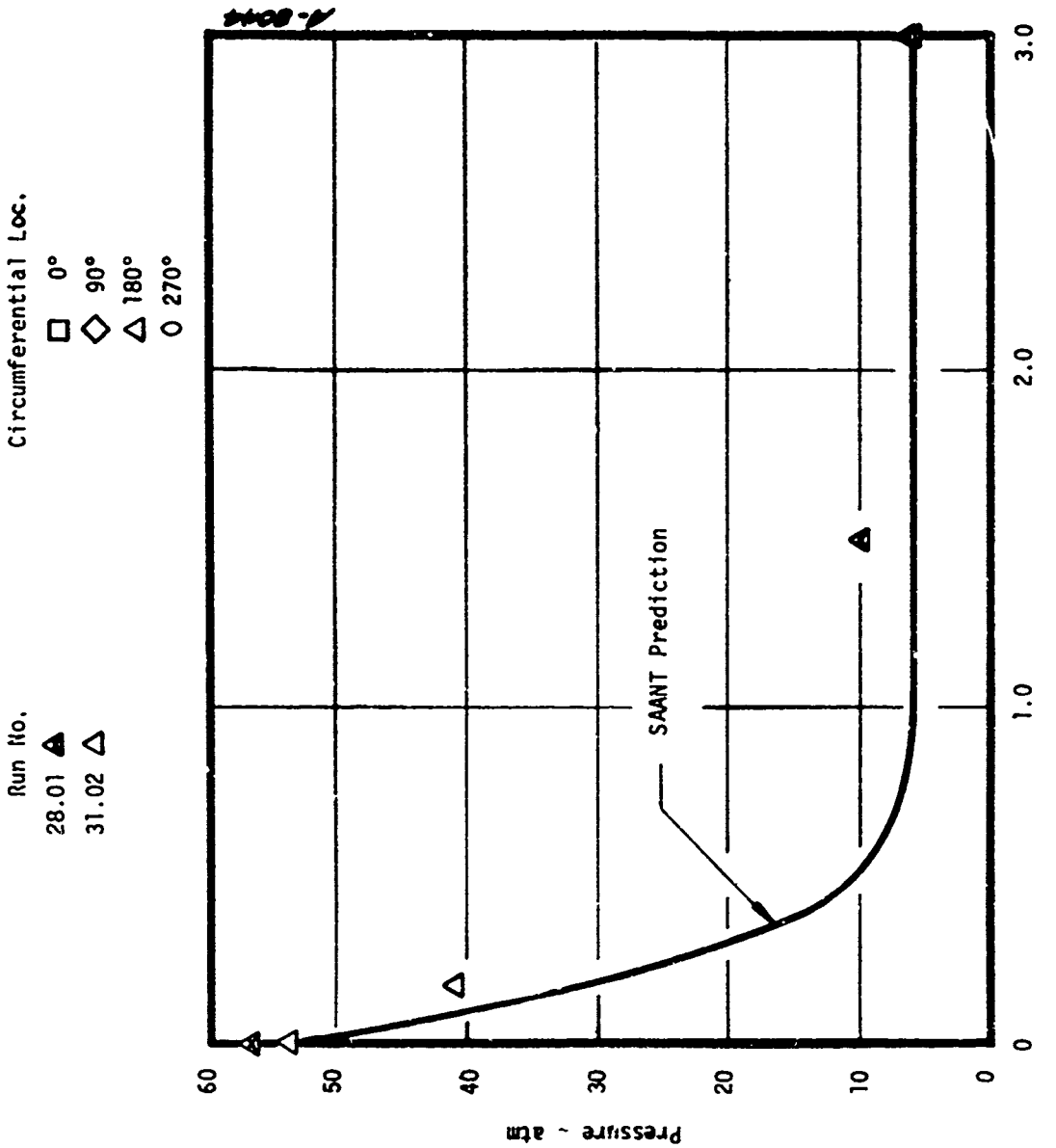

Figure 5. Concluded
b) ABRES Test Condition - P_{t_2} = 50 atm, M_∞ = 2.93

The SAANT pressure distributions were made with a $\gamma = 1.2$ test gas and exhibit excellant agreement with the RAZZIB pressure distribution predictions input to the ARGEIBL code for the convective heating distribution predictions. Observations regarding these comparisons of measured and predicted pressure distributions in Figure 4 are summarized below.

1. At both the high and low impact pressure test conditions, the pressure data are slightly below the predictions at both 1" and 2" axial stations.
2. Run 49.01 missed the center line by about 1.0 inches. The pressure data at the 2 inch axial station agree with the expected asymmetric distribution caused by the misalignment.
3. The static pressure measurements beyond the 2 inch axial station on these large models are within the expansion fan and fall below the predictions.

In summary, the predicted and measured pressure data are in good agreement considering the fact that the predicted distributions assume the nominal 100 and 50 atmosphere impact pressure test conditions. Since the stagnation point impact pressures were not measured by these models it was not possible to verify the absolute level of the predicted distributions.

The pressure calibration data from the 0.75 inch models are compared with SAANT predictions in Figure 5. These models contained 4 pressure ports distributed along the length of the model to an axial distance of 3 inches from the stagnation point. All the pressure ports on these models were within the ABRES test rhombus for all exposures. Observations regarding the pressure distribution data and predictions are summarized below.

1. Pressure distribution data from the model exposed at the high impact pressure test condition (Run 21.01) exhibits excellent agreement with the predicted pressure distribution.
2. Pressure calibration data from models exposed to the high Mach number flow (P_{t_2} = 50 atm, Runs 28.01 and 31.02) also exhibit good agreement with the predicted distribution.

Since the distance between the nozzle exit plane and the model's stagnation point (i.e., model stand-off distance) for these two runs were 0.25 and 5.0 inches respectively, these data verify the uniformity of the large (high Mach number) test rhombus. Both sets of pressure calibration data exhibit good agreement with predictions which verifies that the test stream flow from both nozzles are near the two reported Mach numbers and that the contoured nozzles do yield a uniform free stream flow. Results from the 0.5 inch radius model will be considered in Section 2.1.3 which reviews the test rhombus extent.

2.1.3 Test Rhombus Extent

Flow from both the Mach 2.32 and 2.93 contoured nozzles is underexpanded. As a result, at both flow conditions the test rhombus boundaries are defined by the Mach cone emanating from the lip of the nozzle exit plane. The pressure and calorimeter calibration data reviewed above were analyzed with the intent of rationalizing the extent and uniformity of the ABRES test rhombus.

The pressure calibration measurements provide a clear indication of the boundaries of the test rhombus for an underexpanded flow. The sketch in Figure 6 illustrates how a stagnation point pressure port senses the leading expansion fan from the lip of the nozzle over a relatively large radial distance due to the region of subsonic flow at the stagnation point. This sketch corresponds to the 2.32 Mach number flow and a 0.5 inch radius pressure model.

Figures 7 and 8 compare measured pressure profile data with the three theoretical boundaries described in Figure 6. Figure 7 compares the transverse pressure profile data measured by the stagnation point pressure port on a 0.5 inch radius model as it was swept across the test stream. This model was swept through the test rhombus at a stand-off distance of 0.25 inches from the nozzle exit plane. The agreement between the theoretical boundaries and the pressure profile data is excellent.

Figure 8 compares the theoretical boundaries described above with the pressure data measured at the stagnation point of a 0.75 inch radius model. Both runs were nominally at the same high Mach number test condition. For Run 28.01 the model was swept across the test stream at a stand-off distance of 0.25 inches whereas on Run 31.02 the stand-off distance was 5.0 inches. In both cases the theoretical "inner boundary" exhibits good agreement with the data. The "geometric" and "outer" boundaries agree reasonably with the data at the 0.25 inch stand-off, but not at the 5 inch stand-off. This is expected since at a distance of 5 inches downstream from the nozzle exit plane the expansion region is quite wide. The boundaries described in Figure 6 correspond to the intersection of the inner boundary of the expansion fan with the sonic boundaries in the model's stagnation region. Therefore the true "outer" boundary at the 5 inch stand-off distance should occur at a much larger radial distance than the theoretical "outer" boundary as it does. The pressure and convective heating rates measured by the 0.75 inch radius calibration models at the 0.25 and 5.0 inch stand-off distances in the large test rhombus (Mach 2.93 nozzle) demonstrate that the test rhombus flow is uniform since the centerline pressure and heat flux measurements at both locations exhibit good agreement.

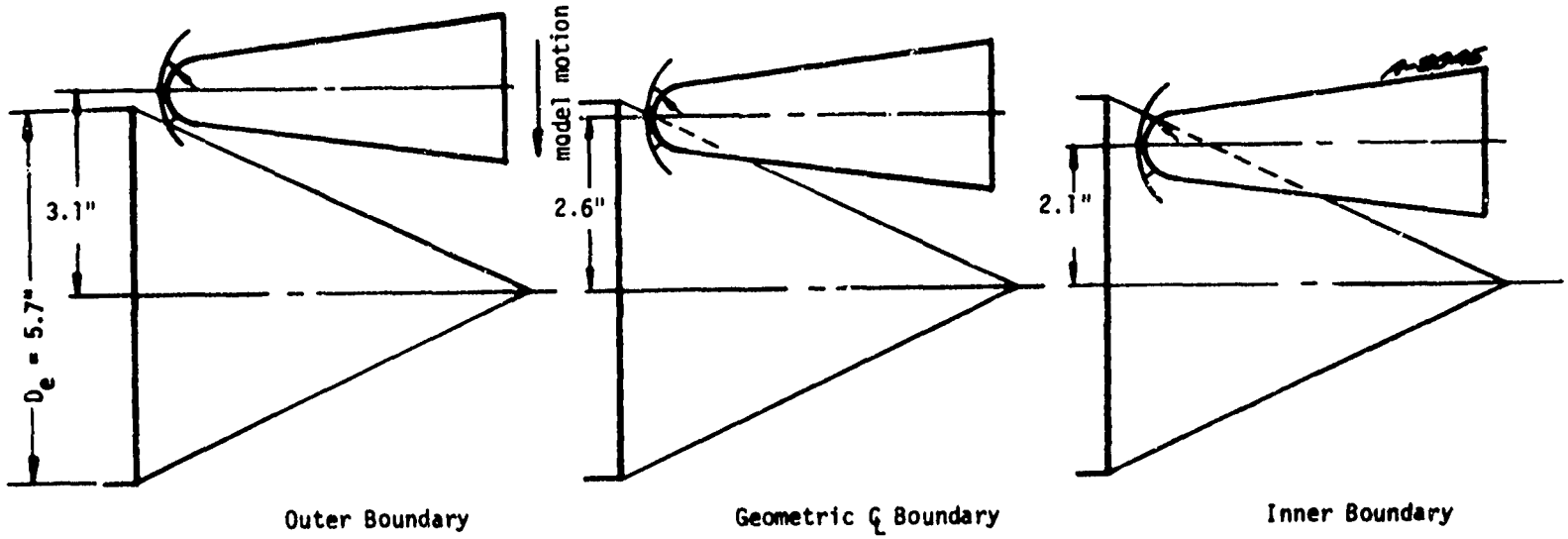

ABRES Test Condition: $M_\infty = 2.32$

Model Stand-off = 0.5 inch

Figure 6. Sequence of Model Insertion Across the Leading Edge of the Nozzle Expansion Fan

ABRES Test Condition - P_{t_2} = 100 atm, M_∞ = 2.32

Run Number 18.01

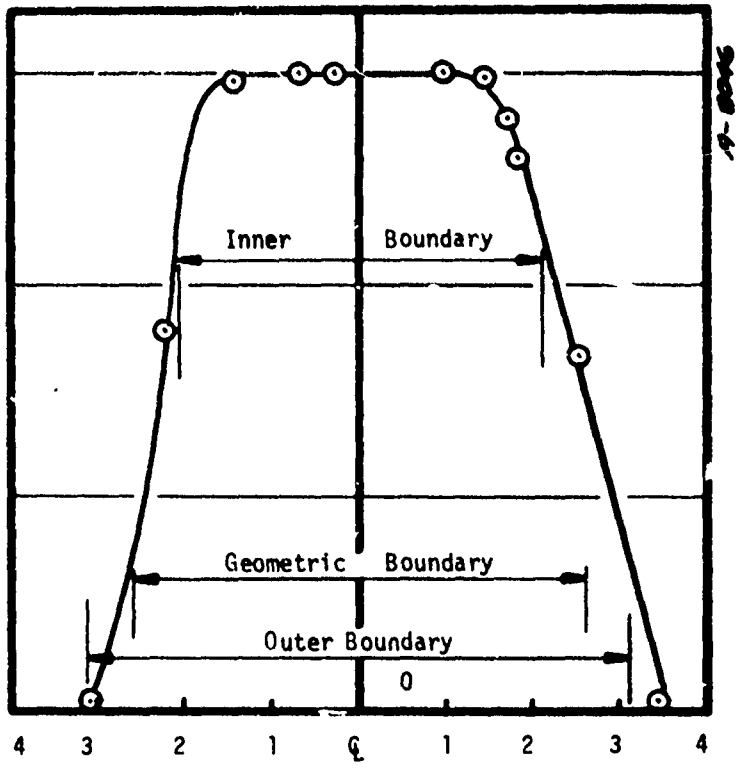

Figure 7. Comparison of Predicted Test Rhombus Boundaries with Pressure Data

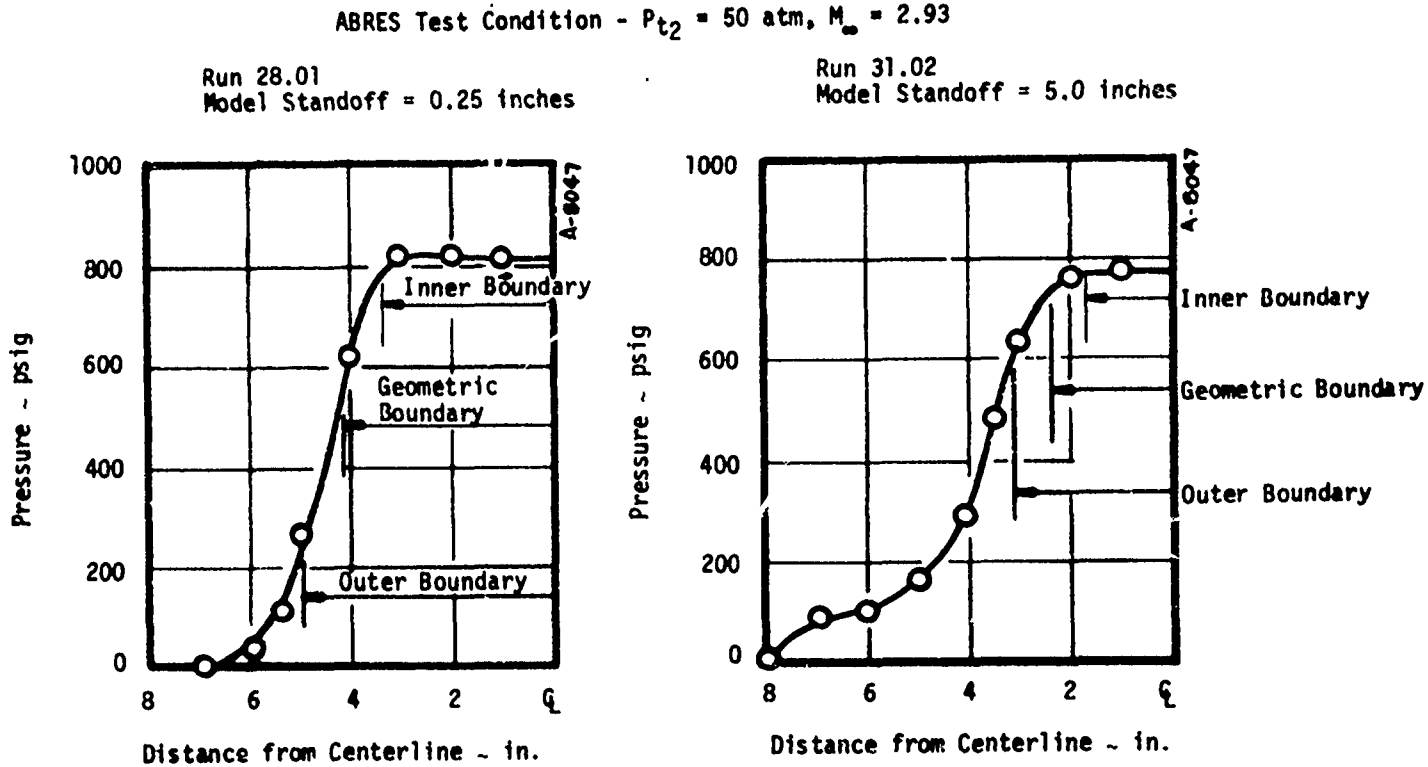

Figure 8. Comparison of Test Rhombus Pressure Profiles at Two Axial Locations within the Mach 2.93 Test Rhombus

Heating and pressure distribution data from the 1.35 inch radius calibration models discussed earlier in Sections 2.1.1 and 2.1.2 showed that the expansion flow intersected the model frustum at the approximate axial location predicted theoretically. All available calibration data from the ABRES combustion test facility conclusively demonstrate that the extent of both the Mach 2.32 and 2.93 test rhombus correspond to theoretical predictions. The theoretical test rhombus for both operational contoured nozzles are sketched in Figure 9.

2.2 FACILITY ENVIRONMENTAL GUIDELINES

Based on the calibration data analyses previously reviewed in Section 2.1, the best estimate of the aerothermal environment over a standard sphere-cone configuration (R_N = 1 inch, CHA = 7°) is presented herein. The intent of these predictions is to provide a convenient set of environmental parameters from which potential users of the facility can estimate environmental conditions for particular configurations of interest to be tested in the ABRES facility.

The predicted cold-wall heating distributions at both the Mach 2.32 and 2.93 test conditions are shown in Figure 10. The predictions were made with the ARGEIBL computer code. The propellent system assumed for these predictions was the standard N_2O_4/Aerozine-50 at a nominal O/F mixture ratio of 2.1. The test stream gas properties were defined by the ACE computer code assuming chemical equilibrium . The convective heating distribution predictions in Figure 10 are accurate, based on predicted and measured heat flux data in Section 2.1.1 with the exception of the stagnation point data. Based on the existing stagnation point calorimeter data, one would estimate that the measured cold-wall heat flux to a 1 inch radius calorimeter would be a factor of 1.5 to 2.0 times the predicted rates in Figure 10. Since these high stagnation point heat rates are possibly a result of two-dimensional conduction effects in the stagnation region, the nominal laminar ARGEIBL predictions are not known to be invalid despite these inconsistencies.

These predicted convective heating distributions are based on an assumed cold-wall (i.e., 530°R). The cold-wall enthalpy potential (based on a chamber enthalpy of 108 Btu/lbm) is -3258 Btu/lbm. This total enthalpy value is referenced to 298°K and is dependent on the injection temperature of the propellants into the combustion chamber listed below and a nominal O/F ratio of 2.1.

	Temperature (°R)	Enthalpy (Btu/lbm)
N_2O_4	530	- 91.6
Aerozine-50	530	516.7

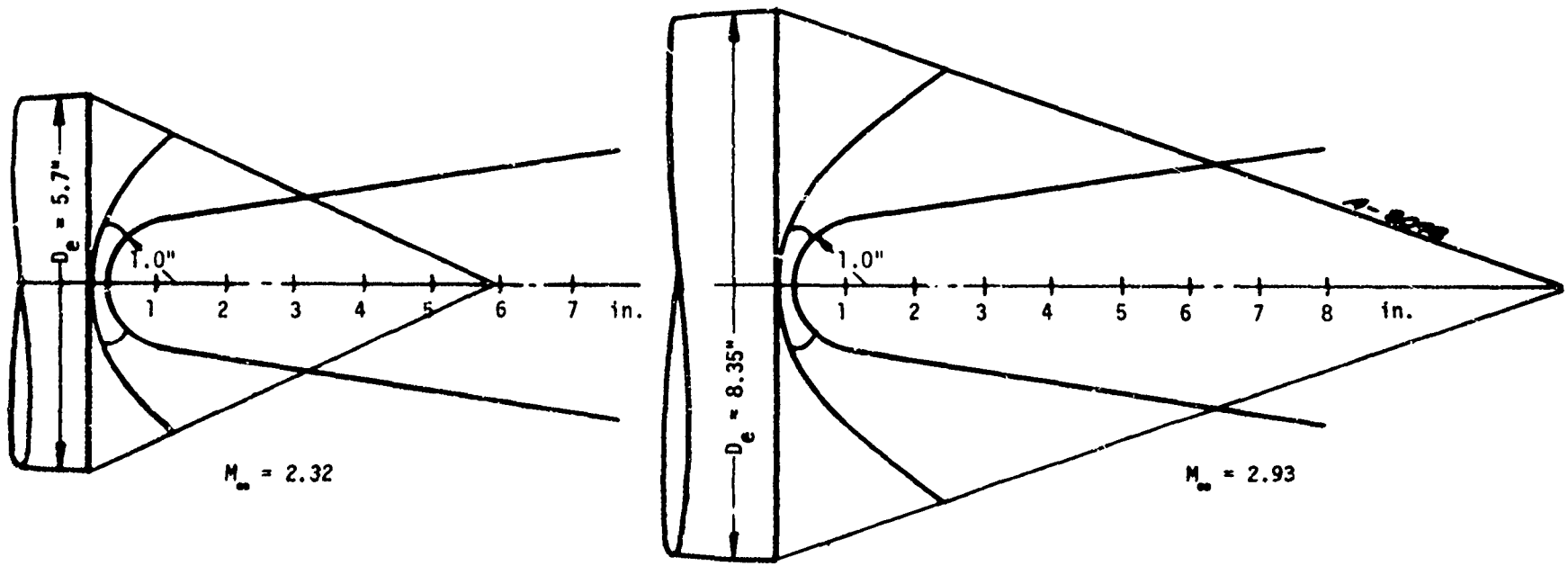

Figure 9. Theoretical Test Rhombuses for the Mach 2.32 and 2.93 Contoured Nozzle Flows in the ABRES Combustion Test

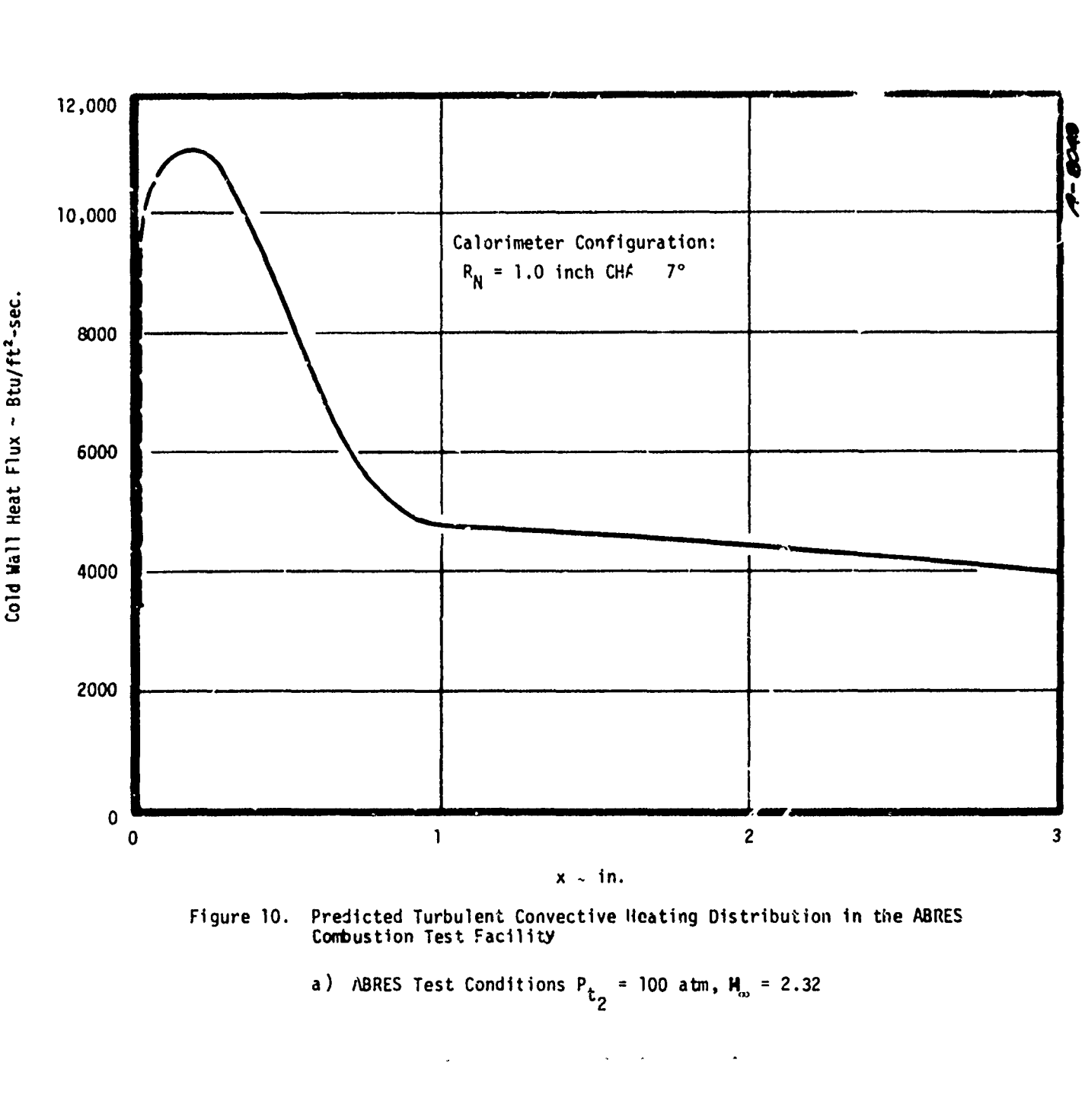

Figure 10. Predicted Turbulent Convective Heating Distribution in the ABRES Combustion Test Facility

a) ABRES Test Conditions P_{t_2} = 100 atm, M_∞ = 2.32

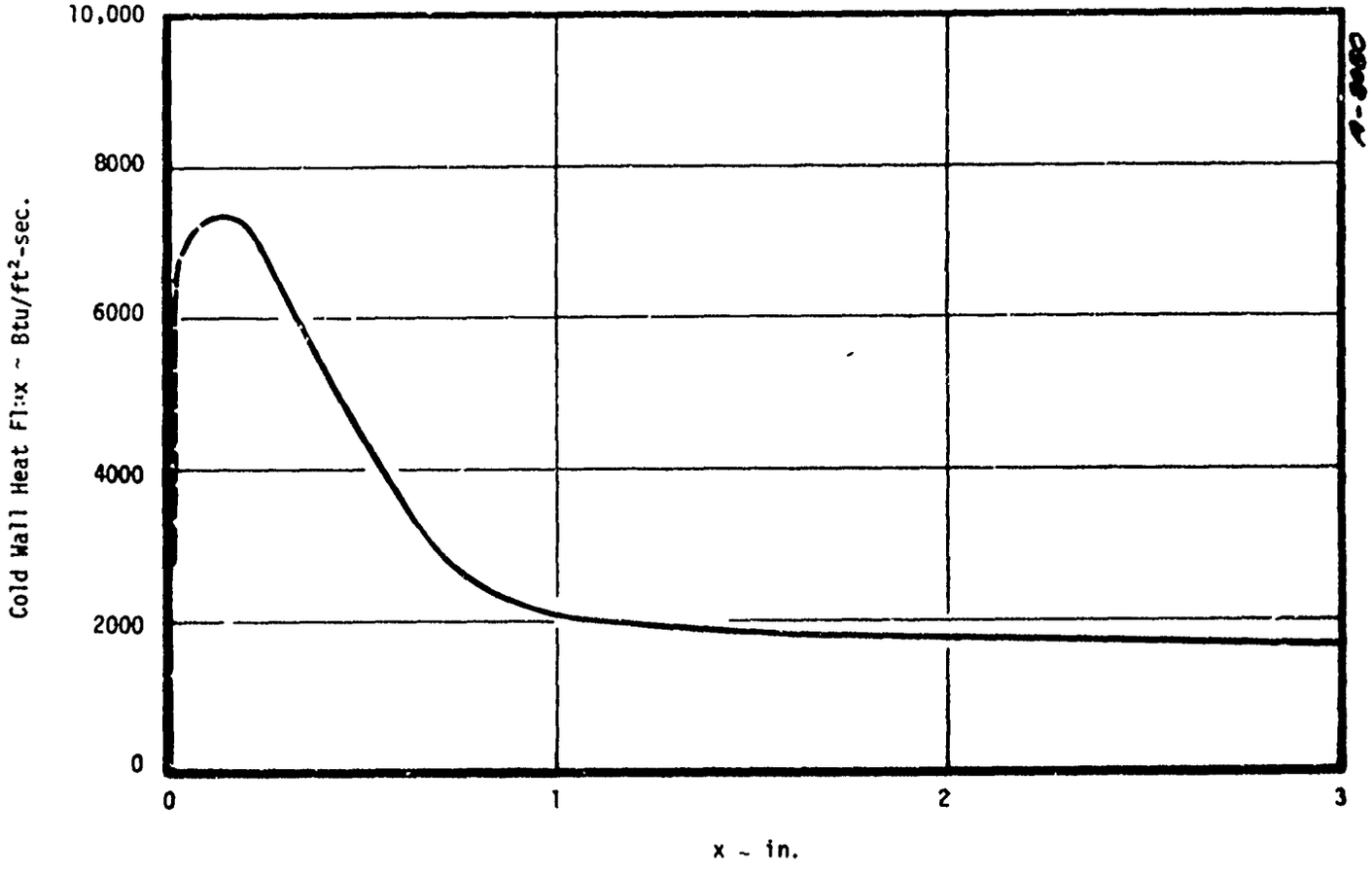

Figure 10. Concluded

b) ABRES Test Condition - P_{t_2} = 50 atm, M_∞ = 2.93

2.3 RECOMMENDED CALIBRATION MEASUREMENTS

The calibration data from the Mach 2.32 and 2.93 nozzles reviewed in Section 2.1 provide a relatively complete set of data for enterpreting these two flow conditions. The stagnation point heating data from these calibration tests do however present an anomaly which is currently not understood. Rationalization of the stagnation point heating anomaly constitutes a part of the additional calibration measurements recommended herein.

A third low Mach number nozzle is presently being fabricated for use with the ABRES facility. Calibration and test rhombus measurements of this nozzle are included in the recommended calibration measurements. The three areas of recommended calibration analyses are listed below:

1. Test rhombus calibration and definition of the "short" low Mach number nozzle flow field.
2. Rationalization of measured stagnation point convective heating rates with theoretical predictions.
3. Evaluation of the uniformity of the test stream chemical composition.

The recommended test rhombus calibration of the "short" high pressure nozzle is discussed in Section 2.3.1. Proposed analyses and calibration tests to rationalize the measured stagnation point convective heating rates are reviewed in Section 2.3.2. A test stream sampling technique to evaluate the uniformity of the test stream chemical composition is presented in Section 2.3.3.

2.3.1 Calibration of "Short" High Pressure Nozzle

The design of the "short" Mach 1.68 nozzle was motivated by the desire to maximize the test rhombus impact pressure attainable in the ABRES facility while protecting the combustion chamber and all support equipment from the highly underexpanded hyperthermal test stream. This conical nozzle which provides approximately a 3.3 inch extension from the end of the combustion chamber was deemed necessary to protect the facility from the hyperthermal exhaust products. Because of its simple conical design, the nozzle flow is complicated by the existence of imbedded shock surfaces. Estimates of the imbedded shock surfaces, based on one-dimensional supersonic gas dynamic analyses are sketched in Figure 11. The nonuniformity of the test rhombus flow caused by these imbedded shock surfaces is best resolved by carefully designed calibration measurements. Proposed calibration measurements include the following.

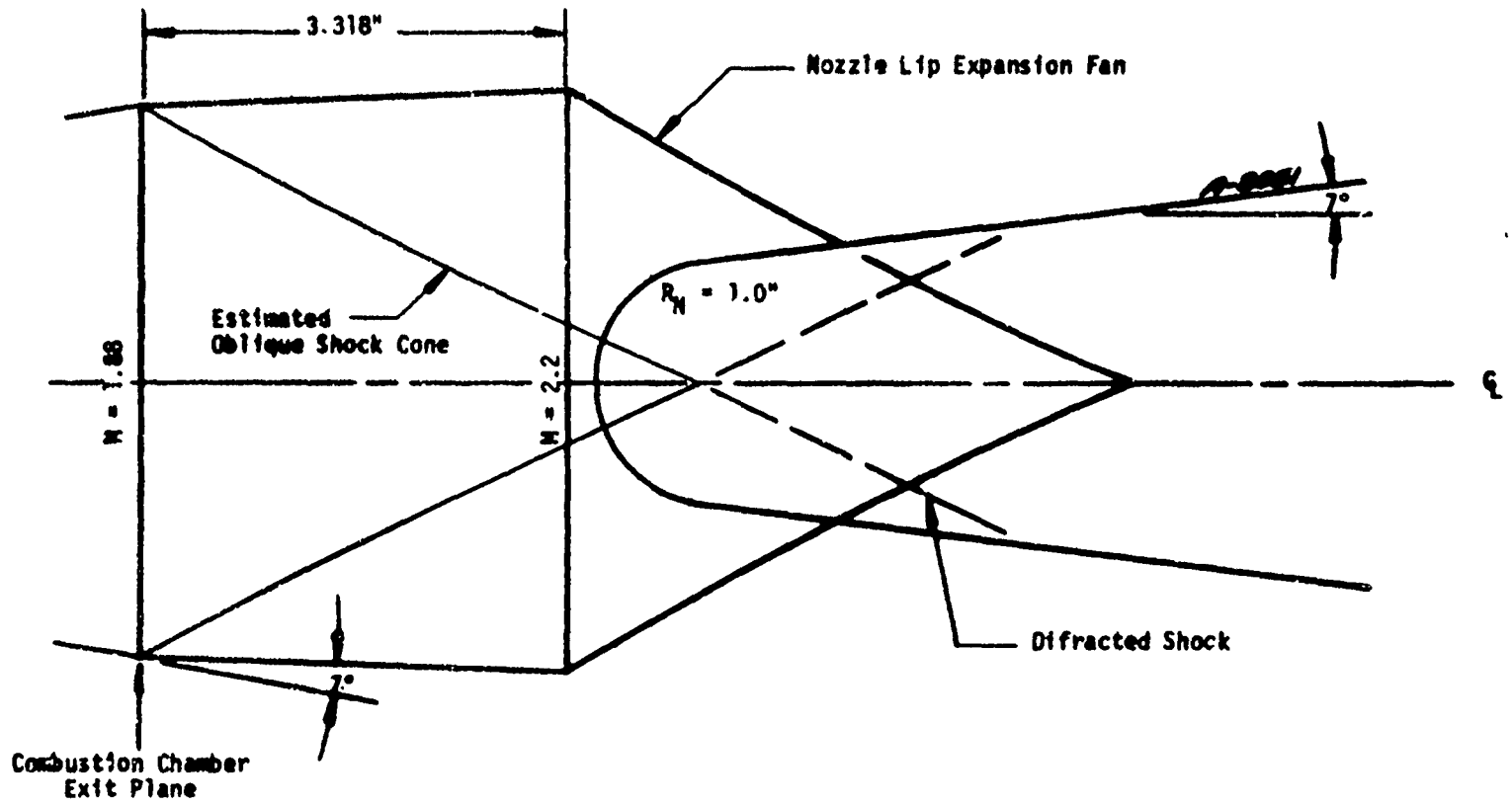

Figure 11. Sketch of "Short" Nozzle Extension to the ABRES Test Facility

1. Expose pressure calibration models with multiple ports with emphasis placed on evaluating perturbations in the pressure distribution data resulting from intersections of the imbedded shock cone boundaries with the model surface. Model configurations should be limited to two nose radii (e.g., R_N = 0.5 and 1.0 inches). Models would be exposed at different stand-off distances with the intent of obtaining sufficient data to map the imbedded shock surfaces and to evaluate their strength. This would be achieved by comparing measured pressure distributions with theoretical predictions.

2. Expose calorimeter models with multiple null point calorimeters. Calorimeter model geometries should be restricted to two nose radii (e.g., R_N = 0.5 and 1.0 inch). Calorimeter models would be exposed to the test rhombus at different stand-off distances inorder to assess the location, strength, and time stability of the imbedded shock surfaces. Calorimeter data reduction would emphasize (a) rationalization of heating distribution data with theoretical predictions and (b) assessment of the significance of anomalies in the heating distribution data in light of the imbedded shock structure.

3. Expose appropriately designed ablative models, stressing the acquisition of high speed film data of the models ablative response within the test rhombus. Gouging or unique shape change phenomena in this test configuration could be correlated with theoretical or empirically deduced nonuniformities within the test rhombus flow.

Such a series of calibration model exposures would provide the data required to qualitatively and quantatively assess the flow field environment of this "short" nozzle. A recommended calibration test matrix is given in Table 5. This calibration test series includes a total of 4 pressure and 4 calorimeter model exposures. The 2 ablation model tests proposed in this test series should provide the qualitative information required to assess the significance of the imbedded shock structures on the uniformity of the "short" nozzles test rhombus.

2.3.2 Rationalization of Stagnation Point Convective Heating Measurements

The objective of this calibration study is rationalization of the current anomaly between measured and predicted stagnation point convective heat rates. The measured stagnation point heat rates made with calorimeter models are above theoretical predictions by factors in the range 1.5 to 2.0.

TABLE 5

PROPOSED CALIBRATION TEST MATRIX FOR THE
ABRES FACILITY "SHORT" NOZZLE

Test No.	Calibration Model	R_N ~ In.	Model Stand-Off Distance ~ In.
1	Pressure	.5	0.25
2	"	.5	1.75
3	"	1.0	0.25
4	"	1.0	1.75
5	Calorimeter	.5	0.25
6	"	.5	1.75
7	"	1.0	0.25
8	"	1.0	1.75
9	Ablator	1.0	0.25
10	"	0.5	1.50

It is theorized that the high stagnation point heat rate measurements result from lateral conduction effects in the stagnation region increasing the effective heat flux to the stagnation point null point calorimeter. The two-dimensional conduction results from the severe thermal gradients in the stagnation region resulting from transition occurring near the stagnation point. Transition occurs on the relatively cold calorimeter models between the stagnation point and the 40° ray since calorimeter data at the 40° station consistently shows the flow to be fully turbulent.

The initial part of this study would analytically assess the significance of two-dimensional conduction effects on the thermal response of the stagnation point null-point calorimeter by using athe ASTHMA computer code (Reference 7). Sensitivity of two-dimensional conduction effects on the null point response would be evaluated by parametrically varying the transition location in the stagnation region, based on real gas heating distribution predictions made with the ARGEIBL computer code. In as much as these analyses do not resolve the anomaly in the measured stagnation point heat rate, additional calorimeter tests are recommended.

Three calorimeter designs are recommended. All calorimeters would be sphere-cone geometries with 7° cone half angles. The three nose radii would be 0.5, 1.0, and 2.0 inches. Each calorimeter would have multiple null points. To increase the resolution of the measured heating data in the stagnation region the "stagnation point" calorimeter on one model of each design would be shifted 10-20° from the axis of symmetry. Calorimeter measurements in this region of the stagnation point would aid in assessing the location of transition on the spherical tip and evaluating the significance of two-dimensional conduction effects in the stagnation region.

Each of the six calorimeters should be exposed to the flow at the Mach 2.32 and 2.93 test conditions. The chamber pressure would be constant at a nominal 3000 psi. This total of twelve calorimeter runs would about double the number of calorimeter exposures run to date. Interpretation of these data would emphasize understanding the measured stagnation point heat rates in light of the previous ASTHMA analyses and the laminar stagnation point heating predictions. The range of calorimeter nose radii proposed (0.5 to 2.0 inches) would be sufficient to evaluate the experimental variation of the stagnation point heat flux with nose radius.

2.3.3 Test Stream Chemical Sampling and Analyses

The proposed test stream chemical sampling and supporting thermochemical analyses would (1) evaluate the uniformity of the ABRES facility test stream and (2) analytically evaluate the effect of any perturbations in the chemical composition on the hypethermal state of the test stream. This task would be accomplished by measuring the uniformity of the test streams elemental composition and inferring variations in the thermodynamic properties based on chemical equilibrium calculations.

This test rhombus gas sampling test series would require design of a multiple port (water cooled) gas sampler probe which would contain 3 or 4 gas ports at different angular and radial locations. This would enable 3 or 4 points in the test stream to be sampled simultaneously. Both the Mach 2.32 and 2.93 test streams would be sampled. The gas samples would be analyzed elementally. Based on these data the variation in the thermodynamic state of the test stream would be calculated with the ACE computer code assuming chemical equilibrium. The state of the test gas at the various sampling points within the test rhombus would be defined assuming a constant pressure and enthalpy. Results of the ACE analyses would show variations in the test stream temperature field caused by nonuniformities in the elemental composition within the test stream. These results would be rationalized with available calorimeter data to assess the significance of the test stream nonuniformities on the facilities nominal hyperthermal environmental test conditions.

SECTION 3

ABRES FACILITY APPLICATION STUDIES

Reentry environments of interest are characterized in terms of the high pressure hyperthermal properties of air. Relating the environmental test conditions within the ABRES combustion facility to those of air during reentry is complicated by the fact that the elemental composition of the ABRES test gas is different than air. The current propellant combination burned in the ABRES facility yields a significant amount of H_2O and CO_2 in the test stream. The predominance of these species within the exhaust gas make the ABRES environment much more corrosive than air. This characteristic, coupled with the relatively low combustion temperature (e.g., T_c = 6250°R) results in a relatively low graphite ablation temperature. Peak graphite ablation temperatures are in the range 4000-4500°R. Thus, significant differences in the aerothermal environment and graphitic material thermal response exist between the ABRES facility test environment and reentry.

The degree of flight simulation currently achieved with graphite ablation tests in the ABRES facility is analyzed in this section. Three aspects of high pressure hyperthermal graphite ablation tests within the ABRES facility are addressed herein:

Thermostructural Simulation

Reentry Sumilation

Nosetip Transition and Ablation/Shape Change

The level of thermostructural simulation achieved in the ABRES facility relative to flight is reviewed in Section 3.1. The level of reentry simulation achieved in the ABRES facility is discussed in Section 3.2. The ablation shape-change response of models tested in the ABRES facility compared to that achieved in the AEDC aeroballistic range and the AFFDL 50 MW RENT arc are reviewed in Section 3.3.

3.1 SIMULATION ACHIEVED IN NOSETIP THERMOSTRUCTURAL TESTS

The intent of thermostructural proof tests of flight scale hardware is to generate the peak strain conditions predicted for flight in ground test facilities. Such tests serve to establish the validity of design criteria used to design graphitic nosetip systems. Evaluation of the level of reentry

thermostructural simulation achieved in any ground test facility is difficult to generalize. The thermostructural response of graphitic materials is strongly dependent on the specific environmental history imposed on a specific material configuration. To facilitate this evaluation of the thermostructural simulation achieved in the ABRES facility compared to flight, a nominal nosetip configuration and two typical reentry trajectories were selected to establish flight levels of the important material response parameters. The material response parameters used to assess the level of thermostructural simulation in the ABRES test envirnment are defined in Section 3.1.1. Results of the evaluation based on these material response criteria are presented in Section 3.1.2. Conclusions regarding the degree of thermostructural simulation achieved in the ABRES facility are discussed in Section 3.1.3

3.1.1 Thermostructural Simulation Criteria

It was not within the scope of this study to make complete thermostructural material response calculations for the flight and ABRES test environments. Due to this limitation, material ablation response criteria were selected which allowed one to relate the thermostructural similarity between flight and ABRES tests. The material response parameters selected to evaluate the degree of thermostructural similitude between flight and ABRES tests were (1) surface temperature (2) surface conductive flux into the material and (3) surface recession rate. If the surface temperature history and surface conductive flux are simulated then the thermal strains are equivalent. However if the surface temperature and indepth conductive flux histories are not similar it is difficult to quantitatively evaluate the level of thermostructural simulation. Despite these limitations one can generally relate high temperatures and high conductive fluxes with potentially high thermal strains. It is this level of comparative analyses which is used in this evaluation.

The two flight trajectories selected for these analyses are summarized in Figures 12 and 13. Trajectory A in Figure 12 is a moderate flight trajectory ($\beta \sim 1500$ lb/ft^2) characteristic of current flight tests. The stagnation point environmental parameters for this trajectory (based on a one inch radius sphere) presented in Figure 12 show a peak pressure slightly above 120 atmospheres and a peak cold wall heat flux of 11,000 Btu/ft^{2}sec. Trajectory B summarized in Figure 13 is a relatively severe trajectory ($\beta \sim 5000$ lb/ft^2) characteristic of advanced reentry flight. The stagnation point environmental parameters for this trajectory (based on a one inch radius spherical tip) show a peak pressure in excess of 200 atmospheres and a peak cold wall heat flux of about 18,000 Btu/ft^{2}sec. Trajectories A and B which bound flight environments of interest were selected to facilitate a more objective comparison of graphitic nosetips response in flight and ABRES tests.

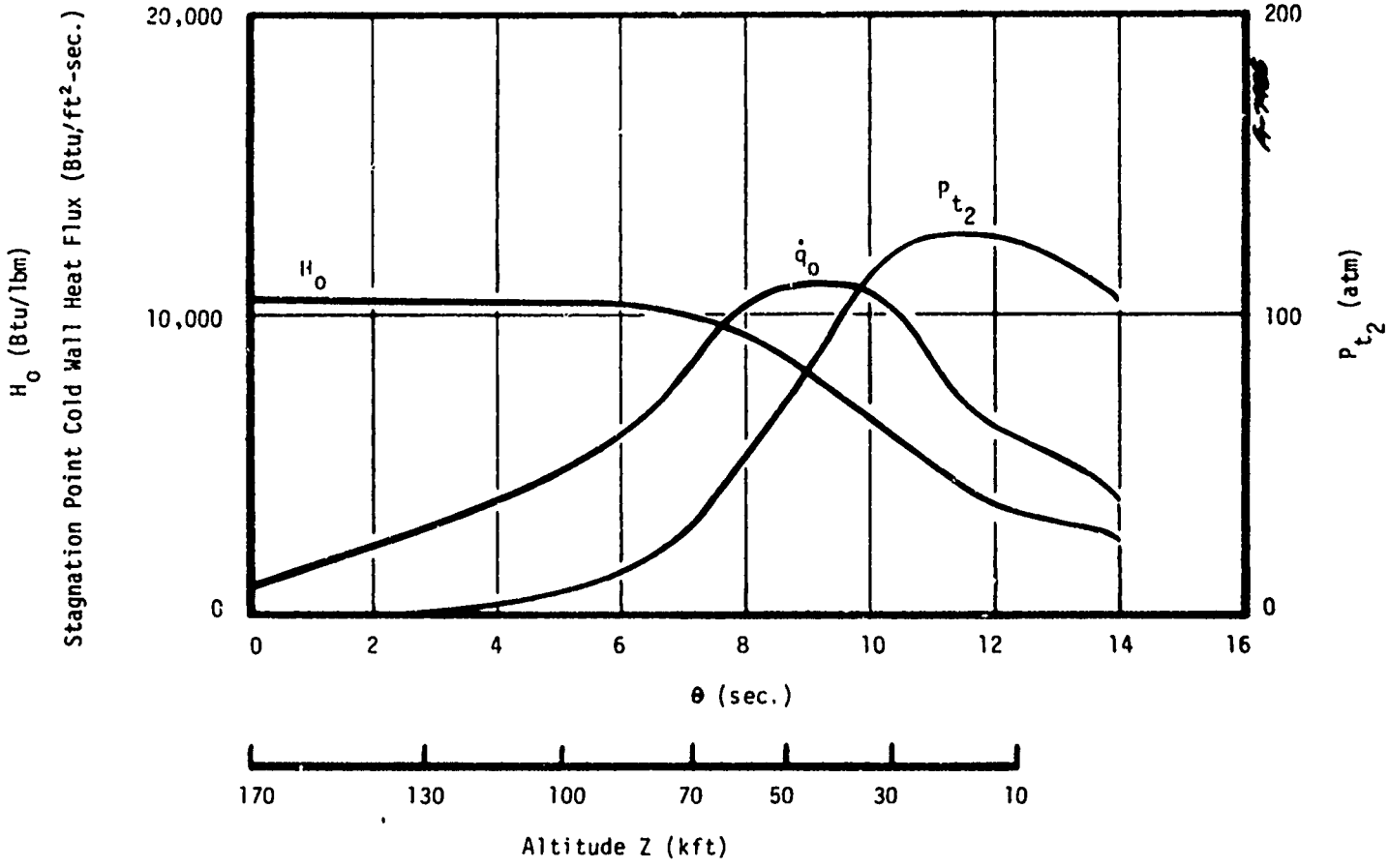

Figure 12. Trajectory A, Stagnation Point Environmental Parameters for a 1.0 in. Radius Spherical Tip

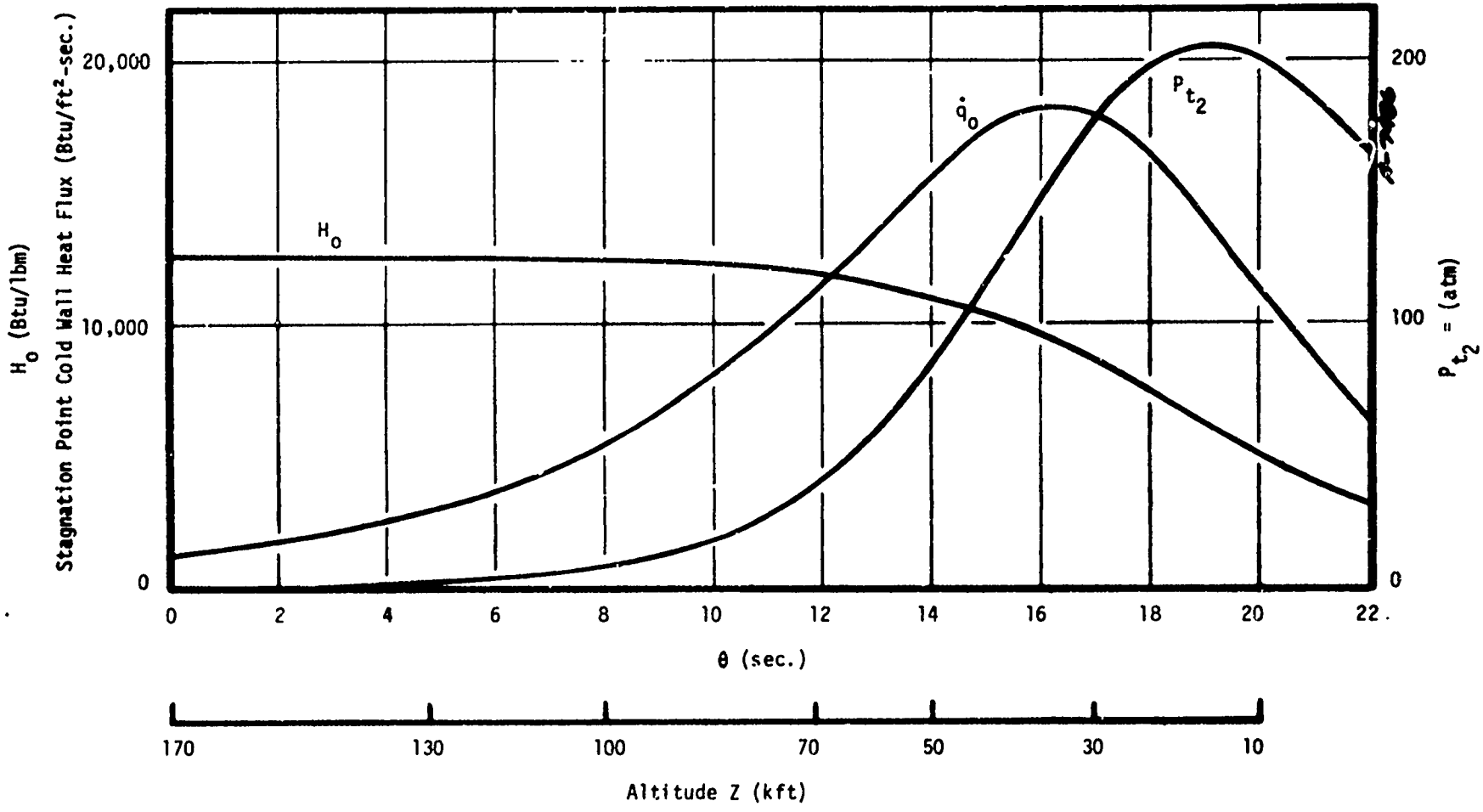

Figure 13. Trajectory B, Stagnation Point Environmental Parameters for a 1.0 inch Radius Spherical Tip

A nominal sphere-cone shell configuration (R_N = 1.0 inch, CHA = 9°) was selected for these analyses. Three body stations were selected for analysis (1) stagnation point (2) tangency point and (3) a frustum station at an axial distance of about 4 inches from the stagnation point. The rational for selecting these three body stations for analysis of the materials thermal response are reviewed below.

1. The stagnation point and tangency point provide the two extremes of surface temperature response on the spherical region of the tip. The peak pressure at the stagnation point results in the peak ablation temperature occuring at this point on the spherical tip despite the fact that the peak heat flux occurs at the sonic point during turbulent flow conditions. The tangency point experiences the minimum convective heat flux and the minimum ablation temperature on the spherical tip.

2. For a shell nosetip configuration with a nominal 4-6 inch overhang, the location of peak strains occurs within the overhang about 3 to 4 inches back from the stagnation point. Thus a frustum location 4 inches back from the stagnation point was selected for these analyses.

The Mach 2.93 test condition was used for these analyses since this nozzle provides the largest test rhombus.

The analytical procedures employed for these ABRES facility ablation response analyses are outlined below.

1. The ACE computer code (Reference 6) was used to generate (1) test stream gas properties assuming chemical equilibrium and (2) general ablation solutions for graphite ablation in the ABRES test stream assuming equilibrium/diffusion controlled heterogenous reactions. The equilibrium test stream properties were input into the ARGEIBL computer code. The generalized ablation tables were input into the CMA computer code.

2. The ARGEIBL code (Reference 4) was used to define the smooth wall aerothermal environment over the entire surface of the nominal sphere cone configuration specified above. This code predicted the convective heat and mass transfer distribution over the entire nosetip surface.

3. The materials ablation response at each of the three locations was predicted with the CMA computer code (Reference 8). This code predicts the materials transient ablation response, based on a one-dimensional indepth conduction and surface ablation solution.

A similar procedure was used to predict the material ablation response for both flights with the following exception.

The smooth wall aerothermal environmental parameters for both flights was predicted with the SAANT computer code (Reference 9). For a given trajectory, this computer code predicts the convective heating environemnt over an entire reentry configuration. Generally the SAANT code is used to predict nosetip ablation shape change response during reentry; however, these environmental predictions were based on the initial shape with no shape change. The in-depth material response predictions were based on thermophysical properties of ATJ-S graphite.

3.1.2 Ablation Results

Results of these analyses are summarized in Figures 14 through 16. Figure 14 compares the surface temperature response predictions at the three nosetip locations with both flight predictions. A nominal ABRES test time of 10 sec. was assumed for these analyses. The peak surface temperatures predicted for the ABRES tests are in the range 3000 to 4000°R, which are 3000 to 4000°R below the corresponding peak temperatures predicted for flight. The predicted surface temperature rise rate in the ABRES facility is certainly much higher than the rise rate predicted for flight. The effect of this difference on the induced thermal strains is difficult to assess. Figure 15 compares the predicted energy storage within the solid for the three nosetip locations. In each case the integrated conductive flux into the material predicted for the ABRES facility tests is less than half that predicted for the mild flight environment. The predicted time rate variation of this parameter in the ABRES facility for the initial 5 seconds of exposure is similiar to that predicted for flight. However, this rate of energy flux into the material does not persist for an extended time period in the ABRES facility. Figure 16 compares the predicted surface recession histories for both flights with the corresponding surface recession rate predictions in the ABRES environment. It should be emphasized that both flight and ground test recession rate predictions are low since the analyses are based on an assumed smooth wall thermochemical ablation model. The predicted stagnation point recession rate in the ABRES environment is less than half of the peak flight recession rates. The predicted ABRES recession rates at the tangency point and frustum body points are comparable to the predicted flight recession rates. This results from the relatively low Mach number and highly oxidizing environment in the ABRES facility.

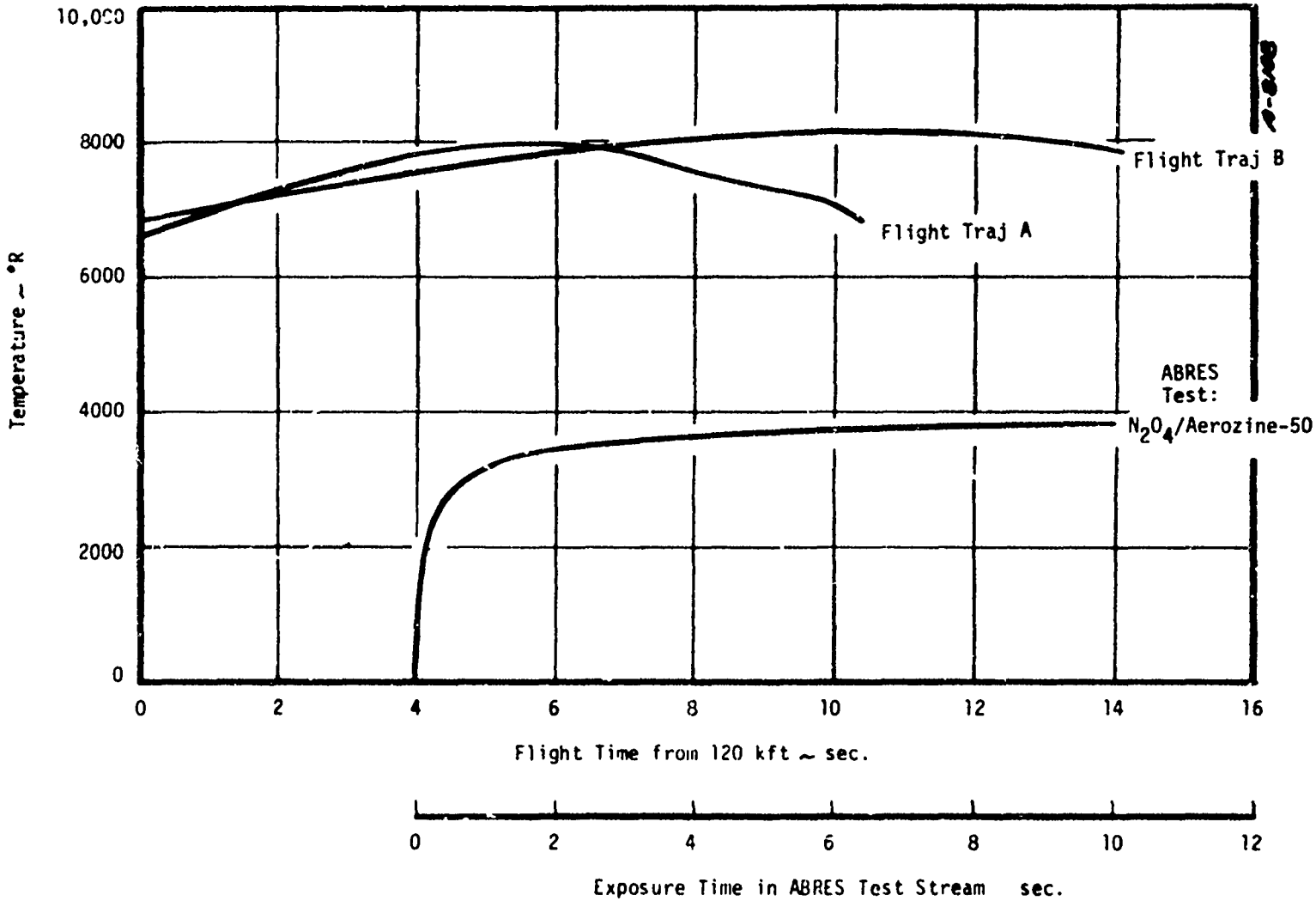

Figure 14. Comparison of Predicted Graphite Ablation Temperature Response in the ABRES Facility with Flight

a) Stagnation Point

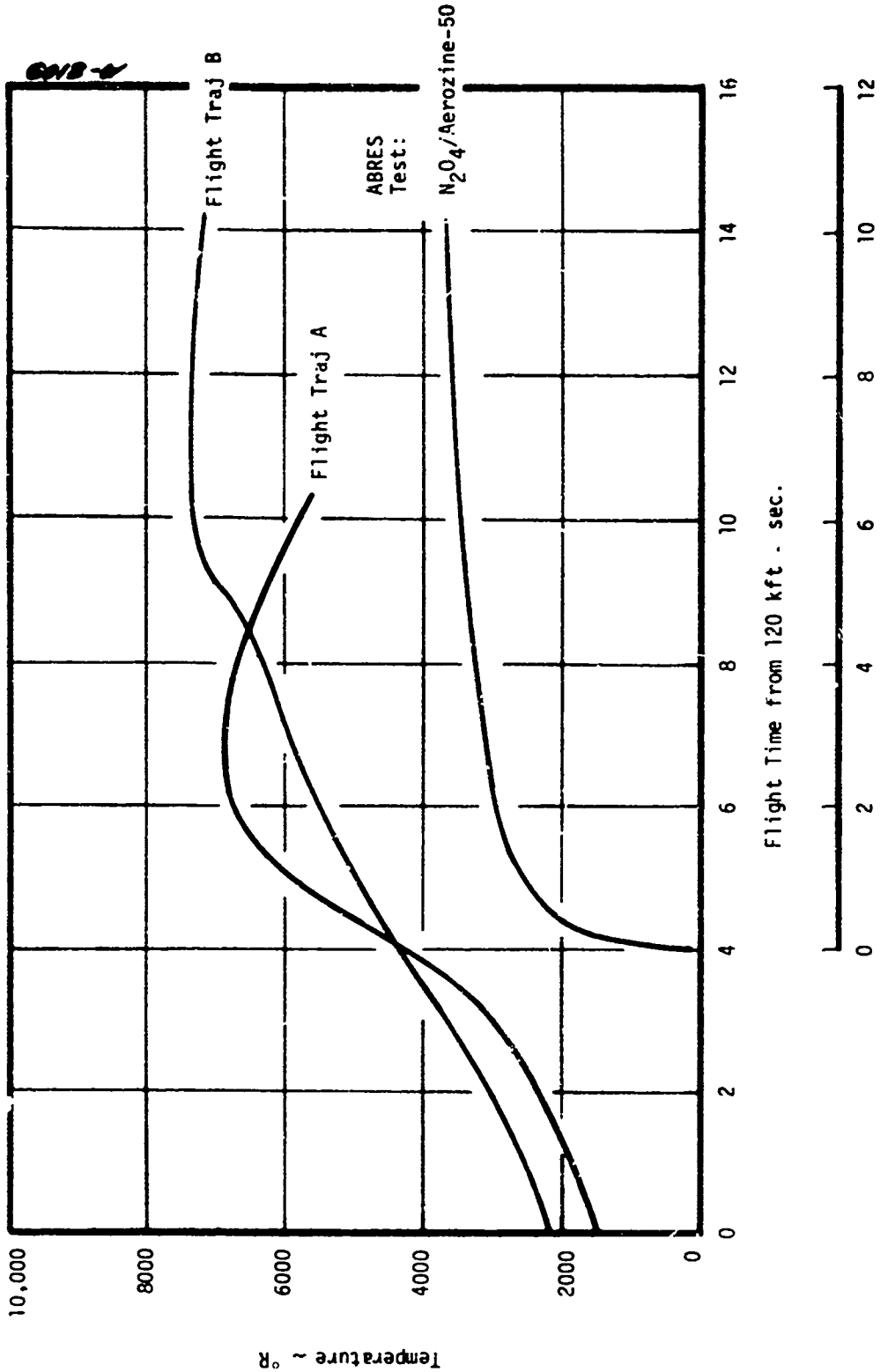

Figure 14. (Continued)
b) Tangency Point (S/R_N = 1.41)

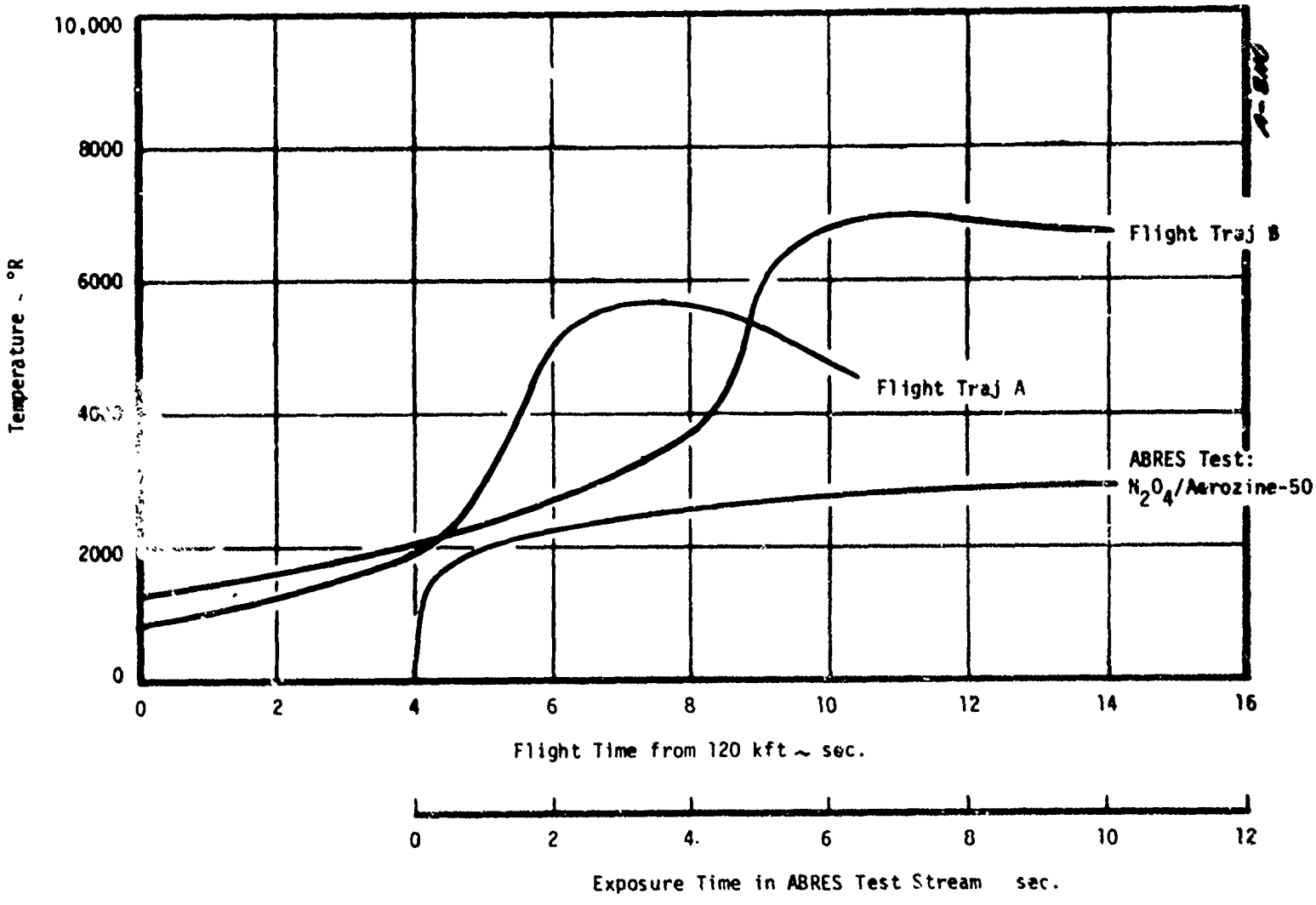

Figure 14. (Concluded)

c) Frustum Body Point (S/R_N = 4.6)

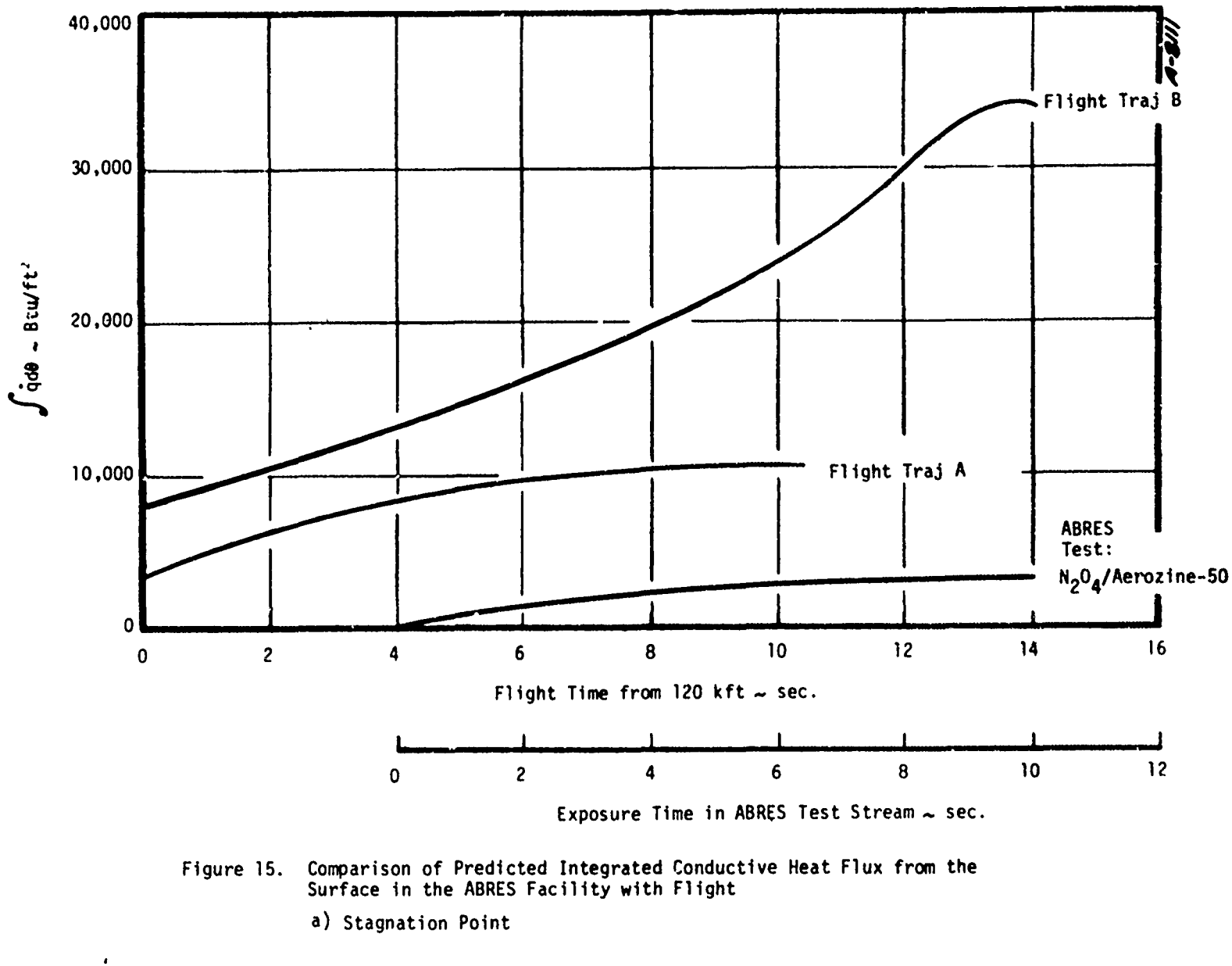

Figure 15. Comparison of Predicted Integrated Conductive Heat Flux from the Surface in the ABRES Facility with Flight

a) Stagnation Point

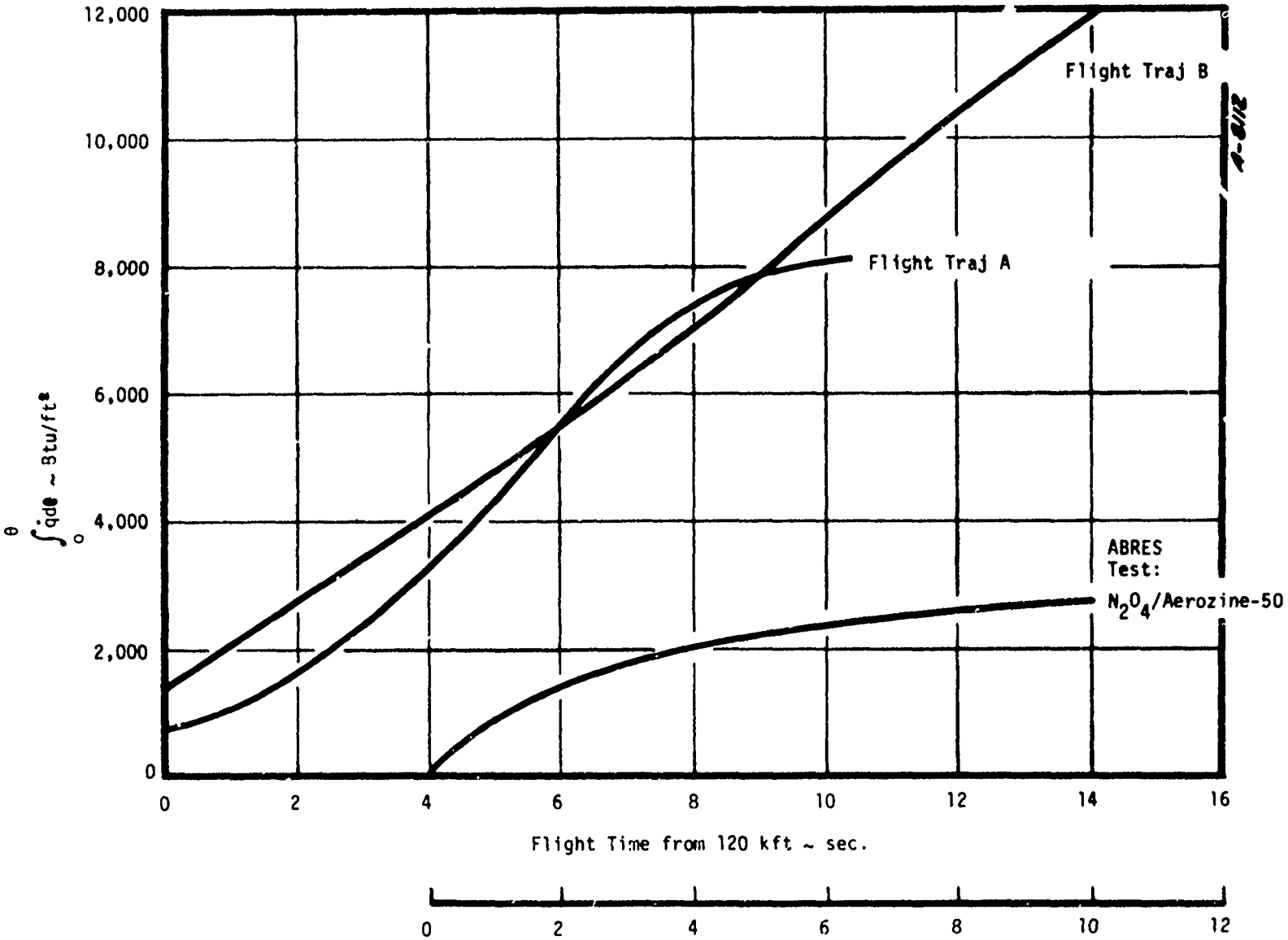

Figure 15 (Continued)

b) Tangency Point (S/R_N = 1.41)

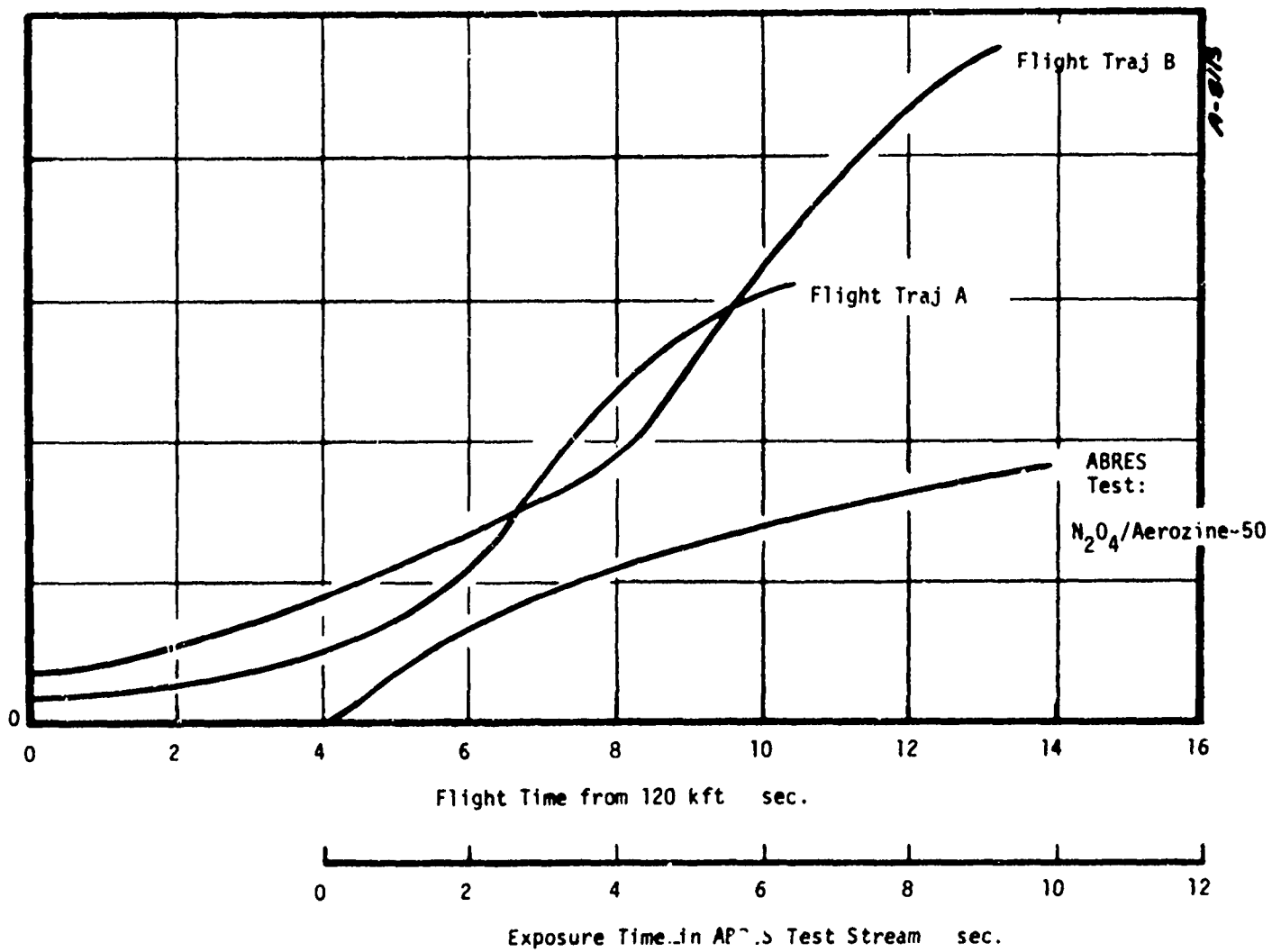

Figure 15 (Concluded)

c) Frustum Body Point (S/R_N = 4.6)

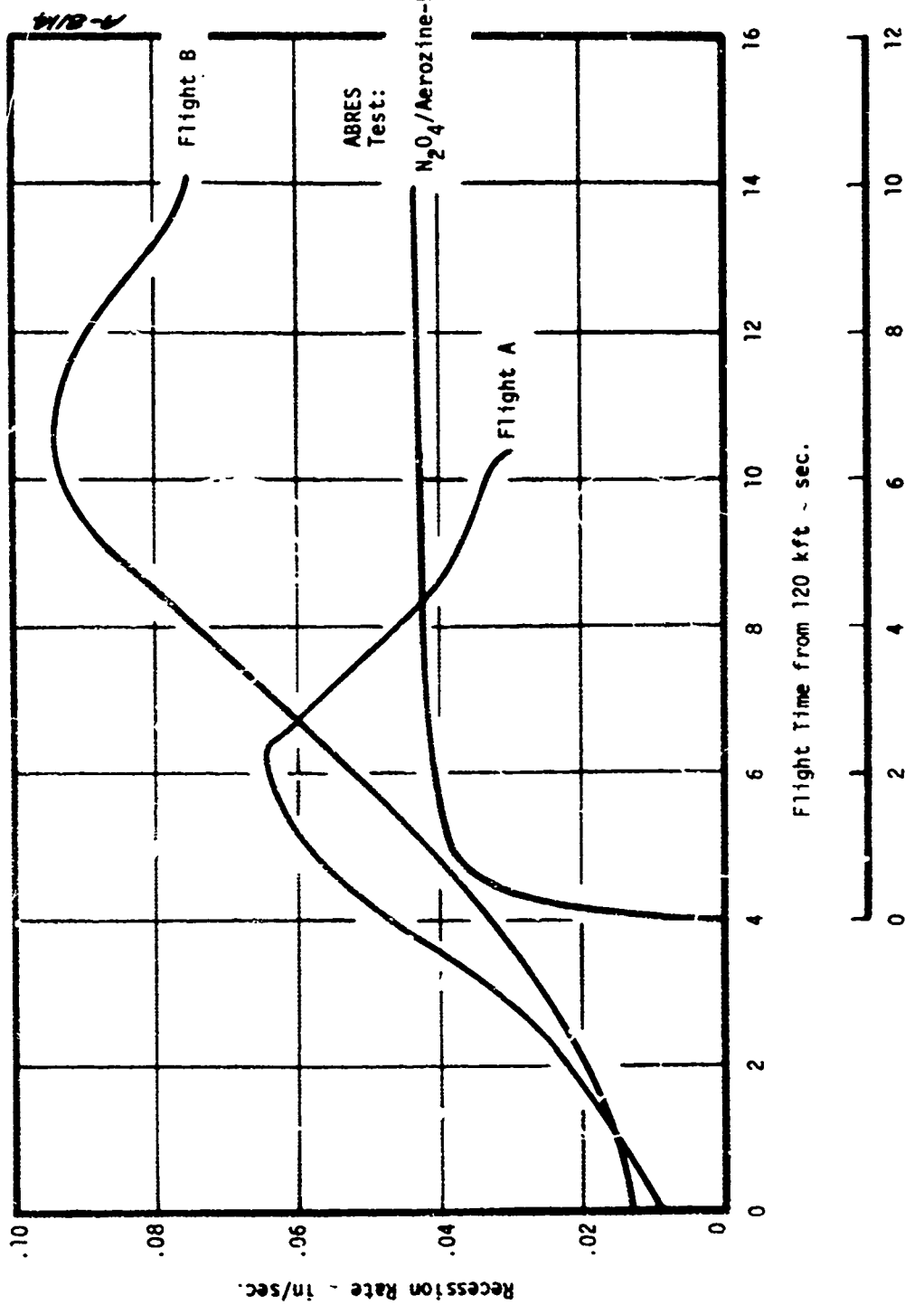

Figure 16. Comparison of Predicted Graphite Surface Recession Rates in the ABRES Facility with Flight
a) Stagnation Point

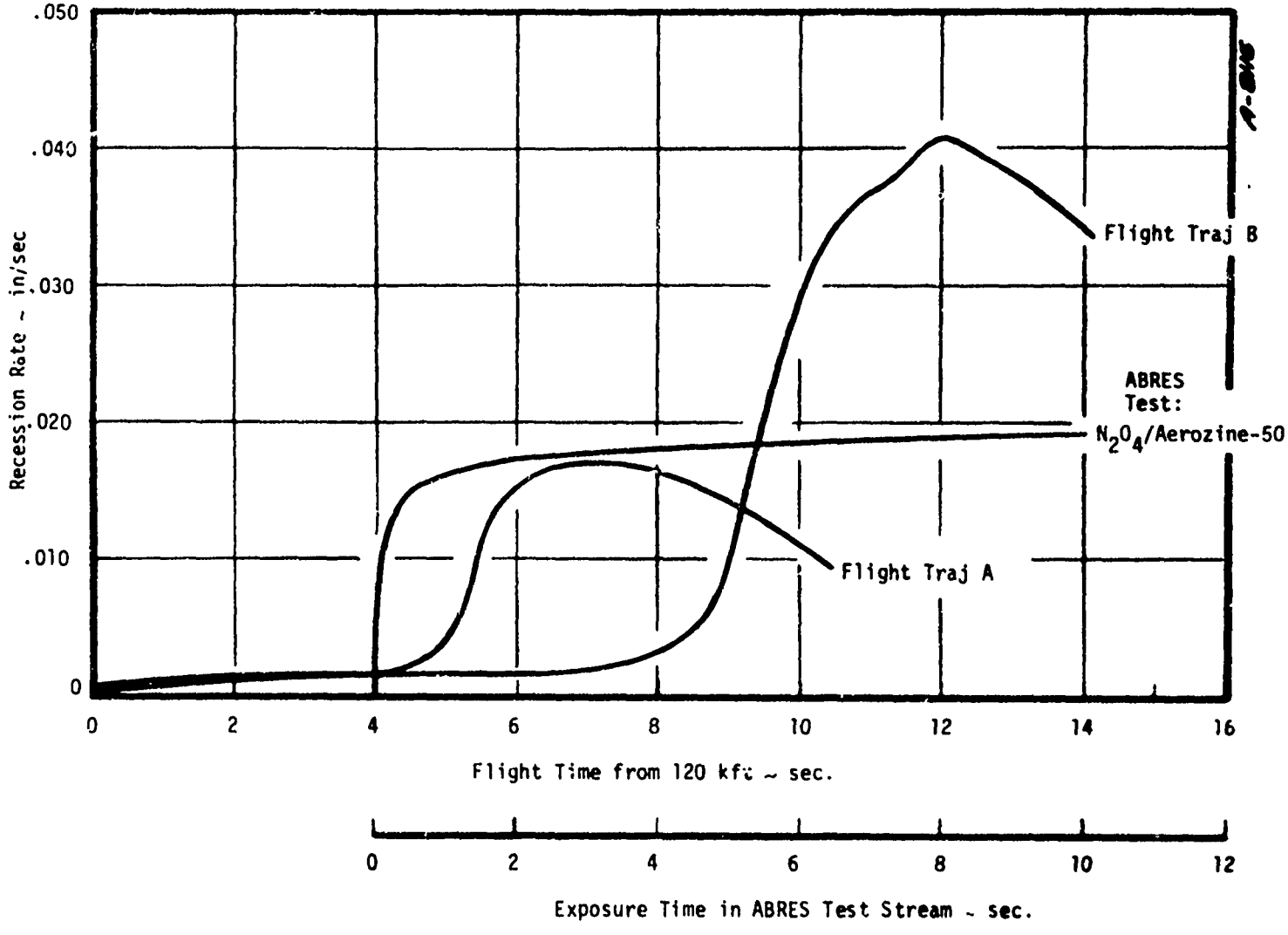

Figure 16. (Continued)

b) Tangency Point (S/R_N = 1.41)

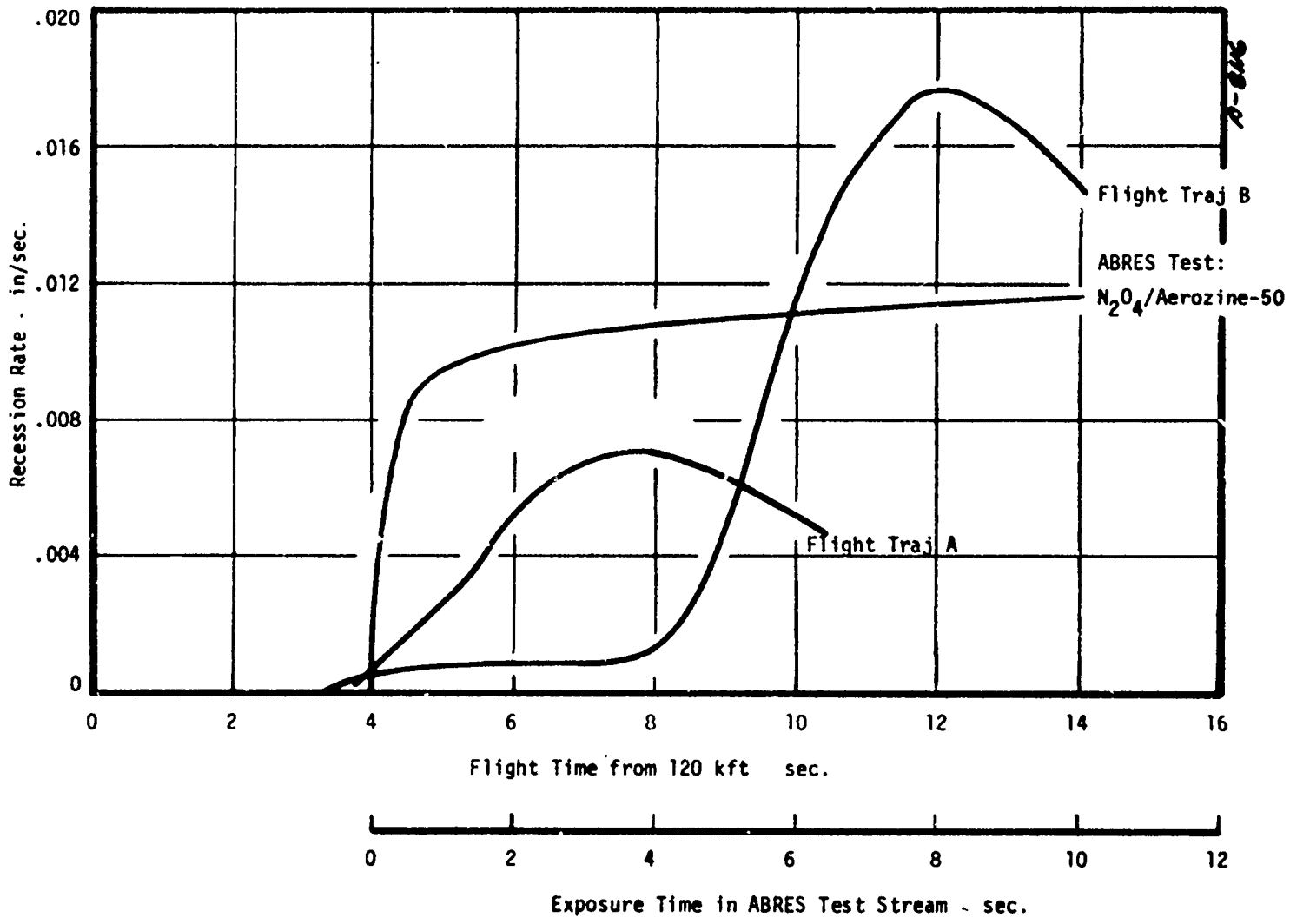

Figure 16. (Concluded)

c) Frustum Body Point (S/R_N = 4.6)

Conclusions drawn from these results regarding the degree of thermostructural simulation are subsequently reviewed in Section 3.1.3.

3.1.3 Conclusions

Based on the ablation predictions reviewed in the previous section it is readily apparent that the severity of the aerothermal environment in the ABRES facility is far below that for flights of interest. Peak graphite ablation temperatures in the ABRES facility are about half of the nominal 8000°R peak for flight. Without the benefit of complete thermostructural calculations it is difficult to quantify the level of similitude achieved with thermostructural tests in the ABRES combustion test facility. In spite of this limitation one concludes that the level of thermostructural simulation achieved with flight is low if the peak ablation temperature in the ABRES facility is 3000 to 4000°R below peak flight values. If thermal strain limits are exceeded in a nominal shell configuration it would occur as a result of the step nature of the ABRES environment although this is unlikely due the thin region of material effected during the initial transient response. It is not possible to comment further on this phenomena since the thermal shock characteristic of the ABRES environment was not quantitatively investigated in this study. In summary one must conclude that the ABRES combustion test facility with the current propellant combination does not provide a sufficiently severe hyperthermal environment to simulate the thermostructural response of graphitic nosetips in flight.

3.2 SIMULATION ACHIEVED WITH RESPECT TO REENTRY

Reentry simulation as interpreted herein implies that the nosetip ablation response should simulate the material ablation and shape change response characteristic of reentry. This implies that the surface temperature, transition, ablation shape change, and total exposure time should simulate that which is characteristic of flight. Reentry simulation implies thermostructural simulation, but the converse is not true since flight levels of thermal strains are currently achieved in subsonic shroud hyperthermal test facilities with no degree of reentry simulation.

The graphite ablation response predictions for the two flight trajectories and the high Mach number ABRES environment compared in Section 3.1.2 are interpreted in this section with respect to the level of reentry simulation achieved with ABRES tests. The comparison of flight and ABRES test environment graphite ablation predictions summarized in Figures 14 through 16 illustrate the following:

1. The maximum graphite ablation temperatures generated in the ABRES combustion test facility are 3000 to 4000°R below peak flight values.

2. The predicted conductive flux from the ablating surface in the ABRES facility is consistently below flight values by factors of 1.5 to 4. over the entire nosetip. This result suggests the level of flight thermostructural simulation achieved in ABRES tests is low, although it can not be quantified.

3. Predicted graphite recession rates in the ABRES test environment are less than half peak flight values in the stagnation region. Predicted recession rates on the frustum surface are above predicted rates for the moderate trajectory and below the peak rates predicted for the severe trajectory. Relative to the stagnation region recession rate predictions, the predicted rates in the low pressure regions of the tip are high. Thus the shape change predicted for the ABRES tests would be dissimilar to that predicted for flight. This results from different thermochemical ablation phenomena in ABRES and the lower Mach number flow in ABRES relative to flight.

The most restrictive features of current graphite ablation tests in the ABRES combustion test facility are (1) the relatively low total temperature (6250°R) and (2) the relatively high concentration of oxidizing species (CO_2 and H_2O) in the test stream. This combination of environmental conditions serves to maximize the surface recession rate of graphitic materials at a relatively low surface ablation temperature compared to flight. This combination of material response phenomena for graphitic materials in the ABRES facility is quite dissimilar to the material response in flight. Thus graphite ablation tests in the ABRES combustion test facility do not presently provide a good simulation of reentry ablation response.

3.3 NOSETIP TRANSITION AND ABLATION (SHAPE CHANGE) IN THE ABRES FACILITY COMPARED WITH OTHER HYPERTHERMAL TEST FACILITIES

This section reviews and compares the high pressure hyperthermal ablation test conditions currently available in the AEDC Aeroballistic Range, the AFFDL 50 MW RENT arc, and the AFRPL ABRES Combustion Test Facility. This comparison emphasizes the steady ablation shapes which develop at the peak Reynolds number test conditions in each facility. The ablation shapes which develop in ground test facilities should compare with ablation shapes characteristic of flight.

Results of the low temperature ablator (LTA) tests in hypersonic flow (M_∞ = 5) show that the steady turbulent ablation shape which develops on sphere-cone models can be categorized by three distinct turbulent shapes sketched in Figure 17. The three nosetip shapes in Figure 17 are defined as (1) slender (2) intermediate and (3) blunt turbulent. At the hypersonic test conditions in NOL tunnel 8 these steady shapes were found to correlate well with the initial transition location on the spherical tip. These results are summarized below:

Turbulent Steady Shape	Transition on Sphere
Slender shape	$S/R_N \geq .5$
Intermediate shape	$.3 \leq S/R_N < .5$
Blunt turbulent shape	$S/R_N < .3$

Therefore, based on these LTA shape change results in hypersonic flow transition should occur forward of $S/R_N = 0.3$ on the sphere for a blunt turbulent shape to develop.

High pressure ablation tests should provide a sufficiently high Reynolds number flow to insure development of a fully turbulent biconic shape, since this shape is most representative of predicted shapes during intervals of peak heating in reentry. Environmental parameters corresponding to the nominal and high pressure operating conditions in the three ablation test facilities are summarized in Table 6. The transition predictions in Table 6 are based on a 0.25 inch radius sphere-cylinder for the 50 MW and ballistic range and a 1 inch radius sphere-cone (CHA = 9°) assuming a nominal 0.4 mil surface roughness height (ATJ-S graphite) and the transition correlation described in Reference 10. Highlights from this summary regarding the test stream Reynolds number regimes and predicted transition locations on the spherical tips in the three high pressure ablation test facilities are summarized below.

1. The sonic point Reynolds number on a one inch radius sphere at the low Mach number test condition is more than a factor of five greater than the peak sonic point Reynolds number on a 0.25 inch radius sphere in both the 50 MW arc and the ballistic range.

2. The higher Mach number and higher pressure in the ballistic range cause the predicted transition location on the 0.25 inch radius spherical tip to be near the predicted transition location on the 1 inch radius sphere in the ABRES test stream. Predicted transition locations in both the ballistic range and ABRES facility is forward of $S/R_N = 0.3$.

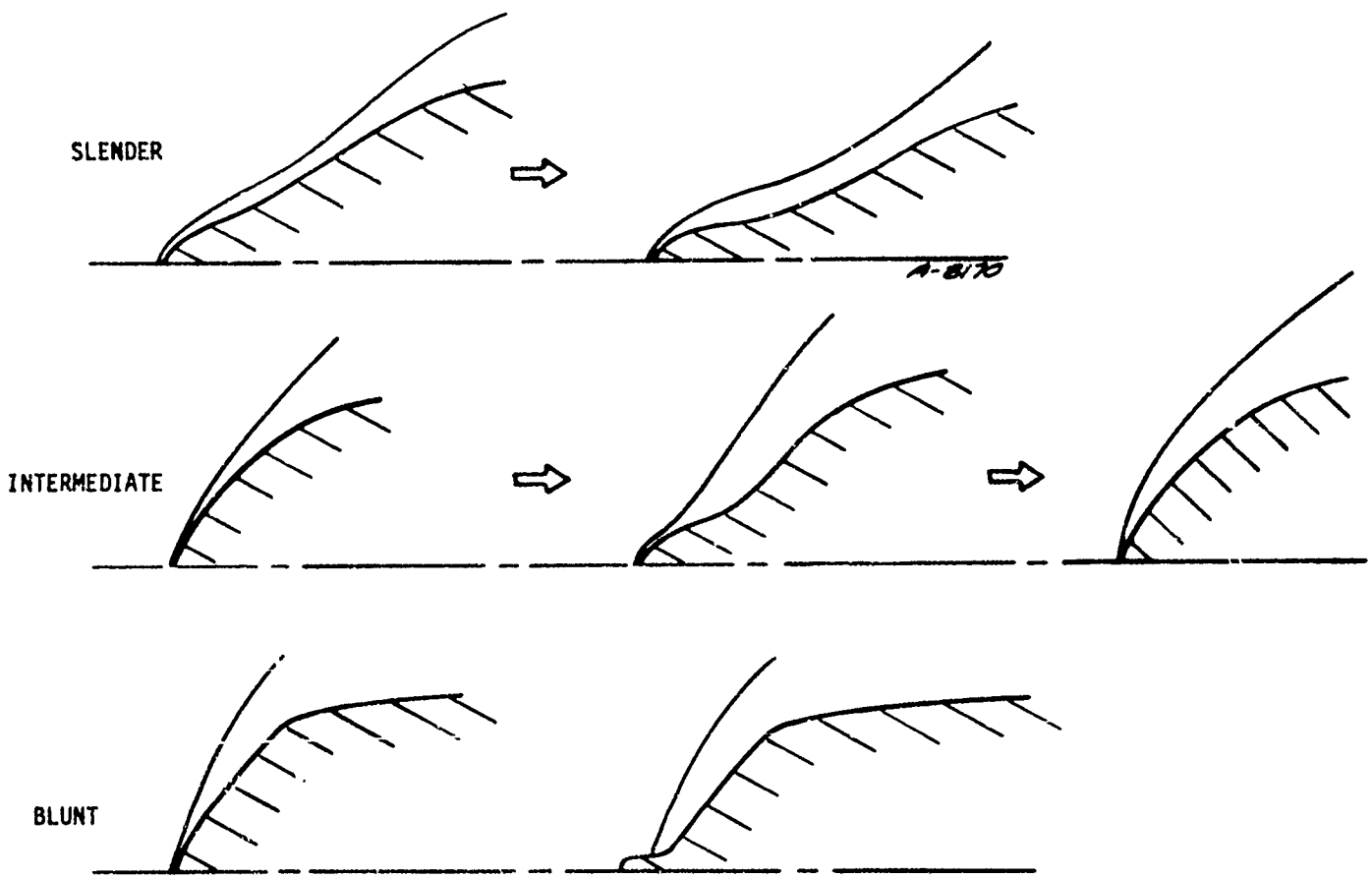

Figure 17. Sketch of Turbulent Ablation Shape Regimes from Hypersonic Low Temperature Ablator Tests

TABLE 6. COMPARISON OF CURRENT TFST FACILITIES ABLATION/SHAPE CHANGE ENVIRONMENTAL PARAMETERS

Facility	Free Stream Properties					Model/Flow Field Parameters					Max Run Time (sec)	Predicted & Observed Steady State Ablation Response				
	Mach No	Re_∞	P_{t_∞} (atm)	$H_o - H_w$ @ 298°K	P_{t_2} (atm)	R_n (in)	S/R_n^*	Re_s^*	Predicted Transition Location ($K = .4$ mil)	Predicted K for Transition Onset		$(\Delta S_o/R_n)_{max}$	$\dot{S}_o$ (in/sec)	T_w	Predicted Steady Ablation Shape†	Observed Steady Ablation Shape
ABLES	2.32	49×10^6/ft	204	3245	100	1	.77	1.59×10^6	$S/R_n = .14$	.08 mils	15.	1.	.07	~4200 (Equilibrium)	Blunt Biconic	Blunt Biconic (Turbulent)
	2.93	25×10^6/ft	204	3245	50	1	.73	$.773 \times 10^6$	$S/R_n = .266$	.17 mils	15.	1.	.05	~4000 (Equilibrium)	Blunt Biconic	Blunt Biconic (Turbulent)
50 MW	1.8 (flat)	13.5×10^6/ft	125	3100	100	.25	.85	$.255 \times 10^6$	$S/R_n = .314$	.18 mils	30	>3.	.06	7260	Intermediate Shape (Convex Biconic)	Blunt Biconic (Turbulent)
	1.8 (peaked)	8.1×10^6/ft	125	5600	100	.25	.85	$.152 \times 10^6$	$S/R_n = .482$	.28 mils	30	>3.	.10	7840	Intermediate Shape (Convex Biconic)	Convex Biconic (Turbulent)
Ballistic Range	16.4 (launch)	77×10^6/ft	1.	6950	360	.25	.61	$.357 \times 10^6$	$S/R_n = .153$	.07 mils	.060	.06	.24	8450	Blunt Biconic	Insufficient Ablation
	13.3 (mid-range)	62×10^6/ft	1.	4640	235	.25	.54	$.352 \times 10^6$	$S/R_n = .155$	.08 mils	.060	.04	.15	7950	Blunt Biconic	Insufficient Ablation

Based on the PANT LTA shape change data, the following criteria can be used to estimate the final stable shapes $M_\infty > 5$.

$.5 \leq S/R_N)_{tran}$ • slender shape

$.3 \leq S/R_n)_{tran} < .5$ • intermediate shape

$S/R_n)_{tran} < .3$ • blunt (turb.) shape

3. The predicted transition location on a 0.25 inch sphere in the 50 MW test stream (P_{t_2} = 100 atm) is between S/R_N = 0.3 and 0.5 which in hypersonic flow should result in an intermediate turbulent shape. Steady ablation shapes which develop in the 50 MW arc at high pressures are generally either blunt conic or convex conic, long triconic shapes are believed to be the result of strong vortical layer effects are not observed to develop in the relatively low Mach number 50 MW test stream.

4. The ABRES test rhombus size at the peak pressure test condition is about a factor of five larger than the Mach 1.8 50 MW test rhombus (neglecting the cold-flow shroud). Launch constraints with the ballistic range restrict models to a nominal half inch diameter, similiar to the 50 MW model sizes.

5. Maximum model exposure times in both the ABRES and 50 MW arc are comparable (on the order of 1 minute). Flight times in the ballistic range are nominally 60 milliseconds. As a result ballistic range models must be preshaped since the total recession which occurs on graphite models is on the order of 50 mils or less.

6. Graphite surface ablation temperatures in both the ballistic range and 50 MW arc are comparable with flight values. The peak graphite ablation temperatures in the ABRES combustion test facility are 3500-4000°R below peak flight values. All three facilities provide a relatively poor simulation of the material thermostructural response in flight. The level of thermostructural simulation in both the ballistic range and the 50 MW arc is low due to the severe restrictions on the model size in both facilities. It should be noted however that by properly designing ablation models and test conditions in the 50 MW arc flight level strains can be generated in subscale models as demonstrated in Reference 11. Thermostructural simulation as used in this discussion however refers to full scale hardware proof testing. Thermostructural simulation with full scale hardware in the ABRES facility is low due to the low graphite ablation temperatures in this facility.

In summary the transition and shape change response of graphitic materials in the the ABRES combustion test facility are comparable with that in the 50 MW arc and the ballistic range. The ABRES facility provides a significantly larger test rhombus than the other two facilities thus enabling proof testing of flight scale hardware. The limitation of this facility is the total lack of graphite ablation simulation in air. Thus, the ABRES facility cannot be used for high pressure hyperthermal graphite ablation response experiments, whereas the 50 MW arc and ballistic range currently service this function.

SECTION 4

PROPELLANT OPTIMIZATION STUDIES

Results presented in the previous section clearly demonstrate that the current propellant combination used in the ABRES combustion test facility does not provide a good reentry environment simulation for graphite ablation. Peak graphite ablation temperatures in the current facility are in the range 4000-4500°R which is about 3500°R below peak graphite ablation tempeatures in flight. In addition the N_2O_4/Aerozine-50 propellant combination provides a highly oxidizing environment with large amounts of H_2O and CO_2 in the test stream. The heterogenous reactions of these species with a graphitic surface produce an unusually high recession rate for graphite at relatively low ablation temperatures.

The intent of this propellant optimization study was to identify propellant combinations suitable for application in the ABRES combustion test facility which would improve the current level of high pressure hyperthermal graphite ablation simulation in this ground test facility.

The alternate propellant combinations analyzed in this review are presented in Section 4.1. The criteria and results of analyses used to evaluate the graphite ablation response in the alternate propellants environments are summarized in Section 4.2. Section 4.3 reviews the results of the transpiration cooling systems propellant optimization studies. Conclusions derived from these analyses regarding optimum propellant combinations for the various hyperthermal testing objectives are reviewed in Section 4.4.

4.1 CANDIDATE PROPELLANTS

Six alternate propellant combinations were analyzed to assess their potential for upgrading the ABRES combustion test facility. These propellant combinations are listed in Table 7. Included in this listing are the nominal oxidizer to fuel (O/F) ratios assumed for these analyses and the predicted chamber conditions. The chamber and cold wall equilibrium gas states listed in Table 7 were calculated using the ACE computer code (Reference 6). Criteria considered in studying alternate propellant combinations for ABRES facility operation are listed below.

TABLE 7. ALTERNATE PROPELLANTS ANALYZED FOR ABRES FACILITY APPLICATION

Propellant	O/F	T_c ~ °R @3000 psi	H_c ~ Btu/lbm @3000 psi	H_w ~ Btu/lbm @530°R	Comments
1. Hydrogen/Fluorine (H_2/F_2)	19	9400	-80.	-5800.	Extremely high chamber temperature. Extremely expensive and relatively high toxicity.
2. Cyanogen/Oxygen (C_2N_2/LOX)	1.1	7400	1100.	-2830	Provides nearly exact simulation of graphite ablation in air. Relatively high toxicity.
3. Benzonitrile/Oxygen (C_1H_5N/LOX)	2.18	7350.	160.	-3910.	Relatively inexpensive propellant with moderate toxicity.
4. Butadiene/Oxygen (C_4H_6/LOX)	2.6	7350	190.	-4390.	Relatively inexpensive propellant with low toxicity.
5. Propyne/Oxygen (C_3H_4/LOX)	2.0	7420.	550.	-4140.	Inexpensive propellant with low toxicity.
6. Hydrogen/Oxygen (H_2/LOX)	8.	6880.	-100.	-6730.	Propellant combination with relatively high cold wall heat rate for transpiration cooling tests.

1. Enhance simulation of reentry thermostructural environments. (Reduction of H_2O content in test stream and increasing combustion chamber total temperature).

2. Minimize toxicity (Increase testing frequency)

3. Minimize test cost

Hydrogen/fluorine is the only propellant combination in Table 7 which has a chamber temperature above 9000°R. The principal limitations of this propellant combination are (1) its high cost and (2) its high toxicity. Cyanogen/LOX provides an extremely desirable graphite ablation test environment since it closely simulates air. This propellant combination is relatively toxic plus the availability of cyanogen is quite restrictive. The three hydrocarbon/LOX propellant combinations in Table 7 are similar. All three are relatively inexpensive and not too toxic. The exhaust products of these propellants contain some H_2O, although each contains significantly less H_2O in the test stream than the current propellant combination. Hydrogen/LOX was included in the list of propellants because of the desire to upgrade environmental test conditions for transpiration cooled systems tests. This propellant combination is nontoxic and can be readily burned in the ABRES facility. The hydrogen/oxygen propellant combination cannot be used for graphitic materials ablation tests due to the high concentration of water in the test stream. The predicted ablation response of graphitic models in the exhaust test stream of each propellant combination in Table 7 are summarized in Section 4.2.

4.2 GRAPHITE ABLATION PREDICTIONS

Relatively complete graphite ablation analyses were made for five of the alternate propellant combinations in Table 7. Hydrogen/oxygen was not considered since it is not suitable for graphite ablation testing. The assumptions and analyses made to predict the graphite ablation response in the various test environments are summarized below.

1. All environmental predictions were based on a nominal sphere-cone configuration (R_N = 1.0 inch, CHA = 9°).

2. The two flight trajectories described in Section 3.1.1 were used to provide flight environmental and material response criteria for comparison.

3. Aerothermal environment predictions for the nominal configuration were made with the SAANT computer code (Reference 9) or the ARGEIBL computer code (Reference 4). The SAANT code was used for flight environmental predictions. THe ABRES facility Mach

2.93 test condition (large test rhombus) was assumed for these aerothermal environment predictions. The test stream transport properties for the various propellant combinations were predicted with the ACE computer code assuming chemical equilibrium. Solution of the inviscid flow field over the model configuration input into the ARGEIBL computer code was made with the RAZZIB computer code (Reference 5) assuming $\gamma = 1.2$. Both the flight and ABRES convective heating environment were smoothwall predictions. The stagnation point convective heat and mass transfer rates predicted by the ARGEIBL code for all propellant combinations in the ABRES facility were doubled since the measured heat rates reviewed in Section 2.1.1 were nominally double the predictions for the N_2O_4/ Aerozine-50 propellant.

4. Material response predictions were made at three locations on the assumed sphere-cone model (1) the stagnation point (2) the tangency point and (3) a frustum body point. The transient material ablation response predictions were made with the CMA computer code. The thermochemical ablation data input into CMA were generated with the ACE computer code assuming equilibrium/diffusion controlled ablation. No chemical kinetics were considered for these analyses.

5. The three material response criteria used to evaluate and rank the propellants with respect to reentry simulation were (1) the integrated conductive flux into the material, $\int \dot{q} d\theta$ (2) the surface temperature history, T_w and (3) the surface recession history, $\dot{s}$.

Results of these analyses are presented in Figure 18 through Figure 20. Figure 18 compares the integrated heat flux from the ablating graphite surface into the material for the six propellant combinations with predictions for the two flight trajectories. These comparisons are made at the three body stations. The ablation analyses for both flight trajectories were initiated at 170 Kft. The results of the flight predictions in Figure 18 are plotted from 120 Kft. The ablation response predictions for the seven ABRES test environments in Figure 18 are displaced from the 120 Kft flight time by four seconds to more closely correspond to the interval of peak heating in flight. The model exposure time in the ABRES facility was assumed to be ten seconds although the maximum facility run time when these analyses were made was 15 seconds and the current maximum run time is 80 seconds. A ten second exposure in the ABRES facility provides a simulation of the peak heating interval for flight. Longer model exposures at the peak heating conditions cause the model to approach the isothermal limit where the surface conductive flux goes to zero.

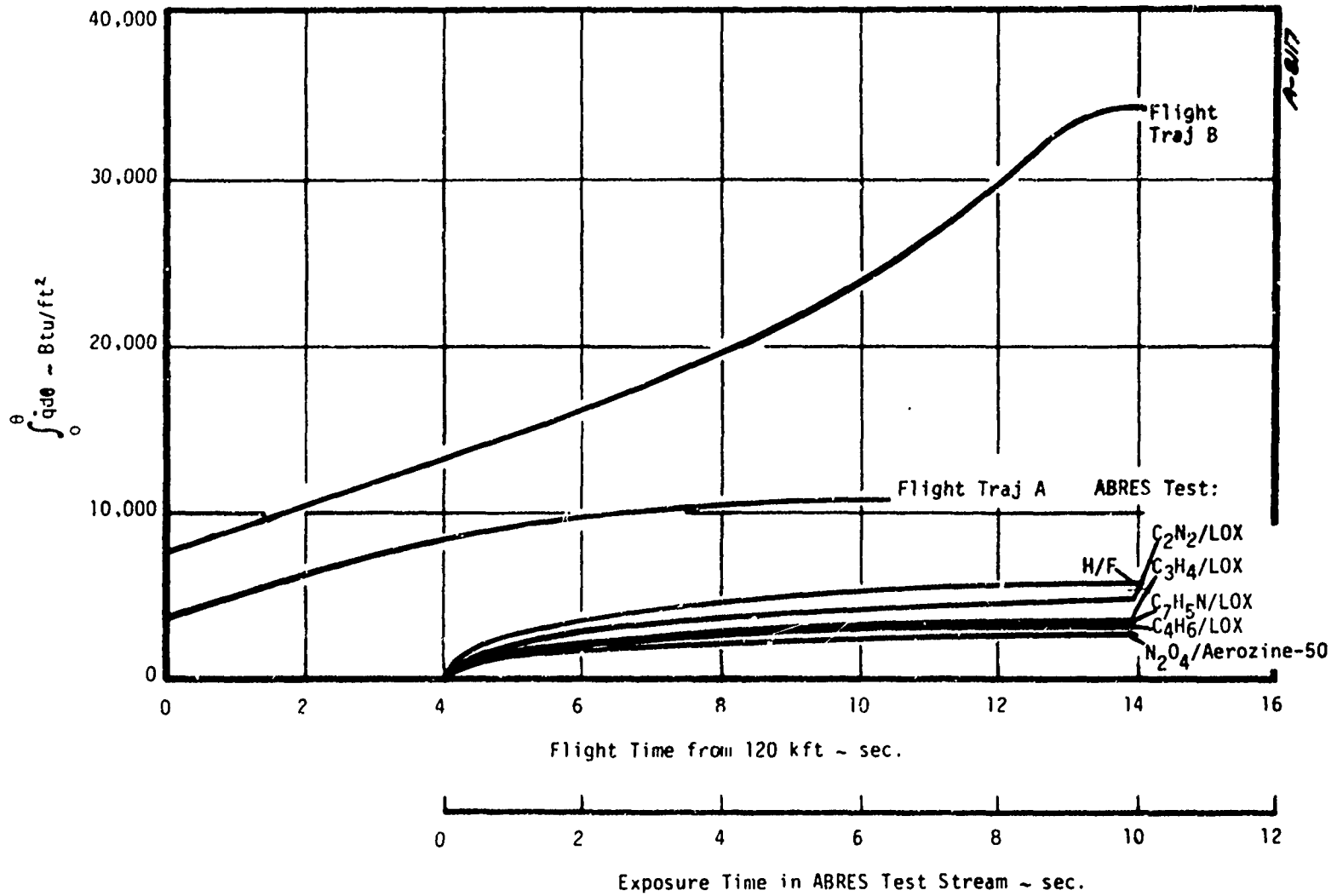

Figure 18. Comparison of Predicted Integrated Energy Flux from the Surface in the ABRES Facility (Alternate Propellants) with Flight

a) Stagnation Point

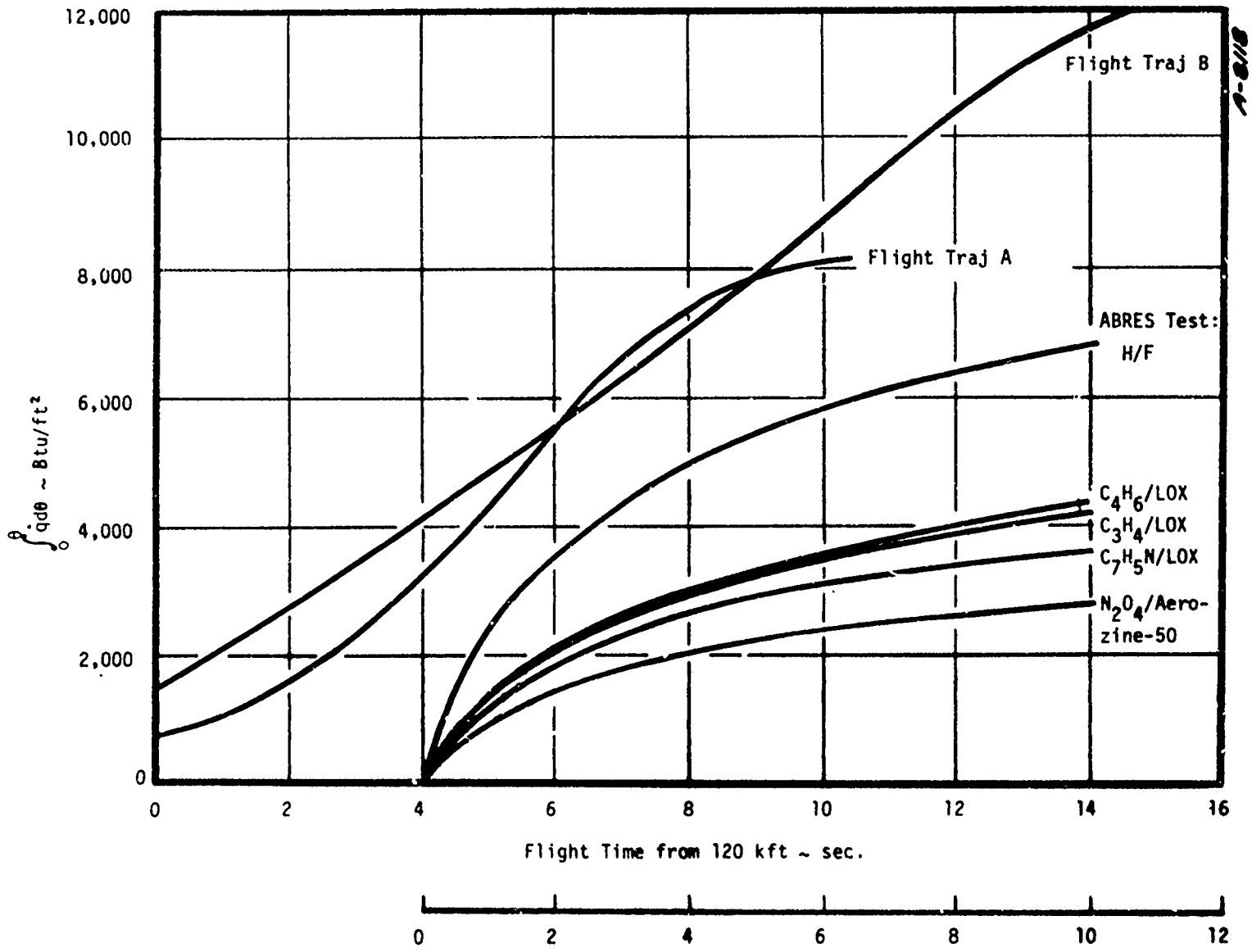

Figure 18. (Continued)

b) Tangency Point (S/R_N = 1.41)

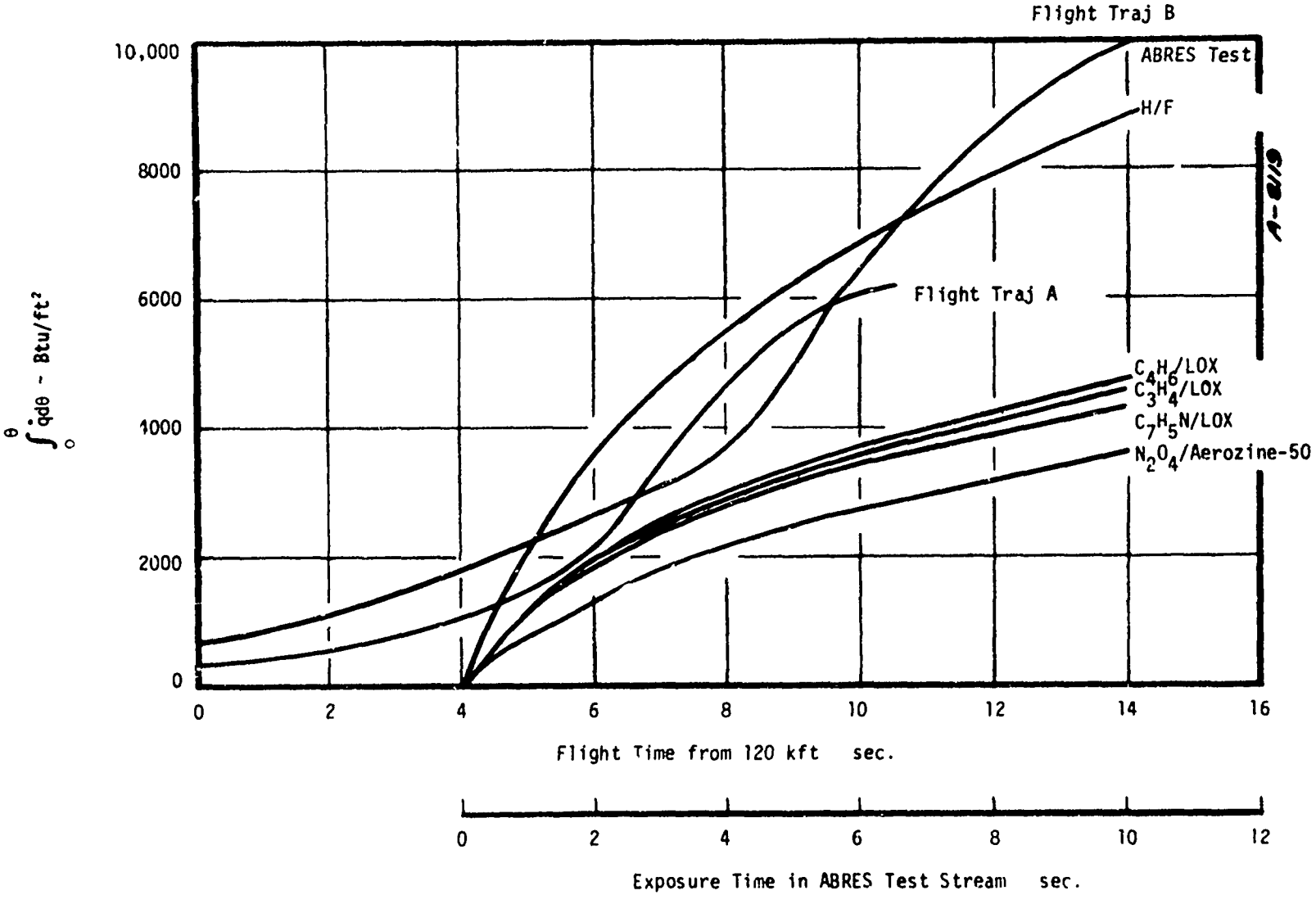

Figure 18. (Concluded)

c) Frustum Body Point (S/R_N = 4.6)

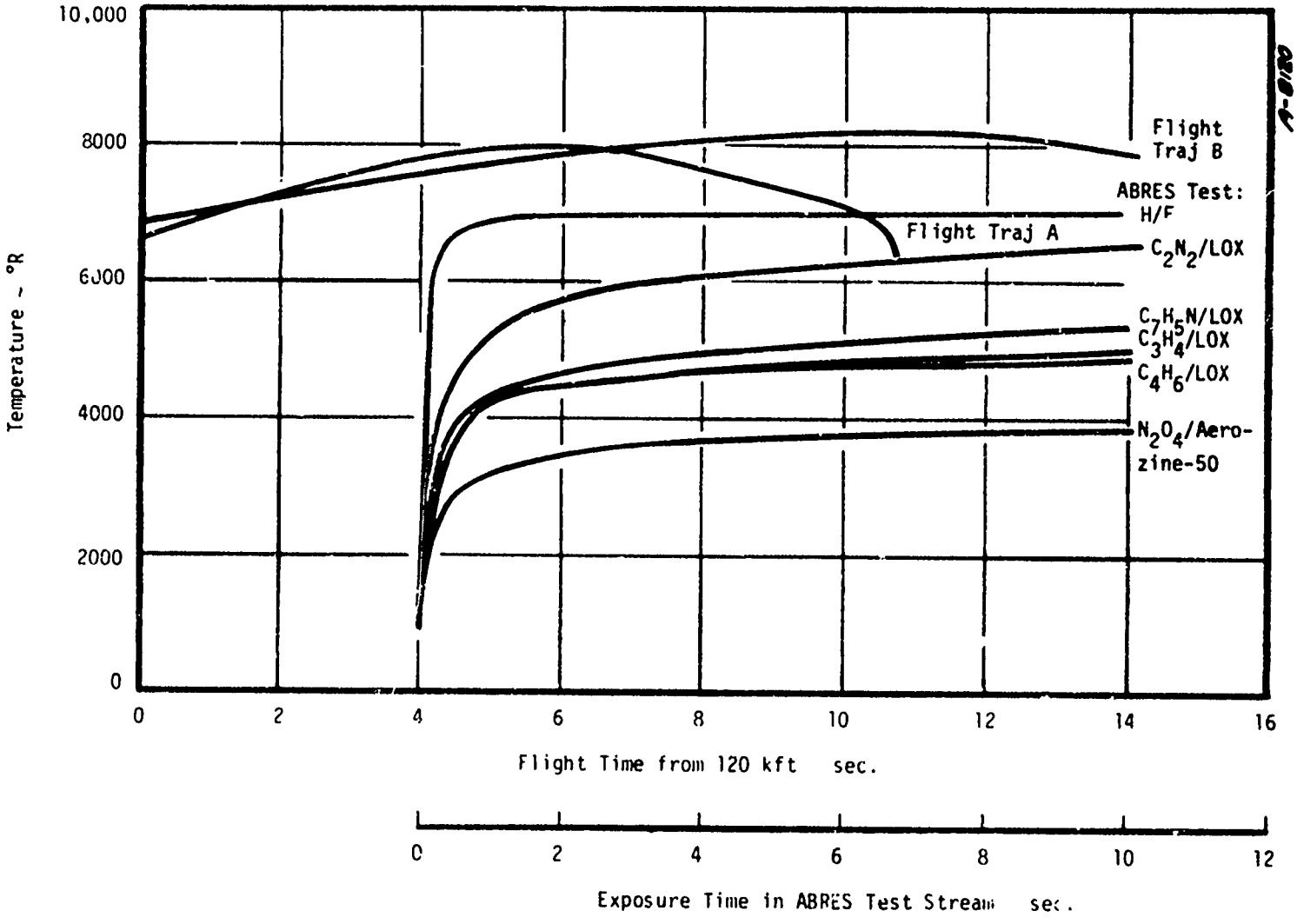

Figure 19. Comparison of Predicted Ablation Temperature Response in the ABRES Facility (Alternate Propellants) with Flight

a) Stagnation Point

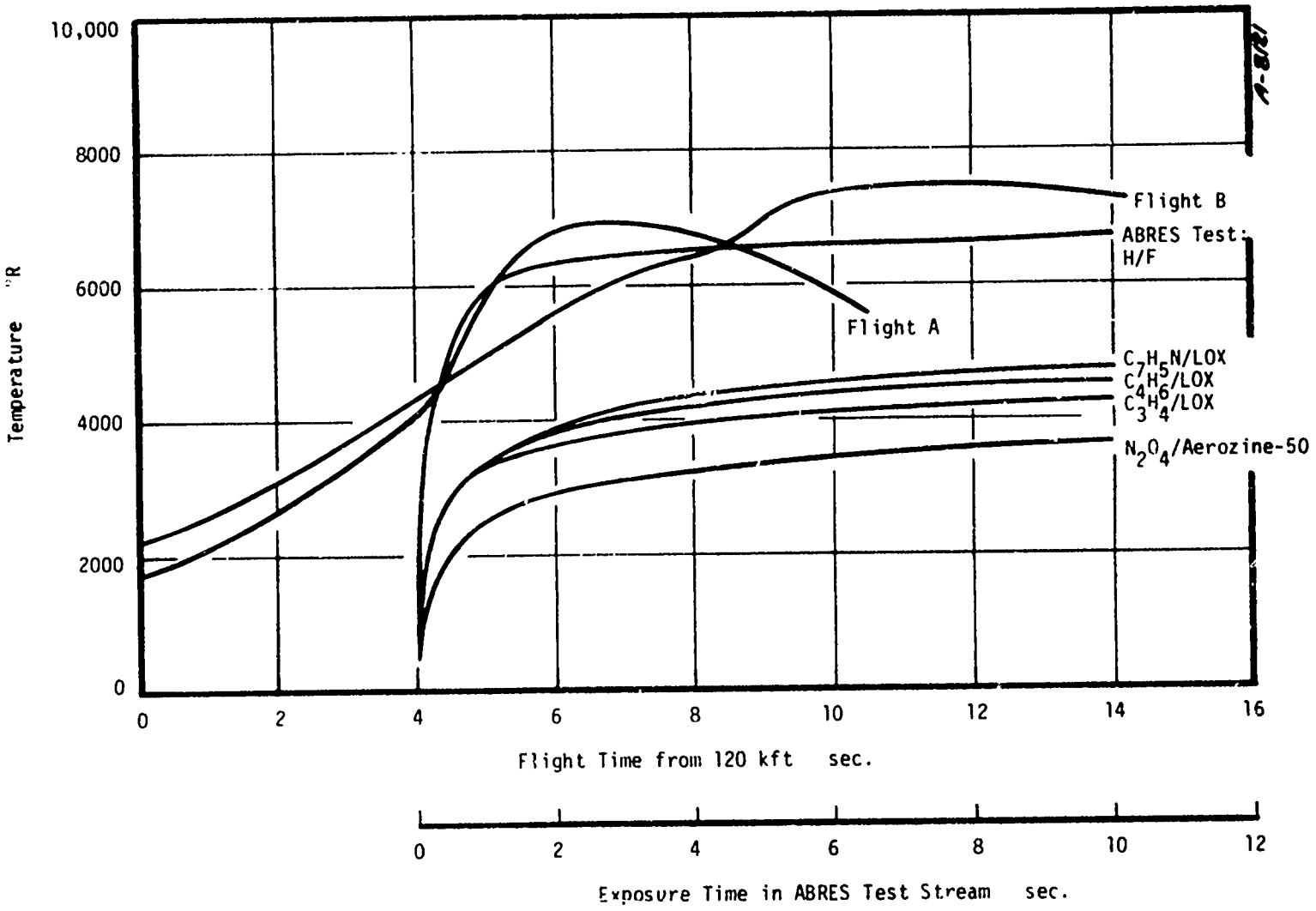

Figure 19.(Continued)

b) Tangency Point

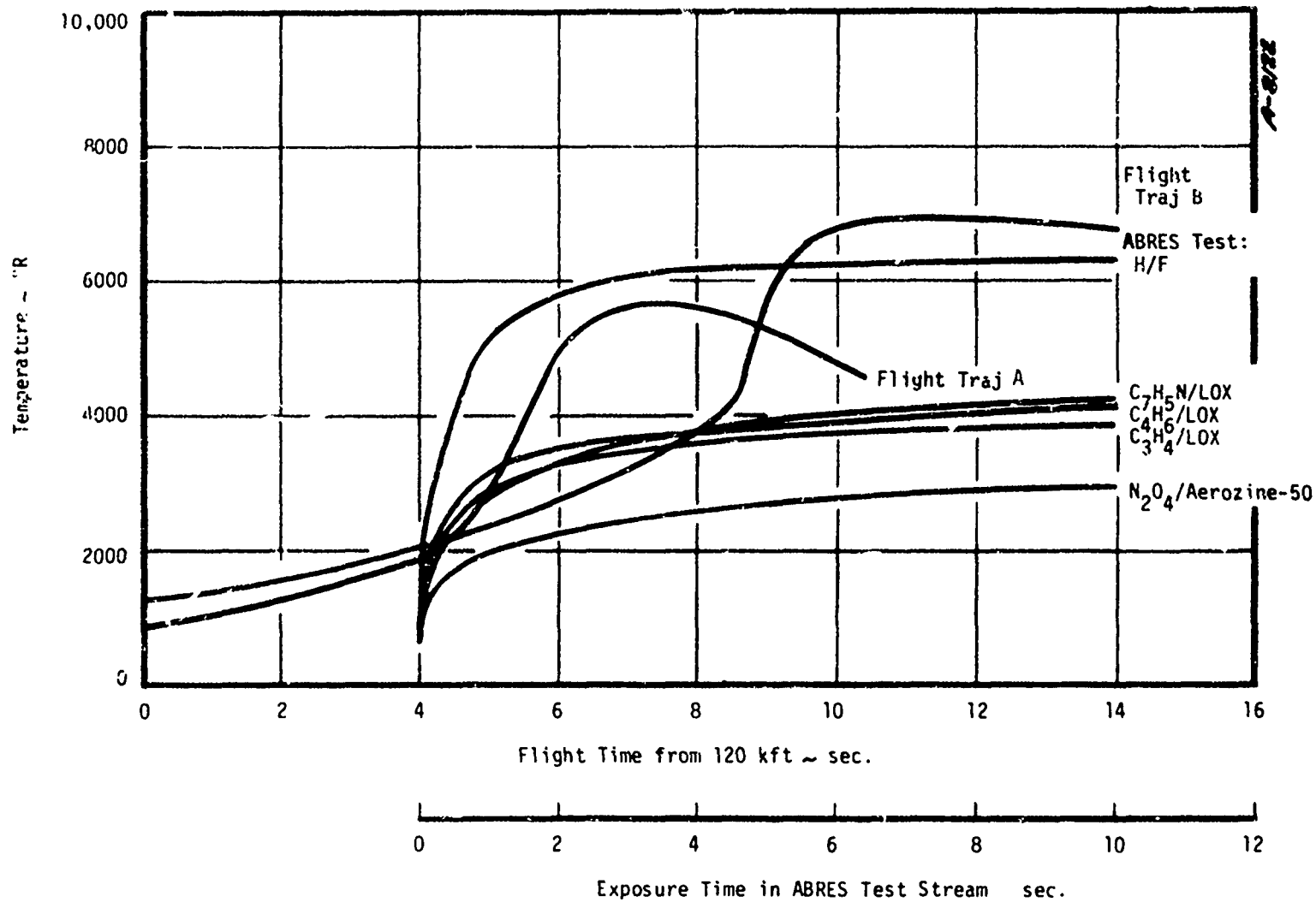

Figure 19. (Concluded)

c) Frustum Body Point (S/R_N = 4.6)

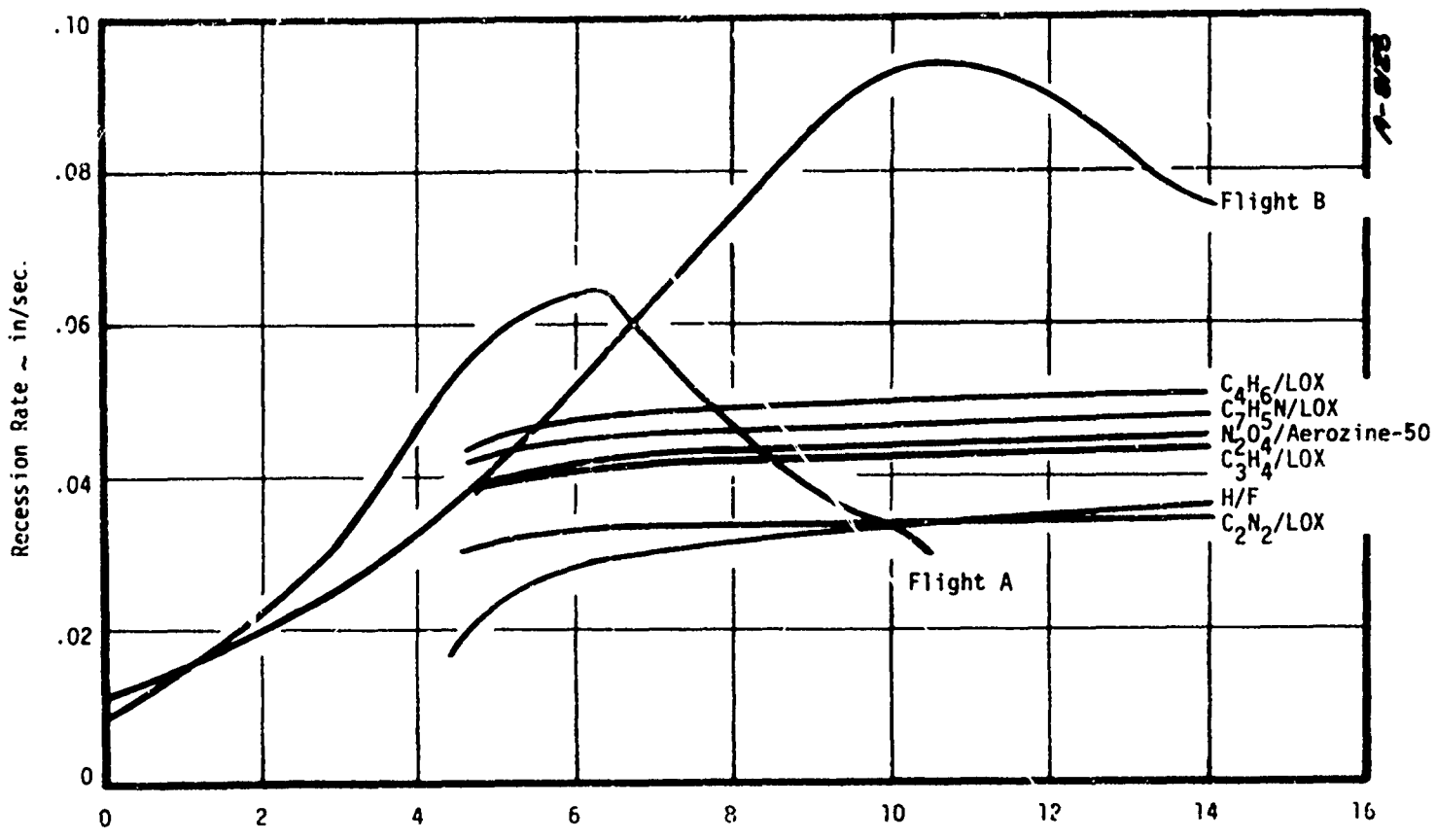

Figure 20. Comparison of Predicted Surface Recession Rates in the ABRES Facility (Alternate Propellants) with Flight

a) Stagnation Point

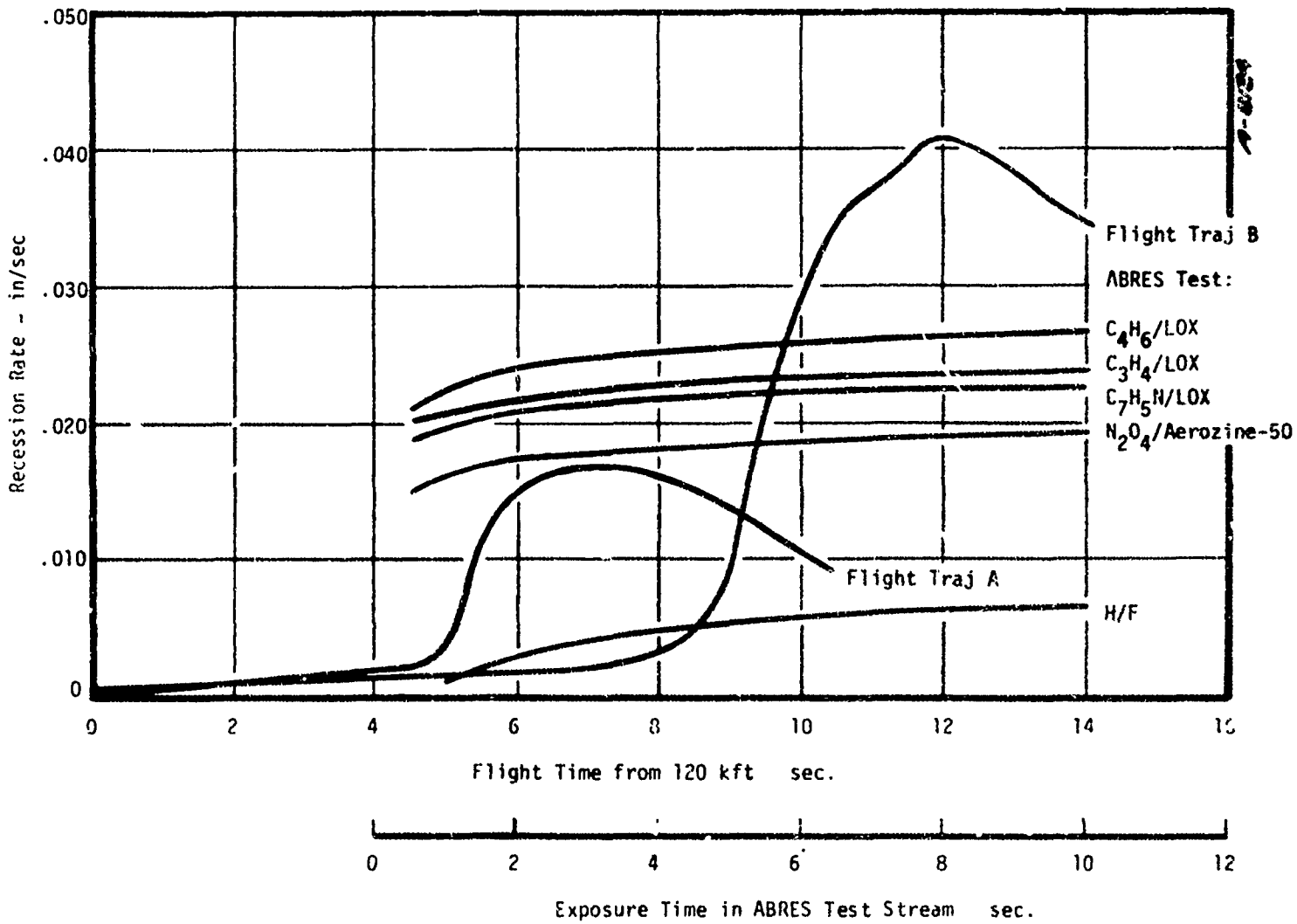

Figure 20. (Continued)

b) Tangency Point

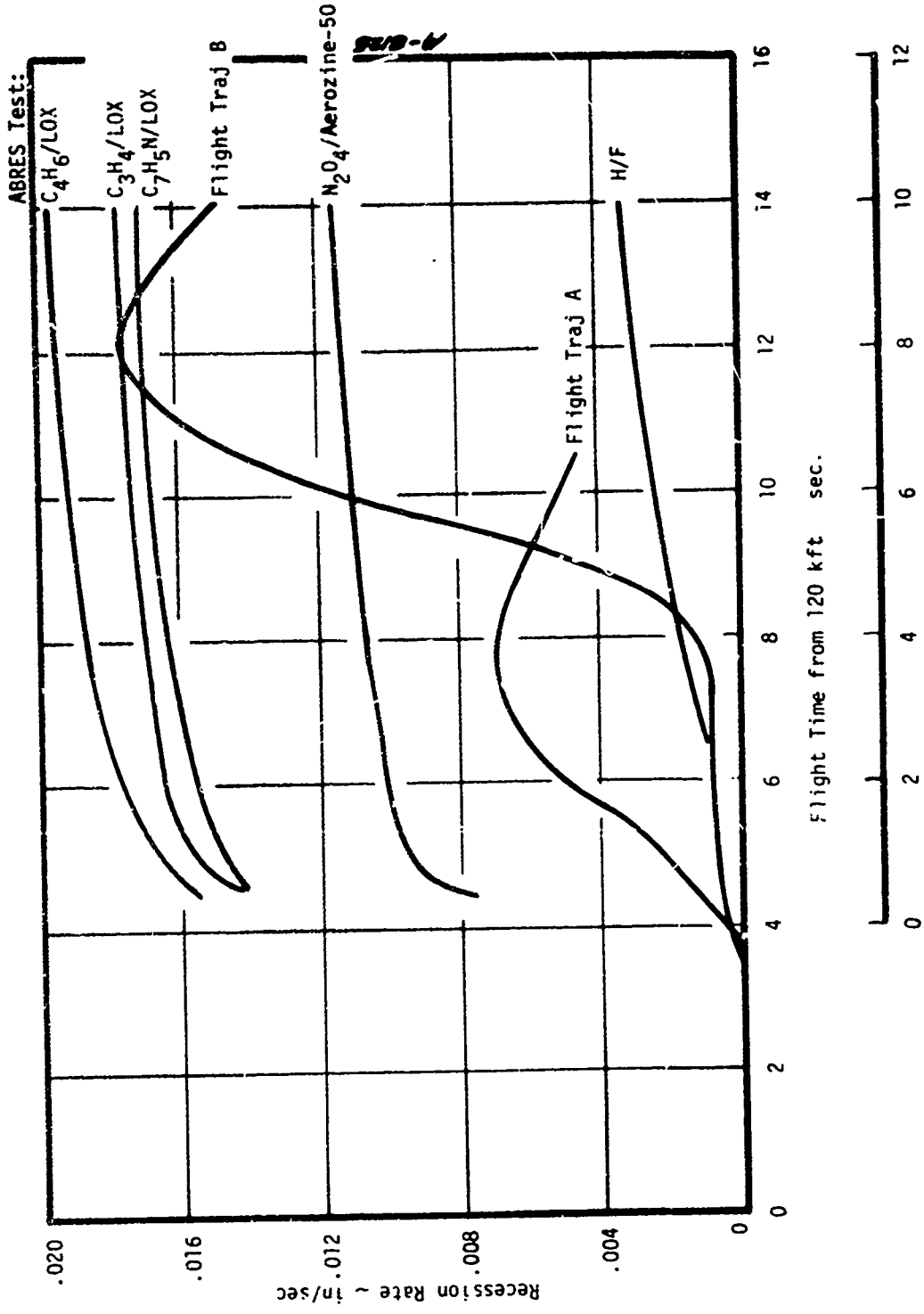

Figure 20.(Concluded)
c) Frustum Body Point

Figure 19 compares the predicted surface temperature histories for both flights and the six propellant combinations in the ABRES facility. Only hydrogen/fluorine produces graphite ablation temperatures in the ABRES facility in the range of flight values. Peak stagnation point ablation temperatures in flight are above the hydrogen/fluorine values by more than 1000°R. At the tangency point and frustum body point the flight and peak ABRES values are in good agreement. Generally, though the peak graphite ablation temperatures in the ABRES facility are about 2000-3000°R below peak flight values.

The predicted surface recession rates are compared in Figure 20. The peak recession rates predicted for the ABRES facility are significantly below the peak flight values at both the stagnation point and tangency point. On the frustum, the predicted surface recession rates for the hydrocarbon/LOX propellants in the ABRES facility are slightly above the peak flight values. Hydrogen/fluorine recession rate predictions are below both the flight and other propellant predictions at all body stations.

These ablation response predictions are interpreted more critically with respect to thermostructural and reentry simulation criteria in Sections 4.2.1 and 4.2.2 respectively.

4.2.1 Thermostructural Simulation

The degree of thermostructural simulation currently achieved in the ABRES combustion test facility is low. Based on the material ablation response analyses reviewed in Section 4.2, the alternate propellants are evaluated from the standpoint of upgrading the thermostructural simulation achieved in the ABRES facility.

Since complete thermostructural analyse of the materials ablation response were not within the scope of this task, it was not possible to quantitatively assess the level of thermostructural simulation achieved with each propellant. As a result, the material ablation response predictions in Sect on 4.2 were utilized to qualitatively rank the proposed propellant combinations for the standpoint of thermostructural simulation. The criteria selected for this evaluation are listed below.

1. Ablation temperature
2. Integrated heat flux into the material (i.e., in-depth material thermal response)
3. Surface recession rate

The higher the surface ablation temperature and the integrated heat flux into the material, the more severe the in-depth thermal gradients and the material thermal strains. The graphite ablation temperature predictions in Figure 19 show that the maximum graphite ablation temperature is achieved in hydrogen/fluorine. Graphite ablation temperatures in H/F are in the range of 6500-7000°R which is about 1000°R below flight level ablation temperatures at the stagnation point. Predicted ablation temperatures in H/F at the tangency and conic surface body points exhibit good agreement with flight ablation temperatures. The predicted graphite ablation temperatures in H/F in Figure 19 exhibit good agreement with measured graphite ablation temperatures in H/F (Reference 12).

Graphite ablation predictions in cyanogen/LOX were limited to the stagnation point since this propellant combination was an unlikely contender due to (1) the limited availability of C_2N_2 and (2) the high toxicity of C_2N_2. The stagnation point ablation predictions with this propellant exhibit an ablation temperature about 500-1000°R below that for H/F.

The hydrocarbon fuels with liquid oxygen yield carbon ablation temperatures from 1000 to 1200°R above the surface temperatures currently achieved in the ABRES facility. These predicted graphite ablation temperatures with hydrocarbon fuels are lower limit ablation temperatures since the CO_2 and H_2O heterogenous reactions kinetics were not included in these analyses. The effect of the heterogenous reaction kinetics is to raise the ablation temperature by 200-400°R while lowering the surface recession rate.

Results in Figure 18 show that the surface conductive flux was predicted to be a maximum for graphite ablation in hydrogen/fluorine. At the stagnation point and tangency point the conductive flux predicted with the H/F propellant is similar to the level predicted for the moderate flight trajectory. On the conic surface the conductive flux with H/F exceeds the moderate flight levels due to the relatively low Mach number and higher conic pressure in the ABRES facility test rhombus.

The stagnation point surface conductive flux predicted with cyanogen/LOX is about double that of the current propellant.

The surface conductive flux predicted with the hydrocarbon fuels are about 40 percent above that of the current propellant. As indicated previously the heterogenous reaction kinetics would increase T_w and decrease $\dot{s}$ which have compensating effects on the surface conductive flux.

Comparison of surface recession rate predictions in Figure 20 show that all recession rate predictions in the ABRES facility are substantially below flight predictions at the stagnation point. At the tangency point the predicted

recession rates are comparable to the moderately severe flight levels with the exception of H/F. On the frustum body point, the predicted recession rates with the hydrocarbon fuels are slightly above the severe flight recession rate predictions. These results clearly show that the recession rate distribution on a sphere-cone model in the ABRES combustion test facility does not compare well with predicted flight distributions.

Based on these graphite ablation predictions, the alternate propellants are ranked in Table 8 with respect to the degree of thermostructural simulation achieved.

TABLE 8

RANKING OF ALTERNATE PROPELLANTS FOR THERMOSTRUCTURAL TESTING OF GRAPHITIC MATERIALS IN THE ABRES FACILITY

Propellant	Comments
hydrogen/fluorine	Provides maximum graphite surface temperature and indepth conductive flux.
cyanogen/LOX benzonitrile/LOX propyne/LOX butadiene/LOX N_2O_4/Aerozine-50	Not possible to rank these propellants without considering kinetics of heterogenous H_2 and CO_2 oxidation reactions

4.2.2 Reentry Simulation

Reentry simulation refers to the material ablation response and shape change similarity between flight and ground-test ablation tests. The graphite ablation predictions previously reviewed clearly demonstrate that the level of reentry simulation achieved in the ABRES combustion test facility is relatively low even with the alternate propellant combinations considered. The reasons for this observation are noted below.

1. The predicted graphite ablation temperatures in H/F are similar to graphite ablation temperatures in flight, however the predicted graphite surface recession rates in H/F are below flight levels by factors of 2 to 6. Thus the level of reentry simulation in the ABRES facility with H/F as a propellant combination is low.

2. The predicted graphite ablation temperatures with the hydrocarbon/LOX propellant combinations are about 3000°R below the peak flight ablation temperatures. In addition, the predicted recession rate distributions over a sphere-cone model exhibit poor agreement with predicted distributions in flight.

3. The stagnation point graphite ablation predictions with cyanogen/LOX show (a) the graphite ablation temperature with this propellant combination in the ABRES facility is about 1500°R below peak flight values and (b) the predicted surface recession rate is a factor of 2 to 3 below the peak flight values. These low recession rates result from the fact that the total enthalpy and pressure in flight are considerably above the peak values in the ABRES facility. This is a restriction which at the present time has bounds dictated by the physical operating constraints of the facility.

Based on these observations regarding the level of reentry simulation achieved with the alternate propellant combinations, the propellants are ranked in Table 9.

TABLE 9

RANKING OF PROPELLANTS FOR ACHIEVING REENTRY ABLATION SIMULATION IN THE ABRES FACILITY

Propellant Combination	Comments
cyanogen/LOX	Simulates carbon ablation in air nearly exactly. The pressure and total enthalpy limits of the ABRES facility greatly reduce the reentry simulation with this propellant.
benzonitrile/LOX propyne/LOX butadiene/LOX	Low graphite ablation temperatures compared to flight with recession rates somewhat comparable with flight levels. It is not possible to rank these hydrocarbon propellant relative to each other without considering the kinetics of the hetergenous H_2O and CO_2 oxidation reactions.
hydrogen/fluorine	High graphite ablation temperature with extremely low surface recession rate.

In summary, reentry ablation simulation is relatively low in the ABRES facility since (1) the peak impact pressure is currently 100 atm with a projected peak impact pressure of 155-170 atmospheres and (2) the total temperature of most propellant combinations is relatively low for these high pressure test conditions.

TABLE 10. PREDICTED HEAT FLUXES AND TRANSPIRATION REQUIREMENTS FOR ALTERNATIVE PROPELLANTS

Propellant	O/F	At Peak Turbulent Heating				
		$H_r - H_{cw}$ (Btu/lbm)	$\rho_e u_e C_H$ (lbm/ft²sec)	Cold Wall $\dot{q}$ (Btu/ft²sec)	B'_{t_c}	Re_s
N_2O_4/Aerozine-50	2.1	3360.	2.3	7,660	3 0	5.498×10^5
C_3H_4/Lox	2.0	4590.	2.7	11,550	3.9	5.485×10^5
C_7H_5N/Lox	2.18	4040.	2.5	10,260	3.7	5.769×10^5
C_4H_6/Lox	2.6	4550.	2.5	11,240	4.0	5.461×10^5
C_2N_2/Lox	1.1	3900.	3.0	11,780	3.5	7.604×10^5
H/F	19.	5590.	2.3	12,750	5.0	4.901×10^5
H_2/O_2	8.	6580	2.0	12,960	5.8	5.098×10^5
Air (Arc Heated)		5000.	2.8	14,000	4.5	3.61×10^5
Flight (Traj. A) P_{t_2} = 130 atm		4900.	3.5	17,200	4.3	9.56×10^5
Flight (Traj. B) P_{t_2} = 210 atm		5000.	3.7	21,800.	5.3	1.03×10^6
Conditions: R_N = 1.0 in., P_{t_2} = 50 atm for ground test						

The ABRES facility can be throttled which provides the flexibility for better simulating reentry environmental conditions. Based on a projected peak chamber pressure of 3500 psi in the ABRES facility, the stagnation point pressure and cold wall heat flux variations in the ABRES facility are compared with the flight values for a relatively severe reentry trajectory in Figure 21. The Mach 2.32 nozzle was assumed for these analyses. The cold wall heat flux predictions for ABRES in Figure 21 are based on the current propellant combination. Peak cold wall heat rates in ABRES are more than a factor of 3 below peak flight values. This descrepancy between peak heat rates in flight and the ABRES facility would be reduced to a factor in excess of 2 with any of the hydrocarbon propellants. The conclusion derived from these results is:

> Throttling of the ABRES combustion test facility to achieve reentry simulation is of marginal utility since the levels of peak heating in the ABRES facility are below peak flight levels by more than a factor of two. However, throttling may provide the desired flexibility of environmental variations for specific thermostructural simulation tests or other unique test objectives.

4.3 TRANSPIRATION COOLING SYSTEMS

The ABRES combustion facility test rhombus is sufficiently large to test full scale transpiration cooled nosetip systems. The current N_2O_4/ Aerozine-50 propellant combination does not provide a sufficiently severe aerothermal environment for testing these nosetip systems. The two principal simulation criteria for transpiration systems test are:

1. Simulation of the cold-wall heat rate in flight
2. Simulation of coolant flow rates (nondimensional mass transfer rates, $B' = \dot{m}/\rho_e U_e C_H$) required for flight

The importance of simulating the static pressure, pressure gradient, and aerodynamic shear depends on the type of porous material being tested. Recent results from the NCT program (Reference 13) regarding distinctions between porous and discrete-injection tips with respect to the coupling of boundary layer and coolant flow phenomena are summarized below.

1. For porous tips, transpiration cooling performance is not sensitive to surface/boundary layer phenomena. The theory is well in hand for predicting the performance of these systems in regimes of high pressure, severe pressure gradients, and aerodynamic shears.

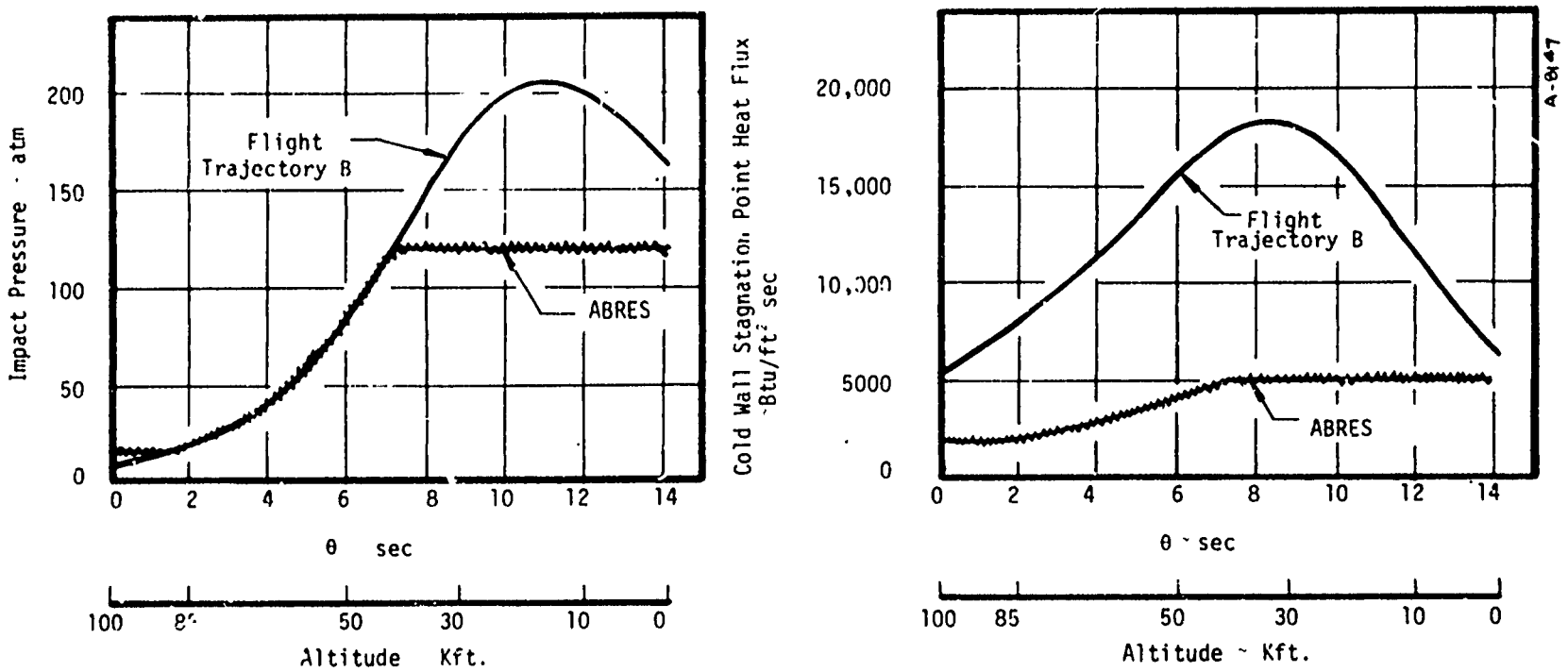

Figure 21. Comparison Of Flight Heat Pulse With ABRES Heat Pulse (With Throttling And N_2O_4/Aerozine-50 Propellant Combination)

2. For discrete-injection tips, transpiration cooling performance is sensitive to surface/boundary layer phenomena. The theory is not developed for predicting the performance of these systems in regimes of high pressure, severe pressure gradients and aerodynamic shears. Discrete injection systems exhibit an effective surface roughness which depends on (a) the slot geometry (b) the boundary layer flow and (c) the injectant flow.

Analyses of the alternate propellant combinations for transpiration cooling tests emphasize porous systems and the two primary simulation criteria listed above. Results of these analyses are summarized in Table 10. Included in Table 10 are transpiration cooling system response predictions at the sonic point of a one inch radius sphere for the two peak flight test conditions and a nominal arc test condition plus the seven propellant combinations in the ABRES test facility.

The peak turbulent cold wall heat rates in the ABRES facility are achieved with hydrogen/oxygen and hydrogen/fluorine. The peak turbulent heat rates in the high Mach number flow field for both of these propellant combinations are 25 and 40 percent below the two peak flight values. The peak cold-wall heat rates predicted for the other alternate propellants are about 10 percent below the peak values with H/F and H_2/O_2. The peak cold wall heat rates for all of the alternate propellants are at least 30 percent above the peak turbulent value with the current propellant combination.

The required coolant mass transfer rates at the point of peak turbulent heating were evaluated by equating the convective heat flux at the surface with the energy absorbed by the vaporizing water, e.g.,

$$\dot{m}\Delta H_v = \rho_e U_e C_{H_o} (H_R - H_w) C_H / C_{H_o}$$

The blowing reduction expression assumed for these calculations was

$$C_H / C_{H_o} = \frac{1.4B'_o}{e^{1.4B'_o} - 1.}$$

Results of these calculations for the environmental test conditions are presented in Table 10 and indicate the following.

1. Peak flight levels of B' are simulated with both H/F and H_2/O_2 propellant combinations in the ABRES facility at the high Mach number test condition.

2. The peak B' levels in the ABRES facility with the hydrocarbon propellant combinations are comparable with flight levels required for a moderate flight, which is not representative of transpiration cooling applications of interest.

3. Cyanogen/LOX provides a relatively poor simulation of flight levels of B' due principally to the relatively low cold wall enthalpy potential of this propellant combination. This propellant combination is only slightly better than the current N_2O_4/Aerozine-50 propellant combination.

Based on these results, the ranking of the alternate propellants with respect to transpiration cooling systems tests are summarized in Table 11.

TABLE 11

RANKING OF PROPELLANTS FOR TRANSPIRATION COOLED SYSTEMS TEST SIMULATION IN THE ABRES COMBUSTION TEST FACILITY

Propellant Combination	Comments
hydrogen/oxygen	Provides environment which maximizes the required coolant mass transfer rate. Easy propellant combination to work with.
hydrogen/fluorine	Provides environment which requires a peak flight level of coolant mass transfer rate. Highly toxic and expensive propellant combination.
benzonitrile/LOX propyne/LOX butadiene/LOX	Marginal propellant combinations for transpiration systems tests since required coolant mass transfer rates are significantly below the peak flight values.
cyanogen/LOX	Inappropriate for transpiration systems tests due to low coolant mass transfer rate requirements.

4.4 CONCLUSIONS

Selecting the optimum propellant combination for general use in the ABRES combustion test facility, based on the results in Sections 4.2.1 through 4.2.3 requires that test environment priorities be established. The environmental priorities used to rank the alternate propellant combinations for general application in this test facility were (1) high temperature thermostructural simulation (2) reentry ablation shape change simulation and (3) high temperature environmental test conditions for transpiration systems tests.

From the standpoint of maximizing the hyperthermal severity of the ABRES test environment, hydrogen/fluorine is the optimum propellant combination. The peak graphite ablation temperature in a hydrogen/fluorine environment is about 2000°R above that generated with the hydrocarbon propellants and about 3000°R above the ablation temperatures generated with the current propellant combination. Hydrogen/oxygen provides the optimum test environment for transpiration cooled systems tests, although this propellant combination is not all all suitable for hyperthermal ablation tests due to the high water content of its exhaust test stream. The hydrocarbon/LOX propellant combinations are all similar with respect to their hyperthermal severity and predicted graphite ablation response. Each of the three hydrocarbon systems (1) benzonitrile/LOX (2) propyne/LOX and (3) butadiene/LOX provide ablation test environments more severe than the current propellant (N_2O_4/Aerozine-50) but significantly less severe than peak flight environments. The desirable aspect of these propellants however are (1) their relatively low cost and (2) their relatively low toxicity. Graphite ablation response in cyanogen/LOX is nearly an exact simulation of graphite ablation in air. The total enthalpy and pressure limitations of the ABRES combustion test facility cause this propellant combination to fall short of simulating flight environmental test conditions. In addition this propellant combination has the restrictions of (1) a relatively high toxicity and (2) a restricted availability.

Within the cost, availability, and operational restrictions discussed above, the most realistic alternate propellant combinations to upgrade the ABRES combustion test facility are the hydrocarbon/LOX systems. It is not possible to select the optimum hydrocarbon fuel and O/F ratio based on the analyses reviewed herein because of their limited scope. No analyses were made to optimize O/F ratios from the standpoint of better simulating reentry ablation test conditions. In addition the heterogenous oxidation reactions kinetics of the important H_2O and CO_2 species in the test stream with the carbon surface were not included. Because of these limitations with the previously described analyses, it is not possible to recommend one hydrocarbon fuel as optimum for simulating reentry ablation response of graphitic materials in the ABRES combustion test facility.

SECTION 5

COMPARISON OF NOSETIP TRANSITION AND ABLATION (SHAPE CHANGE) IN THE ADVANCED ABRES FACILITY WITH OTHER ADVANCED HYPERTHERMAL TEST FACILITIES

Results presented in Section 4 clearly demonstrate the extent to which the ABRES combustion test facility can be upgraded to better simulate reentry environments of interest. This section evaluates the environmental test conditions projected for the upgraded ABRES facility relative to projected test conditions for other advanced or projected ablation test facilities.

Six advanced ablation test facilities were selected for evaluation and comparison with the ABRES facility. The AFFDL 50 MW RENT arc test facility is the only currently operational ablation test facility included in this comparison. The other five facilities are either conceptual designs on paper or under prototype development. The ABRES facility environmental parameters and projected test conditions for benzonitrile/LOX at an O/F ratio of 2.18 are compared with the environmental parameters of the other advanced facilities in Table 12. The facilities listed in Table 12 are limited to those with supersonic flow in the test stream. The subsonic shroud test facilities (References 14 and 15) were not included since high pressure hyperthermal tests in these facilities are restricted to thermostructural proof tests.

Prior to reviewing the results in Table 12 a bief summary of the advanced ablation test facilities selected for this comparison is presented.

Shroud Arc (AFFDL 50 MW): This is a specially designed throat and nozzle configuration for the 50 MW arc which increases the test rhombus size by using a cold flow to envelope the hot core flow. The boundary layer gases over the ablating model originate from the hot core. The cold flow enlarges the test rhombus by increasing the radial location of the expansion fan from about 1.1 to 2.13 inches.

Developmental Segmented Arcs: Work at AEDC is progressing on design and fabrication of a high pressure high enthalpy segmented arc. The projected capability of this facility is a relatively high bulk enthalpy (~4500 Btu/lbm) with a relatively flat enthlapy profile. Peak centerline enthalpy values projected for this facility are in the range 6500-7000 Btu/lbm with peak impact pressures as high as 160 atmospheres.

TABLE 12. COMPARISON OF ABRES OPERATION CHARACTERISTICS WITH OTHER ADVANCED FACILITIES

Facility	FREE STREAM PROPERTIES				TEST RHOMBUS PARAMETERS				Max Model Pt_2 (atm)	Max Test Time	Thermochemical Ablation Response	Status or Projected Operational Date
	Mach No.	Max Re_∞ (1/ft)	Max P_{T_∞} (atm)	H_T (Btu/lbm)	De or Stream Size	Model Size Constraints	Free Stream Uniformity	Convective Heating Distribution				
Advanced ABRES	2.32-2.93	49-25x10⁶	200.	~4870 Btu/lbm equivale . air	5.7"/2.32 8.4"/2.93	R_N= 1-2"	contoured nozzles. uniform free stream,	nominal supersonic heating distribution	100. 50.	80 sec	Benzonitrile/LOx more oxidizing than air	operative in early FY 1975
Shroud Arc (AFFDL 50 MW)	1.8	15x10⁶	125.	~3000.	2.175"	maximum model diameter ~1"	relatively nonuniform free stream	low supersonic distribution	100	~30 sec	air	operative
Developmental Segmented Arcs (AEDC prototype)	~2	8.5x10⁶	presently ~100 projected 150-200	bulk ~ 4500 ℄ ~ 6500-7000	~1"	maximum model diameter ~5"	relatively flat profile	low supersonic distribution	~160.	~30 sec	air	prototype study underway full scale facility downstream 2-3 yrs
AEDC Guided Track Range (projected)	~15-17	77x10⁶	1	5000-7000	not applicable criteria	maximum model diameter ~1"	quiescent gas	hyperthermal high pressure	350.	.3 sec (5000 ft range)	air	prototype study underway full scale facility downstream ~5 yrs
AHES 60 MW	conical: 4.5-8.8 semi-elliptic: 3.9-5.1	.025x10⁶	16.	21,000	41" (conic nozzle)	none for nosetips of interest	relatively uniform	supersonic low pressure	.08	40 min.	air	under development projected operational date mid-year 1974
Explosively Driven Facilities (ARTEC)	3.4	23x10⁶	4170	10,000	~1"	maximum model diameter ~.5"	relatively unknown	supersonic high pressure	500.	.7 sec	air	only conceptual analyses to date
(developmental prototype) Mini-Max Arc (7 MW)	~2.	5x10⁵	100.	6000./bulk	.7"	maximum model diameter ~.25"	relatively uniform due to arc characteristics	low supersonic distribution	~8	unknown	air	prototype under development at AEDC

AEDC Guided Track Range: This ablation test facility is a projected 5000 ft upgrading of the existing 1000 ft aeroballistic range at AEDC. The guided track feature of this facility is required since the model dispersion (i.e., drift from the facility centerline) beyond the existing 1000 ft. range without constraining the model is too great to obtain high quality ablation shape change data.

AMES 60 MW Arc: The 60 MW arc presently being fabricated at NASA Ames is designed for high enthalpy supersonic tests of large panel sections applicable to the space shuttle. The peak chamber pressure for this facility is projected to be 14 atmospheres with the peak impact pressure within the test rhombus slightly less than 0.1 atmospheres.

Explosively Driven Facility Concept (ARTEC): This high pressure hyperthermal testing concept is basically a combustion driven facility. It combines gun technology and combustion driven shock tube technology to develop extremely high pressures and high enthalpies for projected test times in the range of 0.5 to 1.0 second.

Mini-Max Arc:: This arc design combines a stabilizing magnetic field with a high pressure arc which stabilizes the arc into a helical configuration which minimizes the enthalpy peaking in the test stream. To summarize the arc operation it is "vortex-stabilized." A prototype of this arc design is currently being developed at AEDC.

The information in Table 12 summarizing the operational characteristics of these advanced test facilities are compared with those of the advanced ABRES combustion test facility from the standpoint of high pressure, hyperthermal ablation shape change criteria. Based on these criteria, two of the advanced facilities in Table 12 are assessed to be superior to the advanced ABRES facility. These are the AEDC Guided Track Range and the Explosively Driven Facility concept. Both of these conceptual facilities have the potential of generating extremely high pressure (P_{t_2} > 300 atm) and high enthalpy (H_T ~ 7000 Btu/lbm) test conditions. The freestream Reynolds numbers in both facilities and maximum test model sizes are such that transition on an ATJ-S model would be between the stagnation point and an S/R_N location of 0.3. Thus, the steady ablation shapes would be fully turbulent blunt biconics, similar to those which develop on models currently tested in the ABRES facility. The total model exposure time in both facilities is less than one second which is significantly shorter than the 80 second test time in the ABRES facility. The test stream diameter projected for the Explosively Driven Facility is 5 to 8 times less than that of the ABRES test stream which restricts the maximum model diameters to be about 0.5 inches. The maximum diameter of models tested in the Guided Track Range would likely be about 0.5 inches since the gun

launch and sabot constraints restrict the model size. The ablation models tested in both of these facilities are restricted to be subscale replicas of flight hardware. Because of this restriction ablation tests in these facilities would be restricted to material ablation and shape change response tests.

The three advanced high pressure arcs in Table 12 are judged to be comparable to the advanced ABRES facility. The projected peak impact pressures for these advanced arc heaters are in the range 80-160 atmospheres, similar to the pressures generated in the ABRES facility. The peak enthalpy levels projected for both the AEDC Segmented Arc and the Mini-Max Arc are about 2000 Btu/lbm above the projected effective air enthalpy of nominally 4000 Btu/lbm for the advanced ABRES facility. For graphite ablation in air at 100 atmospheres pressure the high enthalpy levels in the advanced arcs result in a 40 percent increase in the predicted steady state ablation rate which is significant for experiments designed to analyze high pressure material ablation response. The peak free-stream Reynolds numbers and model sizes are such that transition would be predicted to occur between $S/R_N = 0.2$ and $S/R_N - 0.4$ on 0.25 inch radius spherically tipped ATJ-S graphite models. Transition in this region of a spherically tipped model generally results in the development of a convex biconic shape (Reference 16) which is sharper than the blunt biconic shapes which develop during the peak heating pulse of most reentry trajectories. The test stream size of these advanced arcs are such that they preclude the possibility of conducting flight hardware proof tests in them.

The NASA Ames 60 MW Arc is not suitable for high pressure hyperthermal ablation tests due to its low maximum chamber pressure. The maximum impact pressure in the Ames 60 MW Arc is less than 0.1 atmospheres. A peak stagnation point pressure in this range is hardly appropriate for conducting material ablation response tests for reentry nosetip application.

In summary, the advanced ABRES combustion test facility is competitive with the advanced arc heater facilities presently in the stage of prototype development. Particularly when one considers the added flexibility of the ABRES facility for proof testing of flight hardware it appears extremely competitive with the advanced arc facilities. Compared to the Guided Track Range and the Explosively Driven Facility concept, the advanced ABRES facility falls short from the standpoint of simulating flight levels of enthalpy and pressure but both of these facilities have maximum test times of only about one second which is quite restrictive for ablation shape change tests. Considering the flexibility of conducting proof tests of full scale flight hardware and the good simulation for transpiration systems tests provided by the ABRES facility, its utility as a high pressure hyperthermal ablation is well established.

SECTION 6

SUMMARY

The high pressure ABRES combustion test facility operating with the N_2O_4/Aerozine-50 propellant has been thoroughly analyzed. Both pressure and calorimeter calibration data have been rationalized with theoretical predictions. Further calibration measurements have been recommended. Alternate propellant combinations have been analyzed for application in the ABRES facility. The ablation shape change simulation achieved in the ABRES facility has been compared with flight and other current ablation test facilities. In addition the ablation shape change simulation with the ABRES facility was compared with other advanced ablation test facility concepts. Results of these analyses are summarized below.

- Calorimeter and pressure calibration data from the ABRES facility exhibit generally good agreement with theoretical predictions with the exception of the stagnation point heating data. Measured stagnation point heat rates are about double the laminar predictions. These calibration data were used to verify the test rhombus boundaries for both the Mach 2.32 and 2.93 nozzles.
- Recommendations for further calibration studies include (1) additional calibration tests and detailed transient heat conduction analyses to resolve the current stagnation point heating anomaly (2) detailed calibration of the Mach 1.68 conical nozzle currently being fabricated (3) gas sampling of the test stream to measure the elemental uniformity within the test rhombus.
- The ablation shape change response of graphitic models in the ABRES test facility is characterized by fully turbulent blunt biconic ablation shapes similar to those which develop during intervals of peak heating in flight. The ablation response of graphitic materials in the ABRES facility however is much different than that predicted for flight due to the relatively low combustion temperature of the N_2O_4/Aerozine-50 propellant combination and the large amounts of H_2O and CO_2 in the test stream. The current level of similitude achieved with the ABRES facility with graphite ablation and thermostructural response in flight is low.

- Results of the propellant optimization studies demonstrated that (1) the optimum propellant combination for thermostructural simulation is hydrogen/fluorine (2) the optimum propellant combination for reentry ablation simulation is cyanogen/LOX despite the relatively low total enthalpy restriction with the ABRES facility and (3) the optimum propellant combination for transpiration systems tests is hydrogen/oxygen.

- Considering the aspects of cost and toxicity associated with selecting an advanced propellant combination for the ABRES combustion test facility resulted in the selection of a hydrocarbon/LOX propellant combination. Conversion of the ABRES facility from the current propellant (N_2O_4/Aerozine-50) to a hydrocarbon/LOX propellant combination represents a compromise from the standpoint of simulating reentry flight environments. These propellants are highly desirable from the standpoint of low cost and low toxicity which increases the allowable testing frequency.

- Comparison of the advanced ABRES combustion test facility (Hydrocarbon/LOX propellant combination) with other advanced ablation test facilities showed that the ABRES facility will continue to provide a unique proof testing capability for flight hardware, not available elsewhere. Compared to several prototype arc heaters the advanced ABRES facility exhibits (1) comparable impact pressures in the range of 50 to 160 atmospheres (2) a test rhombus diameter from five to eight times those of the arcs and (3) a total enthalpy about that of the two advanced facility concepts.

In summary, the ABRES combustion test facility under its current operating constraints provides an ablation test facility for proof-testing flight hardware. Its current operation is consistent with theoretical predictions. Graphite ablation response in the ABRES facility does not simulate flight levels of graphite ablation temperatures or flight strain levels. Alternate propellant combinations can be selected which better simulate the hyperthermal conditions characteristic of flight. High cost and toxicity considerations preclude the use of hydrogen/fluorine and cyanogen/LOX as alternate propellants despite their ability to better simulate flight test conditions. The hydrocarbon/LOX propellant combinations selected for the advanced ABRES facility provide about a 30 percent increase in the cold-wall enthalpy potential and a 1000 to 1200°R increase in the predicted graphite ablation temperature from the current facility. The potential also exists for using hydrogen/oxygen as the propellant for transipiration

systems test wherein peak flight levels of the mass transfer parameter ($B = \dot{m}/\rho_e U_e C_M$) are simulated. The ABRES combustion test facility has to date and will continue to serve an important function in supporting development of high performance nosetip systems for hyperthermal reentry applications.

REFERENCES

1. Driscoll, R. J., "Heat Transfer Over Spherically Blunted Cones Tested in the AFRPL Nosetip Test Facility," AFRPL-TM-73-2, May 1973. (Rough Draft)

2. Kennedy, W. S., Rindal, R. A., and Powars, C. A.: "Heat Flux Measurement Using Swept Null Point Calorimetry," AIAA Paper No. 71-420, April 1971.

3. Moyer, C. B. and Davis, J. N., "Analysis of Advanced Ballistic Reentry Vehicle Nosetip and Heatshield Materials Vol. II Program for Analysis of Null Point Calorimeter Data, Version 2 (PANDA 2): Description and User's Manual," AFML-TR-73-31, March 1973.

4. "Aerotherm Real Gas Energy Integral Boundary Layer Program (ARGEIBL)," Aerotherm Report UM-69-6911, November 1969.

5. Abbett, M. J., "Finite Difference Solution of the Subsonic/Supersonic Inviscid Flow Field About a Supersonic, Axisymmetric Blunt Body at Zero Incidence - Analysis and User's Manual," Aerotherm Report UM-71-34, June 1971.

6. Powars, C.A. and Kendall, R. M., "User's Manual, Aerotherm Chemical Equilibrium (ACE) Computer Program, Version 3," Aerotherm Report UM-70-13, May 1970.

7. Moyer, C. B., "Axi-symmetric Transient Heating and Material Ablation Program (ASTHMA) Description and User's Manual," Aerotherm Report No. 68-27, January 1968.

8. Moyer, C. B. and Rindal, R. A., "Finite Difference Solution for the In-Depth Response of Charring Materials Considering Surface Chemical and Energy Balances." Aerotherm Final Report 66-7, Part II, March 14, 1967 (also NASA CR-1061, June 1968).

9. "Passive Nosetip Technology (PANT) Program, Steady-State Analysis of Ablating Nosetips (SAANT), Volume I - Program Description and Sample Problems," Aerotherm UM-73-38, SAMSO TR-73- , September 1973.

10. Anderson, A. D., "Interim Report Passive Nosetip Technology (PANT) Program, Surface Roughness Effects, Part III Boundary Layer Transition Data Correlation and Analysis," SAMSO-TR-74- , Volume III, Aerotherm Report 74-90, January 1974.

11. Baker, D. L. "50 MW Thermostructural Testing of Graphite RVNT," Aerotherm Program 7055, Final Report to be published June 1974.

12. Personal communication with D. Burnett, Lockheed Missiles and Space Co. Sunnyvale, California, October 1973.

13. Jaffe, N. A., et al., "Final Technical Report Nosetip Cooling Technology (NCT) Program, Investigation of Discrete Injection Cooling," SAMSO-TR-73-380, October 1973.

REFERENCES (CONCLUDED)

14. "Rocket Exhaust Test Facilities Performance and Capabilities," Publication No. U5022, Philco-Ford Corporation, Aeronutronic Division, Newport Beach, California, April 1972.

15. "Thermo Simulation Capabilities," Lockheed Missles and Space Co., Santa Cruz, California 95060.

16. Derbidge, T.C., et al., "Interim Report Passive Nosetip Technology (PANT) Program, Definition of Shape Change Phenomenology From Low Temperature Ablator Experiments, Part III Shape Change Data Correlation and Analysis," SAMSO-TR-74- , Volume V, Aerotherm Report 74-90, January 1974.